UNIVERSIDAD NACIONAL DE COLOMBIA

Bioclimatic evaluation and optimization of the Non-Centrifugal Cane Sugar (NCS) Factory in Caparrapí, Colombia

Evaluación bioclimática y optimización de una Central de Mieles de Panela en Caparrapí, Colombia

Juan David Álvarez Carpintero

Universidad Nacional de Colombia
Facultad de Ingeniería
Bogotá, Colombia
2023

Bioclimatic evaluation and optimization of the Non-Centrifugal Cane Sugar (NCS) Factory in Caparrapí, Colombia

Juan David Álvarez Carpintero

Tesis presentada como requisito parcial para optar al título de:
Magister en Ingeniería de Biosistemas

Director:
Ph.D. Robinson Osorio Hernández

Co-Director:
Ph.D. Jesús Hernán Camacho Tamayo

Línea de Investigación:
Construcciones e infraestructura rural y bioclimática

Universidad Nacional de Colombia
Facultad de Ingeniería
Bogotá, Colombia
2023

La peor prisión es un corazón cerrado.

A Dios, por la vida.

A mis papás, por tanto amor y entrega.

A todos los que me han apoyado en este proceso.

Acknowledgments

I would like to thank the following people for helping me do this research: Universidad Nacional de Colombia for providing its laboratories and sensors, Fedepanela for providing the data and possibility to gather the core data for the research, Professors Robinson Osorio Hernández, and Jesús Hernán Camacho Tamayo for their guidance and Andrea Herrera Cardona for her help in the data gathering in the factory.

Resumen

La producción de panela en Colombia es un importante factor económico y social para las 350.0000 familias campesinas que subsisten de esta actividad. En Colombia, la implementación de fábricas industriales, llamadas Centrales, han intentado mejorar la economía de los trabajadores que ejercen estas actividades sin tecnificación. Hasta el momento no existen estudios de bioclimática aplicada a este tipo de instalaciones agroindustriales. De esta manera, el objetivo del presente estudio fue desarrollar un modelo computacional que representara el entorno real, en el caso específico de la Central de Mieles de Caña, con el fin de predecir su comportamiento ambiental bajo diferentes escenarios. Los resultados mostraron niveles de temperatura adecuados para los horarios de 7 am y 9 am, pero con altas humedades relativas, favoreciendo la condensación de vapor de agua, el goteo y la proliferación de hongos. En horarios de 2 pm, los resultados mostraron valores de temperatura altos, generando estrés térmico en los trabajadores, debido a la naturaleza de las actividades laborales en la Central. Las alternativas propuestas muestran un mejoramiento del ambiente de la Central, no obstante, es necesario acoplar otras medidas para reducir el estrés térmico de los operarios.

Palabras clave: Panela, CFD, caña de azúcar, Índice WBGT, ruido, temperatura, humedad relativa.

Abstract

Non-Centrifugal Cane Sugar production in Colombia is an important economic and social factor for the 350,000 peasant families that subsist on this activity. In Colombia, the implementation of industrial factories, called Centrales, has tried to improve the economy of the workers who carry out these activities without technification. So far, there are no bioclimatic studies applied to this type of agroindustrial facilities. Thus, the objective of this study was to develop a computational model to represent the real environment, in the specific case of the Sugarcane Honey Plant, in order to predict its environmental behavior under different scenarios. The results showed adequate temperature levels for the 7am and 9am hours, but with high relative humidity, favoring water vapor condensation, dripping and fungus proliferation. At 2pm, the results showed high temperature values, generating thermal stress in the workers, due to the nature of the work activities at the plant. The proposed alternatives show an improvement in the plant's environment; however, it is necessary to implement other measures to reduce the thermal stress of the workers.

Keywords: Jaggery, CFD, sugar cane, WBGT Index, noise, temperature, relative humidity.

Content

Acknowledgments vii

Abstract ix

List of Figures xi

List of Tables xiii

1. Introduction 2
- 1.1. Objectives . . . 3
- 1.2. Generalities of NCS in Colombia . . . 3
  - 1.2.1. NCS characterization . . . 4
  - 1.2.2. Production process . . . 5
- 1.3. Bioclimatic simulation . . . 10
  - 1.3.1. Heat transfer . . . 10
  - 1.3.2. Psychrometric characteristics . . . 13
  - 1.3.3. Working comfort . . . 15
  - 1.3.4. Computational Fluid Dynamics (CFD) modeling . . . 16

References . . . 16

2. Hygrometry simulation for a Non-Centrifugal Cane Sugar Factory in Caparrapí, Colombia 24
- 2.1. Introduction . . . 24
- 2.2. Materials and methods . . . 25
  - 2.2.1. Place description and operation . . . 25
  - 2.2.2. Measurement of environmental conditions . . . 26
  - 2.2.3. Simulation process . . . 29
  - 2.2.4. Model validation . . . 32
- 2.3. Results and discussion . . . 33
- 2.4. Conclusions . . . 41

References . . . 42

3. Comfort indexes of work conditions in a Non-Centrifugal Cane Sugar Factory in Colombia 46
- 3.1. Introduction . . . 46

3.2. Materials and methods . . . 47
3.2.1. Place description . . . 47
3.2.2. Simulation procedure . . . 48
3.2.3. Model validation . . . 52
3.2.4. WBGT Index determination and interpretation . . . 53
3.3. Results and discussion . . . 55
3.4. Conclusions . . . 59
References . . . 59

4. Noise mapping technique for an unrefined sugar cane processing factory in Colombia 63
4.1. Introduction . . . 63
4.2. Materials and methods . . . 65
4.2.1. Site description . . . 65
4.2.2. Sound level measure . . . 65
4.2.3. Noise data analysis . . . 66
4.3. Results and discussion . . . 67
4.4. Conclusions . . . 72
References . . . 72

5. Conclusions and recommendations 75
5.1. Conclusions . . . 75

A. Appendix: Temperature profiles for treatments 1 to 4 at 9a.m., 11 a.m. and 3p.m. work shifts 76

B. Appendix: Relative humidity profiles for treatments 1 to 4 at 9a.m., 11 a.m. and 3p.m. work shifts 80

C. Appendix: WBGT Index maps for treatments 1 to 4 at 9a.m., 11a.m. and 3p.m. 84

List of Figures

1-1. NCS production in Colombia from 1961 to 2020. Adapted from FAO (2022) 4
1-2. NCS manufacturing process at Caparrapí's Cane Honey Factory. 8

2-1. Measure of working places in Caparrapí's Cane Honey Factory. 27
2-2. Measure points inside the factory, classified in areas, m. 28
2-3. Geometry of the NCS factory located in Caparrapí, Colombia. 31
2-4. Computed mesh for Caparrapí's Cane Honey Factory model 33
2-5. Boxplot graphics of temperature and relative humidity for different work shifts. (a) Temperature for 7a.m. work shift. (b) Temperature for 2p.m. work shift. (c) Relative humidity for 7a.m. work shift. (d) Relative humidity for 2p.m. work shift. 35
2-6. Temperature profiles for treatments 1 to 4 38
2-7. Relative humidity isometric view for treatments 1 to 4 39

3-1. Temperature measure through thermographic images 49
3-2. Geometry of the NCS factory located in Caparrapí, Colombia. 51
3-3. Computed mesh for Caparrapí's Cane Honey Factory model 55
3-4. Boxplot graphics of WBGT index for different work shifts 56
3-5. WBGT Index profiles for treatments 1 to 4, °C 58

4-1. Measure points inside the factory, m. 66
4-2. Contour maps for noise in working measures, dBA: (a) 7-9 a.m. (b) 9–11 a.m. (c) 11–1 p.m. 70
4-3. TWA noise levels, dBA 71

A-1. Temperature profiles for treatments 1 to 4 for 9a.m. work shift 77
A-2. Temperature profiles for treatments 1 to 4 for 11a.m. work shift 78
A-3. Temperature profiles for treatments 1 to 4 for 3p.m. work shift 79

B-1. Relative humidity profiles for treatments 1 to 4 for 9a.m. work shift 81
B-2. Relative humidity profiles for treatments 1 to 4 for 11a.m. work shift 82
B-3. Relative humidity profiles for treatments 1 to 4 for 3p.m. work shift 83

C-1. WBGT profiles for treatments 1 to 4 for 9a.m. work shift 85
C-2. WBGT profiles for treatments 1 to 4 for 11a.m. work shift 86

C-3. WBGT profiles for treatments 1 to 4 for 3p.m. work shift 87

List of Tables

1-1. Physicochemical requirements for panela and granulated or powdered panela. Adapted from Ministerio de Protección Social (2006) 6

2-1. Properties of the materials of the factory 31
2-2. Boundary conditions used for the CFD models. 32
2-3. Comparison of simulated and measured data for Temperature (T) and Relative Humidity(T) 34
2-4. NMSE values for Temperature (T) and Relative Humidity (RH) variables . . 34
2-5. Statistical information of temperature for each treatment in 7a.m. and 2p.m. work shifts (°C). 36
2-6. Statistical information of relative humidity for each treatment in 7a.m. and 2p.m. work shifts (%). 40

3-1. Properties of the materials of the factory 52
3-2. Boundary conditions used for the CFD models 52
3-3. WBGT Index maximum permitted values. Adapted from Ministério do Trabalho e Previdência (2021). 54
3-4. Comparison of simulated and measured means for WBGT Index, °C 55
3-5. NMSE for WBGT Index values 56
3-6. Statistical information of WBGT Index for each treatment in 7a.m. and 2p.m. work shifts (°C) 57

4-1. Sound level and reference duration sample 68

1. Introduction

Panela, also known as Non-Centrifugal Cane Sugar (NCS), has been a traditional sweetener consumed for cultures all around the world "that preserves most of the nutrients present in sugarcane" (Aguilar-Rivera & Olvera-Vargas, 2021, p. 314). Non-Centrifugal Cane Sugar has received different names, depending on the cultural background it has been related to: "jaggery and gur (South Asia), panela (Latin America), muscovado (Philippines), rapadura and azucar mascavo (Brazil) and kokuto (Japan)" (Jaffé, 2015, p. 2).

The social importance of NCS comes from the gathering of techniques passed from generation to generation and its gastronomical impact in all continents (Aguilar-Rivera & Olvera-Vargas, 2021). Traditional production techniques, which vary from one producer country to another, have been reported to change the final composition of NCS (Flórez-Martínez, Contreras-Pedraza, & Rodríguez, 2021).

Despite its nutritional characteristics, NCS is reported to have inefficient production systems, that usually "depend on firewood for fuel, which is costly and contributes to deforestation" (Aguilar-Rivera & Olvera-Vargas, 2021, p. 316). Additionally, it represents the central economic activity of many rural families and communities worldwide, who depend on its production to survive (Aguilar-Rivera & Olvera-Vargas, 2021; Flórez-Martínez et al., 2021).

In the case of the Caparrapí's Cane Honey Factory, a preliminary data gathering show that there is a deficit in the working comfort of the workers, since the environmental conditions of the building cause thermal stress, presenting high humidity and poor ventilation, resulting in low work efficiency.

Under the current working conditions, it is possible to generate affections to the workers, especially pulmonary diseases, in their general respiratory system, or even at a genetic level (Samet et al., 1987). Additionally, current working conditions lead to low performance, due to the difficulty of working in exposure to high temperatures, causing economic losses (Cai et al., 2018).

1.1. Objectives

To develop a computational model that represents the real environment of the Cane Honey Plant and predicts its behavior under different scenarios. For this purpose, the following specific objectives were proposed:

- To identify the actual internal bioclimatic behavior of the Cane Honey Plant.
- To model the real conditions of the place through the use of computational tools.
- To propose an optimal ventilation system for the Cane Honey Plant to improve worker comfort.

1.2. Generalities of NCS in Colombia

NCS is part of the consumption chain in Colombia, it is "a natural sweetener obtained by concentration of sugarcane juice in establishments called trapiches or Cane Honey Plants, and presented in different forms" (Mujica et al., 2008, p. 1), produced mainly in the departments of Cundinamarca and Antioquia (Rodriguez et al., 2004).

According to the Food and Agriculture Organization (FAO) (2022), Colombia is the tenth largest historical producer of sugarcane in the world, with approximately 26.5 million tons produced from 1961 to 2020. On the other hand, in relation to the use of this crop, Colombia has shown an increase in the production of this product, with a stabilization of around 2.5 million tons per year, as shown in **1-1**.

Currently, Colombia is the second largest producer of NCS in the world, after India, as reported by Mendieta et al. (2016) and Aguilar-Rivera and Olvera-Vargas (2021), registering "a production of 1,388,554 kg for the year 2014, with an average yield of 6.4 ton/ha". However, panela is produced, mainly, in systems that do not meet the demand capacity or quality required by international markets (Velásquez et al., 2019).

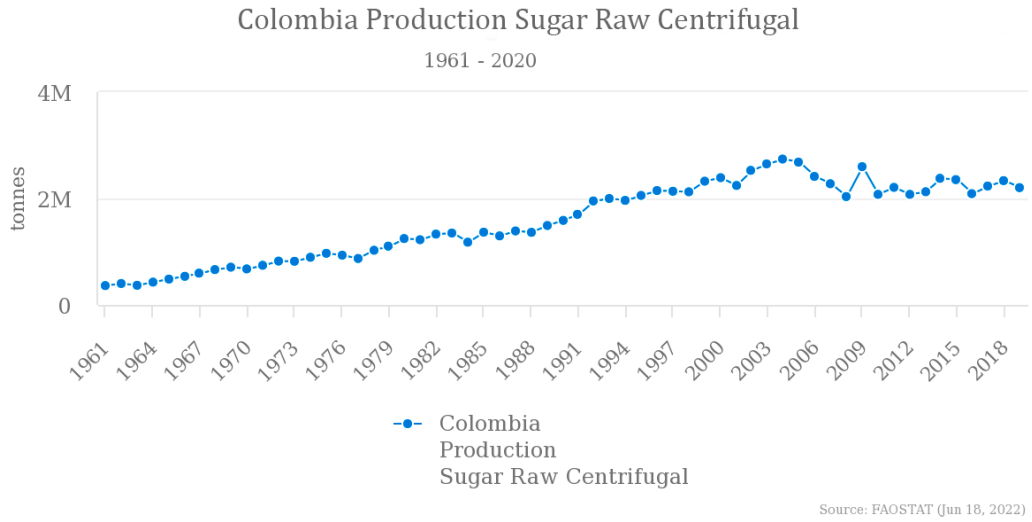

Figure 1-1.: NCS production in Colombia from 1961 to 2020. Adapted from FAO (2022)

In Colombia, NCS is one of the most important food products, since it is "the second most important agroindustry in the country, after coffee, with 220 thousand hectares" (Ministerio de Agricultura y Desarrollo Rural, 2019, p. 5). Due to this, it is necessary to optimize the processes present in this production, guaranteeing the safety of the product and the producer's security, since it not only affects agricultural systems, but also the country's cultural spheres.

However, the importance of sugarcane production is not only reflected at a social level, as it has proven to be important in the agricultural economy of the country. Cundinamarca presented, for the year 2018, the highest production in the country by department, "reaching 60315 Has of area cultivated in sugarcane, for the production of panela" (Ministerio de Agricultura y Desarrollo Rural, 2018, p.5). At the same time, for this production, the department presented very low levels of technification of crops and processing plants, with high levels of vapor production and exposure to high temperatures (Rodriguez et al., 2004).

1.2.1. NCS characterization

Due to its origin from sugarcane, along with the handling in the different processes required for its manufacture, "NCS can present variations in its nutritional composition, bioactive and sensory characteristics" (Jaffé, 2015). Despite this variation, sucrose is the component with the highest presence in this product (65-85%), followed by reducing sugars (10-15%), with traces of different materials such as proteins, minerals, phosphorus, among others (3-10%) (Velásquez et al., 2019). Additionally, (Jaffé, 2015) adds that there are records of compounds such as fats and ashes corresponding to 0.13% and 1.47%, respectively, due to

the manufacturing processes.

Similarly, García, Narváez, Heredia, Orjuela, and Osorio (2017) reported that NCS contains mainly two enzymes responsible for the characteristic odor of the final product, these components being 2-Methylpyrazine and Furfural. Additionally, the same study by García et al. (2017) presents, in the case of Colombia, low pH differences between panela produced in Cundinamarca due to the use of alkaline compounds for pH balance during the evaporation process.

As for the mineral composition reported in the literature, "there is a wide variety due to sugarcane varieties, soil type, fertilization, harvesting and manufacturing activities" (Velásquez et al., 2019, p. 33). Consequently, the same Jaffé (2015) reports, among other minerals, calcium, chlorides, cobalt, copper, chromium, iodine, iron, magnesium, manganese. On the other hand, the vitamins found in panela, in a more recurrent way, are thiamine, riboflavin, niacin, vitamins B5 and B6, as well as a deficiency in vitamin B12 (Jaffé, 2015).

In the case of antioxidants, a clear correlation has been determined where "high evaporation temperatures, produce higher amounts of phenolic compounds and, consequently, higher amounts of antioxidants" (Asikin et al., 2016). Additionally, Rao and Singh (2022, as cited in Jaffé, 2015) reported a phenolic compound content between 280-320 mg/100 g of panela. This, demonstrating a higher nutritional potential than conventional sugar (Shrivastava & Singh, 2020). Furthermore, (Ebadi & Azlan, 2021) reports that NCS has "anti-diabetic, anticariogenic, antioxidant and has radical scavenging activity due to the presence of vitamins, minerals, phenolic acids and flavonoid components as well as total antioxidant capacity", presenting the importance of the product and its benefits to human health.

On the other hand, NCS has been considered as a medicinal element since 800 - 1000 B.C., according to (Shrivastava & Singh, 2020). Asikin et al. (2012) reported the detection of Polyconazole, "a primary alcohol chain of great interest, due to its effects that include reduction of platelet aggregation, reduction of blood lipoprotein levels, inhibition of cholesterol synthesis and prevention of the development of arteriosclerosis". Finally, Weerawatanakorn et al. (2016) found a value of 2.63 to 3.69 mg of Polyconazole per 100 g of panela, reaffirming its benefits on human health.

1.2.2. Production process

In Colombia, sugarcane production is governed by Resolution 779 of 2006 of Ministerio de Protección Social (2006), which establishes the requirements and prohibitions, sanitary conditions and provisions for packaging, packing, labeling, repackaging, storage, distribution,

transportation and commercialization in the production of panela (Ministerio de Protección Social, 2006). The physical-chemical requirements requested in this regulation are shown in Table **1-1**.

Subsequently, Resolution 3462 of 2008 modified the sanitary conditions requested for the production of panela and added the Good Manufacturing Practices for Panela (Ministerio de Protección Social, 2008). Additionally, through Resolution 3544 of 2009, the regulation of the packaging of panela, as well as the individual labeling of the same came into force (Ministerio de Protección Social, 2009).

Table 1-1.: Physicochemical requirements for panela and granulated or powdered panela. Adapted from Ministerio de Protección Social (2006)

	NCS		***Granulated or powdered NCS***	
Requirements	**Minimum**	**Maximum**	**Minimum**	**Maximum**
Reducing sugars, expressed in glucose, in %	5.5%	-	5.74%	-
Non-reducing sugars, expressed in sucrose, in %	-	83.0%	-	90%
Proteins, in % (N x 6.25)	0.2%	-	0.2%	-
Ashes, in %	0.8%	-	1.0%	-
Humidity, in %	-	9%	-	5.0%
Lead expressed as Pb in mg/kg	-	0.2	-	20%
Arsenic expressed as As in mg/kg	-	0.1	-	10%
SO2	NEGATIVE	NEGATIVE	NEGATIVE	NEGATIVE
Colorants	NEGATIVE	NEGATIVE	NEGATIVE	NEGATIVE

In Colombia, the production process of NCS is carried out through conventional and artisanal methods, especially in farms dedicated to it, called "trapiches paneleros" (sugarcane mills). Given the importance of having standardized processes that guarantee the healthiness and preserve the quality of each part of the process, studies have been conducted on phytosanitary management during cultivation and production (Tarazona Parra, 2011; Osorio, 2007).

The quality of the product is affected in each of the parts of the production chain involved in the production of panela(Velásquez et al., 2019). In the first place, during sugarcane cultivation there are numerous factors that affect the development of the varieties, as well as their sugar concentration (Osorio, 2007). Thus, according to Osorio (2007), site characteristics such as temperature, climate, luminosity and altitude above sea level, generate changes in production times and sugar concentration.

Afterwards, during the sugarcane cutting process, the shortest possible times must be achieved to obtain the best quality of the final product (Rozo, 2013). To carry out this process, there are two commonly used methodologies: "cutting by thinning and cutting by paring" (Osorio, 2007, p. 98). Where, "cutting by thinning is commonly used in small-scale farms, but with continuous production and (...) cutting by paring is used in technified productions" (Osorio, 2007, pp. 98-99).

After this, the juice must be extracted from the sugarcane, through a process traditionally known as "milling"(Rozo, 2013). Osorio (2007) described that, after the sugarcane passes through the mill, cane honey is obtained, which is used for panela production. In addition, the residue of this process is called bagasse, which can be stored and used to obtain energy by burning it.

The obtained cane honey in the extraction must undergo an initial cleaning process, where "thick impurities of non-nutritional character are removed by physical (decantation and flotation in the precleaner), thermal (in the first pailas) and biochemical (with the agglutinants) means. It comprises three operations: pre-cleaning, clarification and liming" (Osorio, 2007, p. 114).

According to Rozo (2013), pre-cleaning is carried out through a decanting system, in which the heavier elements are extracted, while lighter residues, such as leaves and insects, are eliminated by buoyancy. Subsequently, during the clarification process, elements such as sand, soil residues and soluble solids are separated, due to the "heating provided by the stove and the agglutinating action of certain natural compounds allowed within the Good Manufacture Practices (GMP), such as cadillos, balsa, guásimo, juan blanco, san joaquín, among others" (Osorio, 2007, p. 116). Finally, within the pre-cleaning process, liming is carried out to obtain a pH value of 5.8 (Osorio, 2007).

Next, the process of evaporation and concentration of the cane juice begins. At this stage, the aim is to reach the "panela point", reaching a temperature of 96°C, which guarantees the necessary concentration of Brix degrees and temperatures between 120 and 125°C, to achieve the necessary molding texture (Osorio, 2007; Rozo, 2013), also adding natural anti-adherents to avoid burning the panela and homogenize the cane honey (Osorio, 2007).

After that, to guarantee the correct oxygenation of the honeys, the tapping process is carried out. This is done in specific containers for this task, through manual beating, depending on the experience of the worker for its correct performance (Osorio, 2007). Subsequently, the honeys are deposited in the molds, where they take their final shape (Rozo, 2013). Finally, after the cooling time, the panela is packaged and stored for its commercialization (Osorio, 2007).

In Colombia, on the other hand, the incorporation of honey mills for the production of NCS has begun on a massive scale. In particular, the production process of the "Central de Mieles de Caparrapí" or Caparrapi's Cane Honey Factory, in Cundinamarca, Colombia, differs from the traditional system by the concentration of honeys (after the extraction of juices, described above) and the production of NCS of up to 250kg/h. This process is described below according to the description made on site and recorded by Fedepanela (2019), as can be seen in Figure **1-2**.

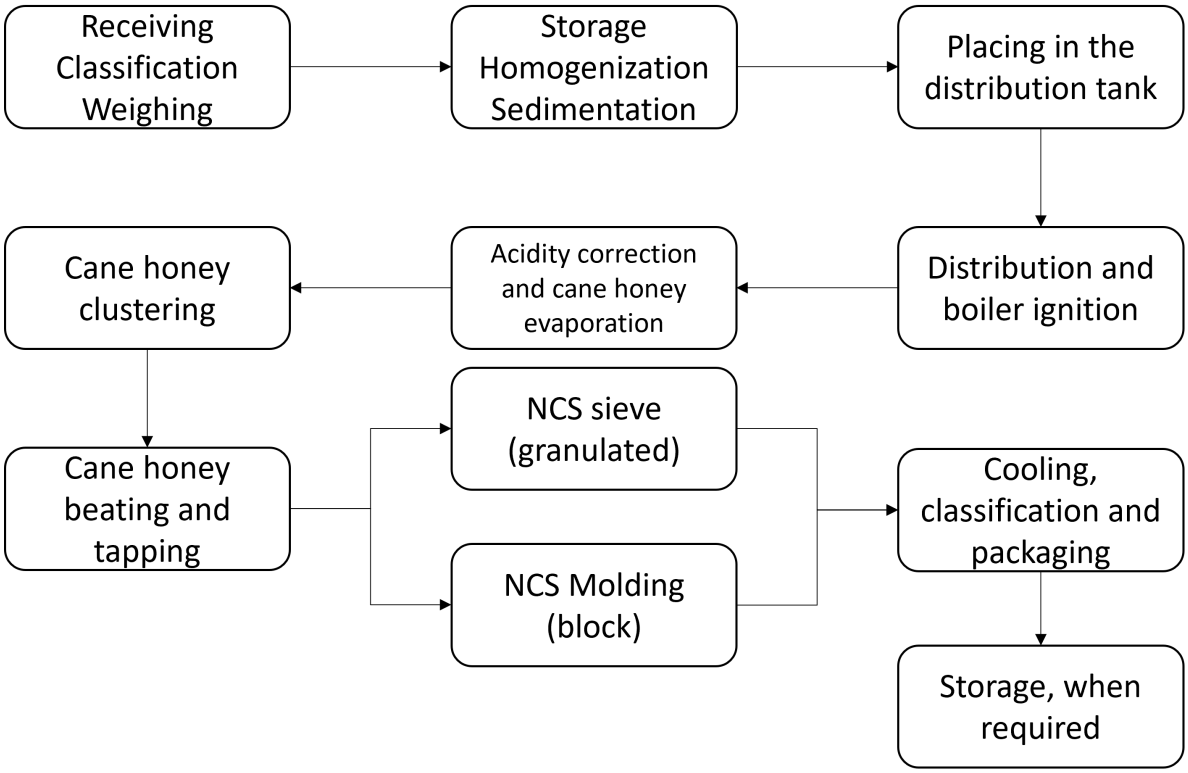

Figure 1-2.: NCS manufacturing process at Caparrapí's Cane Honey Factory.

- **Receiving of the cane honey**: To contextualize, the production process is described as follows (Fedepanela, 2019). First, the Factory receives the cane honeys, extracted from the cane and purchased from the farmers, on which pH and Brix degrees (°Brix) are measured to determine their quality. Based on the results obtained there, these honeys can be classified as type A or type B, according to those of higher and lower quality, respectively.

- **Storage and homogenization**: Subsequently, the cane honeys are sent to their respective tanks and the cleaning process by decantation is carried out, which lasts 24

hours. At the same time, the homogenization process is carried out by mixing different honeys from different farms to obtain a single uniform honey. Finally, the settled honey can be used for the production of honeys for animal consumption.

- **Placing in the distribution tank**: Before starting the production, the cane honeys are sent to the distribution tank, which has a capacity of 5 tons, through a pumping system. Here, the honey can be blended to achieve the desired characteristics. From the distribution tank, the honey is sent by gravity to the evaporators, where its inflow can be controlled through valves. In this way, partial or complete operation of the plant can be guaranteed.

- **Distribution and boiler ignition**: During the arrival of the honey to the evaporators, prior to reaching 60°C, the honey acidity correction must be carried out. If the honey has an acidity of 5.2 or less, it must be corrected with the addition of hydrated lime type E, edible for humans. The correction is made until reaching a pH of 5.6 - 5.8 for NCS in block shape and 6.0 for pulverized NCS.

- **Acidity correction and cane honey evaporation**: The lime is prepared by dissolving a ratio of 500 g of lime/10 liters of water, which then remains in a decanting process for 4 hours. Finally, the upper section of the mixture is separated and used as an alkalizing agent.

- **Evaporation process**: On the other hand, the evaporator system operates by means of a piping network, through which air flows at 120°C. Initially, this air is heated in the boiler, which is located at the back of the building and operates by burning coal.

- **Cane hoy clustering**: Once the boiler has been ignited, the honey is deposited in a system of containers with coils, which favor heat exchange with the air pipes. During this process, the honey reaches 85°Brix, when it reaches approximately 105 °C, according to site-specific measurements taken by the workers. After this process, the valves are opened to allow the passage of the cane honey to the evaporators, adding vegetable oil, in the same way, to avoid adhesion of the honeys and reduce the production of foam. There, the water evaporation process begins until the "panela point" is obtained, when a temperature between 120 to 130°C is reached. Usually, this point is recognized by the workers' expertise.

- **Cane honey beating and tapping**: At the end of the water evaporation process, the honey is transferred to the honey pans, where the churning process is carried out. This has three main objectives, essential for the commercialization of the final product: to dry the honey until a texture is obtained that allows the correct molding, to oxygenate the honeys and to guarantee the change of color.

- **NCS molding or sieving**: Once the desired texture is reached, the honey is deposited in the molds, also called gravel pits, where it is distributed homogeneously in all cavities, to ensure homogeneity in the shape and amount of honey used. Finally, after 3 minutes inside the mold, the product extraction process is carried out on the table. During this procedure it is essential that there is no water in the molds or on the table, to avoid unwanted stains on the product and the presence of fungi.

- **Cooling, classification and packaging**: Finally, NCS remains in cooling until it reaches thermal equilibrium with the ambient temperature. During this stage it is important to ensure that the NCS is not packaged at high temperature, as this can cause physical and biological damage to the product, due to the steam produced by the NCS. Finally, the NCS is classified according to its weight, to be packaged accordingly.

1.3. Bioclimatic simulation

1.3.1. Heat transfer

Heat transfer study for buildings can help create a safe environment for workers and increase productivity (Davies, 2004). Heat transfer, specially in rural activities, is characterized for the influence of solar radiation and, in some cases, presenting high temperature processes (Parkes et al., 2022).

For instance, heat transfer and its way of transferring have been studied by many authors (Cengel & Ghajar, 2014; Xu et al., 2019). Historically, in agriculture, heat transfer has been studied mainly for greenhouses (Mobtaker et al., 2019), whereas other processes have been left aside.

For this study, all ways of heat transfer were studied, due to the nature of the processes carried inside the NCS Factory. Here is a brief description of the interaction of each way of heat incidence in the NCS production.

Heat transfer through conduction is "the transfer of energy from the more energetic particles of a substance to the adjacent less energetic ones as a result of interactions between the particles" (Cengel & Ghajar, 2014, p. 17), and it is represented by Equation 1-1. This type of heat transfer can be found specially in walls and ceilings, for agricultural buildings, in the proximity to burners, ovens, among other sources of heat (Tarigan, 2018).

$$\dot{Q} = kA\frac{T_1 - T_2}{\Delta x} \tag{1-1}$$

Where:

$\dot{Q}$ is heat (W).

k is the thermal conductivity of the object $(W \cdot m^{-1} \cdot K^{-1})$.

A is the area through which the transfer takes place (m^2).

T_1 **and** T_2 are the temperatures of the ends of the surface (K).

x is the width of the surface (m).

Another way of heat transfer is convection. It can be defined as "the energy transfer between a solid surface and the adjacent liquid or gas that is in motion, and it involves the combined effects of conduction and fluid motion" (Cengel & Ghajar, 2014, p. 25). In agriculture, this type of heat transfer is usually found in drying and storage systems (Ekka & Palanisamy, 2020; Lingayat et al., 2020), in ventilation (Ghernaout et al., 2020; Çerçi & Daş, 2019), among others. Heat transfer by convection is calculated by the use of Equation 1-2 (Cengel & Ghajar, 2014).

$$\dot{Q} = h \cdot A_s \cdot (T_s - T_\infty) \tag{1-2}$$

Where:

$\dot{Q}$ is heat (W).

h is the type of convection $(W \cdot m^{-2} \cdot K^{-1})$.

A_s is the area through which the transfer takes place (m^2).

T_s is the surface temperature (K).

T_∞ is the temperature far from the surface (K).

Also, radiation is a way of heat transfer, that can be defined as "the energy emitted by matter in the form of electromagnetic waves (or photons) as a result of the changes in the electronic configurations of the atoms or molecules", and calculated by using Equation 1-3 (Cengel & Ghajar, 2014, p. 27). For instance, in agriculture, high temperature processes related with burning materials, such as air heating, and drying, usually present this type of heat transfer (Salehi, 2020; Dhiman, Sethi, Singh, & Sharma, 2019).

$$\dot{Q}_{emit} = \epsilon \cdot \sigma \cdot A_s \cdot T_s^4 \tag{1-3}$$

Where:

$\dot{Q}_{emit}$ is heat (W).

ϵ is the emissivity of the surface ($0 < \epsilon < 1$).

σ is the Stefan-Boltzman constant (SI=$5.670 \cdot 10^{-8} W \cdot m^{-2} \cdot K^{-4}$).

A_s is the surface area (m^2).

T_s is the emitted temperature from a surface (K).

In addition, according to Cengel and Ghajar (2014), heat transfer through walls can be defined by Equation 1-4. The overall heat transfer can be defined as $U = 1/R$, where R is the overall unit thermal resistance, depending on the material of the walls. Due to the adverse ambient conditions of the rural areas, treatments with heat transfer require this characteristic.

$$\dot{Q} = UA \cdot (T_i - T_o) \tag{1-4}$$

Where:

$\dot{Q}$ is heat (W).

U is the overall heat transfer coefficient ($W \cdot m^{-2} \cdot^{\circ} C^{-1}$).

A is the heat transfer area (m^2).

T_i is the indoor temperature ($^{\circ}C$).

T_o is the outdoor temperature ($^{\circ}C$).

On the other hand, for food products, specific heat of food is an important property of the products, specially for cooling processes (Tun, 2019). NCS' specific heat has been studied during its production process (Alarcón et al., 2020) and in its final state (Kumar & Kumar, 2021a). For the current study, specific heat was used to calculate the temperature of exposition for each one of the task in the factory.

Furthermore, vapor emission in NCS production can contain harmful components (Tyagi et al., 2022). Also, high emission levels increase risk of fungus development in the final product (Attri & Varma, 2018) and can cause pulmonar illnesses with high exposure (Jaffé, 2012; Tong et al., 2019).

1.3.2. Psychrometric characteristics

In order to understand the internal conditions of the site during production periods at the Caparrapí's Cane Honey Factory, it is necessary to study the characteristics of the air present at the site. The concepts used in this research are described below.

Firstly, dry bulb temperature, defined as the temperature traditionally measured by a thermometer exposed to air (Yaciuk, 1981), is commonly used for the determination of other characteristics, due to the ease in its measurement (Hanif et al., 2022).

On the other hand, the wet bulb temperature, "is the temperature obtained with a thermometer, the bulb of which is covered by a piece of muslin, which is kept wet with clean or distilled water, exposed to air and free from radiation" (Legg, 2017, p. 23). This is also defined as "the dynamic temperature equilibrium reached by a water surface, when the rate of convective heat transfer equals the external mass transfer from the surface" (Fox et al., 2014). Equations describing the relationship between dry bulb temperature, relative humidity, and wet bulb temperature have been determined empirically, as described by Stull (2011), and shown in equation 1-5.

$$T_{wb} = T * \arctan[0.151977 * (RH * 18.313659)^{1/2}] + \arctan(T + RH) - \arctan(RH - 1.676331) + 0.00391838 * (RH)^{3/2} * \arctan(0.023101 * RH) - 4.686035 \quad (1\text{-}5)$$

Where:

T_{wb} is wet-bulb temperature (°C).

T is dry-bulb temperature (°C).

RH is relative humidity (%).

Likewise, the black globe temperature is used in thermal comfort measurement processes. Its operation is based on a black globe, with a thermometer inserted in its center (Dimiceli et al., 2013). Additionally, it can be calculated based on the dry-bulb temperature, for indoor environments below 40°C, according to Dimiceli et al. (2013), as shown in Equation 1-6.

$$T_g = 0.456 + 1.0335 * T \tag{1-6}$$

Where:

T_g is the black globe temperature (°C).

T is dry-bulb temperature (°C).

Relative humidity determines the environment the readiness of the air for illnesses and contamination, therefore it is important to maintain its levels low (Ahlawat et al., 2020). It can be defined as "the percentage ratio of the vapor pressure of water vapor in the air to the saturated vapor pressure at the same temperature" (Legg, 2017, p. 5). Relative humidity can be calculated by applying Equation 1-7.

$$RH = \frac{e}{e_s} \cdot 100 \tag{1-7}$$

$$e = e_{sh} - AP(T - T_{bh}) \tag{1-8}$$

$$e_s = 6.107 \cdot 10^{\left(\frac{7.5 \cdot T_{bh}}{237.3 + T_{bh}}\right)} \tag{1-9}$$

$$e_{sh} = 6.107 \cdot 10^{\left(\frac{7.5 \cdot T}{237.3 + T}\right)} \tag{1-10}$$

Where:

RH is the relative humidity (%).

e is the partial pressure exerted by water vapor (hPa).

e_s is the saturation pressure at dry-bulb temperature (hPa).

A is the psychrometer constant for aired and non-aired psychrometers (constant).

P is the absolute pressure of the location (Pa).

T is dry-bulb temperature (°C).

T_{bh} is wet-bulb temperature (°C).

Additionally, through Equations 1-8, 1-9, and 1-10 vapor pressure can be calculated, according to the environmental conditions (Junzeng et al., 2012).

1.3.3. Working comfort

Thermal comfort is an important area of research, due to its direct impact in production, along with benefiting workers and their health (Lipczynska et al., 2018; Budd, 2008). Additionally, it can have a positive impact on products, by decreasing the risk of damage by fungus and bacteria that live in environments with high temperature and relative humidity (Guerra García et al., 2022).

Additionally, the measurement of the Wet Bulb Globe Temperature (WBGT) index is important in the agro-industry because of the nature of its tasks (Dillane & Balanay, 2020). For instance, radiant environments, high humidity levels and high vapor production need to be addressed in a particular way, because of its impact in human health (Cai et al., 2018; Dillane & Balanay, 2020).

Thermal comfort was evaluated through the calculation and measurement of the WBGT Index, following the instructions ruled by Ministerio de Trabajo y Seguridad Social (1979); Ministério do Trabalho e Previdência (2021), to determine thermal stress and its sources. WBGT Index for indoor conditions is determined by equation (1-11), as reported by Yoshida et al. (2020).

$$\text{WBGT} = 0.7 \cdot T_{wb} + 0.3 \cdot T_g \tag{1-11}$$

Where:

T_{wb} is wet-bulb temperature (Equation 1-5).

T_g is globe temperature (Equation 1-6).

For instance, when workers are exposed to high temperatures and humidity, due to vapors escaping without air movement, they can generate complications at the genetic level, or chronic pulmonary diseases, including reproductive system affections (Samet et al., 1987). Similarly, studies have shown how high temperatures in the workplace are reflected in significant economic losses, since the work performance of workers decreases in such conditions (Cai et al., 2018).

Additionally, studies using the same tools to analyze environmental behaviour have been conducted for comfort in animals (Tong et al., 2019; Dziubata et al., 2020; Kim et al., 2019; Zhou et al., 2019), and workers in some agricultural labors, such as coffee production (Guerra García et al., 2022), greenhouses (OLIVEIRA et al., 2019; Takakura et al., 2019; Jung & Kim, 2022), maize production (Sadiq et al., 2019; Orlov et al., 2021), among other production types. In addition, for determining thermal comfort in working places, previous studies have been determined in radiant temperature (Guo et al., 2020; Manavvi & Rajasekar, 2020).

1.3.4. Computational Fluid Dynamics (CFD) modeling

CFD presents an alternative to current measure-based systems, due to the economic and time-demanding activities required to complete measuring tasks (Tong et al., 2019). This technology is usually used "to address pertinent issues relating to technologies for clean and renewable power and meeting strict regulation challenges of emission control and substantial reduction of environmental pollutants" (Tu et al., 2018, p. 1).

An important research area for CFD creation is meshing, specially due to its impact in the simulation results (Lintermann, 2021). For instance, previous studies have shown determinant impact with the meshing application (Cheng et al., 2021; Tran et al., 2021).

Previous studies have been done in the economic impact through CFD application(Kumar & Kumar, 2021b), poultry production (Cheng et al., 2021; Dziubata et al., 2020), cattle (Zhou et al., 2019; Bustos-Vanegas et al., 2019), swine production (Kim et al., 2019; Xie et al., 2019), among other animal production. Additionally, for plants, CFD studies have been conducted specially in greenhouses (Villagrán-Munar & Bojacá-Aldana, 2019; Saberian & Sajadiye, 2019; Guzmán et al., 2018; Zhang et al., 2020).

At the moment, several studies have been conducted for evaporation pans in rural production processes (Osorio, 2007; Aguilar-Rivera & Olvera-Vargas, 2021). Nevertheless, studies on Honey Factories have not been conducted nor have been published, leaving a hole in knowledge about this type of production.

In that way, CFD tools were used to determine alternatives to correct the current situation inside the factory, without local intervention to the structure. Additionally, studying in detail the local behavior of air.

References

Aguilar-Rivera, N., & Olvera-Vargas, L. A. (2021). Innovations for Sustainable Production of Traditional and Artisan Unrefined Non-centrifugal Cane Sugar in Mexico. In *World sustainability series* (pp. 313–330). doi: 10.1007/978-3-030-78825-4_19

Ahlawat, A., Wiedensohler, A., Mishra, S. K., et al. (2020). An overview on the role of relative humidity in airborne transmission of sars-cov-2 in indoor environments. *Aerosol and Air Quality Research*, *20*(9), 1856–1861. doi: https://doi.org/10.4209/aaqr.2020.06.0302

Alarcón, Á. L., Orjuela, A., Narváez, P. C., & Camacho, E. C. (2020). Thermal and rheological properties of juices and syrups during non-centrifugal sugar

cane (jaggery) production. *Food and Bioproducts Processing*, *121*, 76–90. doi: https://doi.org/10.1016/j.fbp.2020.01.016

Asikin, Y., Hirose, N., Tamaki, H., Ito, S., Oku, H., & Wada, K. (2016). Effects of different drying–solidification processes on physical properties, volatile fraction, and antioxidant activity of non-centrifugal cane brown sugar. *LWT - Food Science and Technology*, *66*, 340-347. Retrieved from https://www.sciencedirect.com/science/article/pii/S0023643815302577 doi: https://doi.org/10.1016/j.lwt.2015.10.039

Asikin, Y., Takahashi, M., Hirose, N., Hou, D.-X., Takara, K., & Wada, K. (2012). Wax, policosanol, and long-chain aldehydes of different sugarcane (saccharum officinarum l.) cultivars. *European Journal of Lipid Science and Technology*, *114*(5), 583-591. Retrieved from https://onlinelibrary.wiley.com/doi/abs/10.1002/ejlt.201100300 doi: https://doi.org/10.1002/ejlt.201100300

Attri, M. K., & Varma, A. (2018). Comparative study of growth of piriformospora indica by using different sources of jaggery. *Journal of PurE and aPPliEd Microbiology*, *12*(2), 933–942. doi: http://dx.doi.org/10.22207/JPAM.12.2.56

Budd, G. M. (2008). Wet-bulb globe temperature (wbgt)—its history and its limitations. *Journal of Science and Medicine in Sport*, *11*(1), 20-32. Retrieved from https://www.sciencedirect.com/science/article/pii/S1440244007001478 (Heat Stress in Sport) doi: https://doi.org/10.1016/j.jsams.2007.07.003

Bustos-Vanegas, J. D., Hempel, S., Janke, D., Doumbia, M., Streng, J., & Amon, T. (2019). Numerical simulation of airflow in animal occupied zones in a dairy cattle building. *Biosystems Engineering*, *186*, 100–105. doi: https://doi.org/10.1016/j.biosystemseng.2019.07.002

Cai, X., Lu, Y., & Wang, J. (2018). The impact of temperature on manufacturing worker productivity: Evidence from personnel data. *Journal of Comparative Economics*, *46*(4), 889–905. doi: 10.1016/j.jce.2018.06.003

Cengel, Y. A., & Ghajar, A. J. (2014). *Heat and mass transfer: Fundamentals and applications* (5th ed ed.). McGraw-Hill Professional.

Çerçi, K. N., & Daş, M. (2019). Modeling of heat transfer coefficient in solar greenhouse type drying systems. *Sustainability*, *11*(18), 5127. doi: https://doi.org/10.3390/su11185127

Cheng, Q., Feng, H., Meng, H., & Zhou, H. (2021). Cfd study of the effect of inlet position and flap on the airflow and temperature in a laying hen house in summer. *Biosystems Engineering*, *203*, 109–123. doi: https://doi.org/10.1016/j.biosystemseng.2021.01.009

Davies, M. G. (2004). *Building heat transfer*. John Wiley & Sons.

Dhiman, M., Sethi, V., Singh, B., & Sharma, A. (2019). Cfd analysis of greenhouse heating using flue gas and hot water heat sink pipe networks. *Computers and Electronics in Agriculture*, *163*, 104853. doi: https://doi.org/10.1016/j.compag.2019.104853

Dillane, D., & Balanay, J. A. G. (2020). Comparison between osha-niosh heat safety tool app and wbgt monitor to assess heat stress risk in agriculture. *Journal of occupational and environmental hygiene*, *17*(4), 181–192. doi: https://doi.org/10.1080/15459624.2020.1721512

Dimiceli, V. E., Piltz, S. F., & Amburn, S. A. (2013). Black globe temperature estimate for the wbgt index. In H. K. Kim, S.-I. Ao, & B. B. Rieger (Eds.), *Iaeng transactions on engineering technologies: Special edition of the world congress on engineering and computer science 2011* (pp. 323–334). Dordrecht: Springer Netherlands. Retrieved from https://doi.org/10.1007/978-94-007-4786-9_26 doi: 10.1007/978-94-007-4786-9_26

Dziubata, Z., Trokhaniak, V., Rogovskii, I., Titova, L., Luzan, P., & Popyk, P. (2020). Using cfd simulation to investigate the impact of fresh air valves on poultry house aerodynamics in case of a side ventilation system.
doi: https://doi.org/10.35633/inmateh-62-16

Ebadi, S., & Azlan, A. (2021). Nutritional composition and role of non-centrifugal sugar (ncs) in human health. *Current Nutrition & Food Science*, *17*(3).

Ekka, J. P., & Palanisamy, M. (2020). Determination of heat transfer coefficients and drying kinetics of red chilli dried in a forced convection mixed mode solar dryer. *Thermal Science and Engineering Progress*, *19*, 100607. doi: https://doi.org/10.1016/j.tsep.2020.100607

FAO. (2022). *Crops and livestock products database.* Retrieved junio 18, 2022, from https://www.fao.org/faostat/en/#data/QCL/visualize (Production/Yield quantities of Sugar Raw Centrifugal in Colombia. Última actualización: 07/02/2022.)

Fedepanela. (2019). *PROTOCOLO DE TRAZABILIDAD PARA OBTENCIÓN DE PANELA*. BOGOTÁ, D.C.. Unpublished writing.

Flórez-Martínez, D. H., Contreras-Pedraza, C. A., & Rodríguez, J. (2021). A systematic analysis of non-centrifugal sugar cane processing: Research and new trends. *Trends in Food Science & Technology*, *107*, 415-428. Retrieved from https://www.sciencedirect.com/science/article/pii/S0924224420306828 doi: https://doi.org/10.1016/j.tifs.2020.11.011

Fox, B., Bellini, G., & Pellegrini, L. (2014). Chapter 14 - drying. In H. C. Vogel & C. M. Todaro (Eds.), *Fermentation and biochemical engineering handbook (third edition)* (Third Edition ed., p. 283-305). Boston: William Andrew Publishing. Retrieved from https://www.sciencedirect.com/science/article/pii/B9781455725533000143 doi: https://doi.org/10.1016/B978-1-4557-2553-3.00014-3

García, J. M., Narváez, P. C., Heredia, F. J., Orjuela, Á., & Osorio, C. (2017). Physicochemical and sensory (aroma and colour) characterisation of a non-centrifugal cane sugar ("panela") beverage. *Food Chemistry*, *228*, 7–13. doi: 10.1016/j.foodchem.2017.01.134

Ghernaout, B., Attia, M. E., Bouabdallah, S., Driss, Z., & Benali, M. L. (2020). Heat

and fluid flow in an agricultural greenhouse. *Int. J. Heat Technol*, *3*, 92–98. doi: https://doi.org/10.18280/ijht.380110

Guerra García, L. M., Osorio Hernández, R., Osorio Saráz, J. A., Carlo, J. C., & Damasceno, F. A. (2022). Bioclimatic performance of wet coffee processing facilities: conditions for workers and coffee. *Revista Facultad Nacional de Agronomía Medellín*, *75*(1), 9763–9772. doi: https://doi.org/10.15446/rfnam.v75n1.96247

Guo, H., Aviv, D., Loyola, M., Teitelbaum, E., Houchois, N., & Meggers, F. (2020). On the understanding of the mean radiant temperature within both the indoor and outdoor environment, a critical review. *Renewable and Sustainable Energy Reviews*, *117*, 109207. doi: https://doi.org/10.1016/j.rser.2019.06.014

Guzmán, C. H., Carrera, J. L., Durán, H. A., Berumen, J., Ortiz, A. A., Guirette, O. A., ... others (2018). Implementation of virtual sensors for monitoring temperature in greenhouses using cfd and control. *Sensors*, *19*(1), 60. doi: https://doi.org/10.3390/s19010060

Hanif, M. A., Nadeem, F., Tariq, R., & Rashid, U. (2022). Chapter 4 - solar thermal energy and photovoltaic systems. In M. A. Hanif, F. Nadeem, R. Tariq, & U. Rashid (Eds.), *Renewable and alternative energy resources* (p. 171-261). Academic Press. Retrieved from https://www.sciencedirect.com/science/article/pii/B9780128181508000071 doi: https://doi.org/10.1016/B978-0-12-818150-8.00007-1

Jaffé, W. R. (2012). Health effects of non-centrifugal sugar (ncs): a review. *Sugar tech*, *14*(2), 87–94. doi: http://dx.doi.org/10.1007/s12355-012-0145-1

Jaffé, W. R. (2015). Nutritional and functional components of non centrifugal cane sugar: A compilation of the data from the analytical literature. *Journal of Food Composition and Analysis*, *43*, 194–202. doi: 10.1016/j.jfca.2015.06.007

Jung, W., & Kim, H. (2022). Evaluation of heat stress levels inside greenhouses during summer in korea. *International Journal of Environmental Research and Public Health*, *19*(19), 12497. doi: https://doi.org/10.3390/ijerph191912497

Junzeng, X., Qi, W., Shizhang, P., & Yanmei, Y. (2012). Error of saturation vapor pressure calculated by different formulas and its effect on calculation of reference evapotranspiration in high latitude cold region. *Procedia Engineering*, *28*, 43-48. Retrieved from https://www.sciencedirect.com/science/article/pii/S187770581200690X (2012 International Conference on Modern Hydraulic Engineering) doi: https://doi.org/10.1016/j.proeng.2012.01.680

Kim, R.-w., Kim, J.-g., Lee, I.-b., Yeo, U.-h., & Lee, S.-y. (2019). Development of a vr simulator for educating cfd-computed internal environment of piglet house. *biosystems engineering*, *188*, 243–264. doi: https://doi.org/10.1016/j.biosystemseng.2019.10.024

Kumar, R., & Kumar, M. (2021a). Performance evaluation of improved and traditional two pan jaggery making plants: A comparative study. *Sustainable Energy Technologies and*

Assessments, *47*, 101462. doi: https://doi.org/10.1016/j.seta.2021.101462

Kumar, R., & Kumar, M. (2021b). Thermoeconomic analysis of a modified jaggery making plant. *Heat Transfer*, *50*(5), 4871–4891.

Legg, R. (2017). Chapter 1 - properties of humid air. In R. Legg (Ed.), *Air conditioning system design* (p. 1-28). Butterworth-Heinemann. Retrieved from https://www.sciencedirect.com/science/article/pii/B9780081011232000017 doi: https://doi.org/10.1016/B978-0-08-101123-2.00001-7

Lingayat, A. B., Chandramohan, V., Raju, V., & Meda, V. (2020). A review on indirect type solar dryers for agricultural crops–dryer setup, its performance, energy storage and important highlights. *Applied Energy*, *258*, 114005. doi: https://doi.org/10.1016/j.apenergy.2019.114005

Lintermann, A. (2021). Computational meshing for cfd simulations. In K. Inthavong, N. Singh, E. Wong, & J. Tu (Eds.), *Clinical and biomedical engineering in the human nose: A computational fluid dynamics approach* (pp. 85–115). Singapore: Springer Singapore. Retrieved from https://doi.org/10.1007/978-981-15-6716-2_6 doi: 10.1007/978-981-15-6716-2_6

Lipczynska, A., Schiavon, S., & Graham, L. T. (2018). Thermal comfort and self-reported productivity in an office with ceiling fans in the tropics. *Building and Environment*, *135*, 202–212. doi: https://doi.org/10.1016/j.buildenv.2018.03.013

Manavvi, S., & Rajasekar, E. (2020). Estimating outdoor mean radiant temperature in a humid subtropical climate. *Building and Environment*, *171*, 106658. doi: https://doi.org/10.1016/j.buildenv.2020.106658

Mendieta, O., García, M., Peña, A., & Rodríguez, J. (2016). *Las buenas prácticas de manufactura en la producción de panela* (1st ed.; Corpoica, Ed.). Mosquera (Colombia).

Ministerio de Agricultura y Desarrollo Rural. (2018). Cadena Agroindustrial De La Panela. *El Renacer del Campo*, 2018.

Ministerio de Agricultura y Desarrollo Rural. (2019). *Cadena agroindustrial de la panela.*

Ministerio de Protección Social. (2006). *Resolución Número 779 de 2006.* Retrieved from https://fedepanela.org.co/gremio/descargas/resolucion-779-de-2006/

Ministerio de Protección Social. (2008). *Resolución Número 3462 de 2008.* Retrieved from https://fedepanela.org.co/gremio/descargas/resolucion-3462-de-2008/

Ministerio de Protección Social. (2009). *Resolución Número 3544 de 2009.* Retrieved from https://fedepanela.org.co/gremio/descargas/resolucion-3544-de-2009/

Ministerio de Trabajo y Seguridad Social. (1979). *RESOLUCIÓN 2400 DE 1979.* BOGOTÁ, D.C.. Retrieved from https://minvivienda.gov.co/sites/default/files/normativa/2400 - 1979.pdf

Ministério do Trabalho e Previdência. (2021). *Portaria n.º 426 de 07 de outubro de 2021.* Retrieved from https://www.gov.br/trabalho-e-previdencia/pt-br/composicao/orgaos-espec

ificos/secretaria-de-trabalho/inspecao/seguranca-e-saude-no-trabalho/sst-portarias/2021/portaria-mtp-no-426-anexos-i-vibracao-e-iii-calor-da-nr-09.pdf (Anexo 3)

Mobtaker, H. G., Ajabshirchi, Y., Ranjbar, S. F., & Matloobi, M. (2019). Simulation of thermal performance of solar greenhouse in north-west of iran: An experimental validation. *Renewable Energy*, *135*, 88–97.

Mujica, M., Guerra, M., & Soto, N. (2008). Efecto de la variedad, lavado de la caña y temperatura de punteo sobre la calidad de la panela granulada. *Interciencia*, *33*, 598–603.

OLIVEIRA, B. F. A., Silveira, I. H., Feitosa, R. C., Horta, M. A. P., Junger, W. L., & Hacon, S. (2019). Human heat stress risk prediction in the brazilian semiarid region based on the wet-bulb globe temperature. *Anais da Academia Brasileira de Ciências*, *91*. doi: https://doi.org/10.1590/0001-3765201920180748

Orlov, A., Daloz, A. S., Sillmann, J., Thiery, W., Douzal, C., Lejeune, Q., & Schleussner, C. (2021). Global economic responses to heat stress impacts on worker productivity in crop production. *Economics of Disasters and Climate Change*, *5*(3), 367–390. doi: https://doi.org/10.1007/s41885-021-00091-6

Osorio, G. (2007). *Manual: Buenas Prácticas Agrícolas -BPA- y Buenas Prácticas de Manufactura -BPM-en la Producción de Caña y Panela.* (Primera ed.). FAO.

Parkes, M. G., Azevedo, D. L., Domingos, T., & Teixeira, R. F. (2022). Narratives and benefits of agricultural technology in urban buildings: A review. *Atmosphere*, *13*(8), 1250.

Rao, G. P., & Singh, P. (2022). Value Addition and Fortification in Non-Centrifugal Sugar (Jaggery): A Potential Source of Functional and Nutraceutical Foods. *Sugar Tech*, *24*(2), 387–396. Retrieved from https://doi.org/10.1007/s12355-021-01020-3 doi: 10.1007/s12355-021-01020-3

Rodriguez, G., Garcia, H., Roa, Z., & Santacoloma, P. (2004). Producción de panela como estrategia de diversificación en la generación de ingresos en áreas rurales de América Latina Producción de panela como estrategia de diversificación en áreas rurales de America Latina. *FAO*, 98.

Rozo, T. (2013). *Manual técnico de buenas prácticas de manufactura (BPM) para el proceso tecnológico de producción de panela.* Retrieved from https://www.onfandina.com/images/Publicaciones/Panela_/Manual Técnico BPM Trapiches.pdf

Saberian, A., & Sajadiye, S. M. (2019). The effect of dynamic solar heat load on the greenhouse microclimate using cfd simulation. *Renewable Energy*, *138*, 722–737. doi: https://doi.org/10.1016/j.renene.2019.01.108

Sadiq, L. S., Hashim, Z., & Osman, M. (2019). The impact of heat on health and productivity among maize farmers in a tropical climate area. *Journal of environmental and public health*, *2019*. doi: https://doi.org/10.1155/2019/9896410

Salehi, F. (2020). Recent applications and potential of infrared dryer systems for drying various agricultural products: A review. *International Journal of Fruit Science*, *20*(3), 586–602. doi: https://doi.org/10.1080/15538362.2019.1616243

Samet, J. M., Marbury, M. C., & Spengler, J. D. (1987). State of Art: Indoor Air Pollution. *The American Review of Respiratory Disease*(136), 1486–1508.

Shrivastava, A., & Singh, P. (2020, 12). Jaggery (gur): The ancient indian open-pan non-centrifugal sugar. In (p. 283-307). doi: 10.1007/978-981-15-6663-9_19

Stull, R. (2011). Wet-bulb temperature from relative humidity and air temperature. *Journal of Applied Meteorology and Climatology*, *50*(11), 2267–2269. doi: 10.1175/JAMC-D-11-0143.1

Takakura, J., Fujimori, S., Takahashi, K., Hijioka, Y., & Honda, Y. (2019). Site-specific hourly resolution wet bulb globe temperature reconstruction from gridded daily resolution climate variables for planning climate change adaptation measures. *International journal of biometeorology*, *63*(6), 787–800. doi: https://doi.org/10.1007/s00484-019-01692-3

Tarazona Parra, G. A. (2011). *Manejo fotosanitario del cultivo de caña panelera - Medidas para la temporada invernal*. BOGOTÁ, D.C..

Tarigan, E. (2018). Mathematical modeling and simulation of a solar agricultural dryer with back-up biomass burner and thermal storage. *Case studies in thermal engineering*, *12*, 149–165.

Tong, X., Hong, S.-W., & Zhao, L. (2019). Cfd modelling of airflow pattern and thermal environment in a commercial manure-belt layer house with tunnel ventilation. *Biosystems engineering*, *178*, 275–293. doi: https://doi.org/10.1016/j.biosystemseng.2018.08.008

Tran, V. T., Duong, Y. H., & Le, T. M. (2021). The influence of meshing strategies on the numerical simulation of solar greenhouse dryer. In *Iop conference series: Earth and environmental science* (Vol. 947, p. 012007).

Tu, J., Yeoh, G. H., & Liu, C. (2018). *Computational fluid dynamics: a practical approach*. Butterworth-Heinemann.

Tun, A. (2019). Review of the specific heat of food models. (3), 82–86. doi: https://doi.org/10.17586/1606-4313-2019-18-3-82-86

Tyagi, S., Kamboj, S., Himanshu, Tyagi, N., Narayanan, R., & Tyagi, V. (2022). Technological advancements in jaggery-making processes and emission reduction potential via clean combustion for sustainable jaggery production: An overview. *Journal of Environmental Management*, *301*, 113792. Retrieved from https://www.sciencedirect.com/science/article/pii/S0301479721018545 doi: https://doi.org/10.1016/j.jenvman.2021.113792

Velásquez, F., Espitia, J., Mendieta, O., Escobar, S., & Rodríguez, J. (2019). Non-centrifugal cane sugar processing: A review on recent advances and the influence of process variables on qualities attributes of final products. *Journal of Food Engineering*,

255(November 2018), 32–40. doi: 10.1016/j.jfoodeng.2019.03.009

Villagrán-Munar, E. A., & Bojacá-Aldana, C. R. (2019). Determination of the thermal behavior of a colombian hanging greenhouse applying cfd simulation. *Revista Ciencias Técnicas Agropecuarias*, *28*(3), 1–10.

Weerawatanakorn, M., Asikin, Y., Takahashi, M., Tamaki, H., Wada, K., Ho, C.-T., & Chuekittisak, R. (2016). Physico-chemical properties, wax composition, aroma profiles, and antioxidant activity of granulated non-centrifugal sugars from sugarcane cultivars of Thailand. *Journal of Food Science and Technology*, *53*(11), 4084–4092. Retrieved from https://doi.org/10.1007/s13197-016-2415-5 doi: 10.1007/s13197-016-2415-5

Xie, Q., Ni, J.-Q., Bao, J., & Su, Z. (2019). A thermal environmental model for indoor air temperature prediction and energy consumption in pig building. *Building and Environment*, *161*, 106238. doi: https://doi.org/10.1016/j.buildenv.2019.106238

Xu, H. J., Xing, Z. B., Wang, F., & Cheng, Z. (2019). Review on heat conduction, heat convection, thermal radiation and phase change heat transfer of nanofluids in porous media: Fundamentals and applications. *Chemical Engineering Science*, *195*, 462–483.

Yaciuk, G. (1981). 24 - solar crop drying. In A. JANZEN & R. SWARTMAN (Eds.), *Solar energy conversion ii* (p. 377-396). Pergamon. Retrieved from https://www.sciencedirect.com/science/article/pii/B9780080253886500490 doi: https://doi.org/10.1016/B978-0-08-025388-6.50049-0

Yoshida, S., Yoshida, A., & Kinoshita, S. (2020). Chapter 5 - evaluation methods of adaptation cities. In H. Takebayashi & M. Moriyama (Eds.), *Adaptation measures for urban heat islands* (p. 115-159). Academic Press. doi: https://doi.org/10.1016/B978-0-12-817624-5.00005-1

Zhang, Y., Yasutake, D., Hidaka, K., Kitano, M., & Okayasu, T. (2020). Cfd analysis for evaluating and optimizing spatial distribution of co2 concentration in a strawberry greenhouse under different co2 enrichment methods. *Computers and Electronics in Agriculture*, *179*, 105811. doi: https://doi.org/10.1016/j.compag.2020.105811

Zhou, B., Wang, X., Mondaca, M. R., Rong, L., & Choi, C. Y. (2019). Assessment of optimal airflow baffle locations and angles in mechanically-ventilated dairy houses using computational fluid dynamics. *Computers and Electronics in Agriculture*, *165*, 104930. doi: https://doi.org/10.1016/j.compag.2019.104930

2. Hygrometry simulation for a Non-Centrifugal Cane Sugar Factory in Caparrapí, Colombia

Abstract

NCS production is an important economic and social factor for rural families who subsist with this activity. In Colombia, the implementation of industrial factories, called "Centrales" has attempted to improve economy for people who do this activities without technification. Nevertheless, the characteristics of the factories show ventilation problems, generating risks for the workers and the product. Therefore, the objective of this study was to analyze the current situation of the work place and propose an alternative to improve the ventilation systems, through a Computational Fluid Mechanics (CFD) model. Results show that the proposed treatment creates a favorable environment for workers just as much for the NCS product.

2.1. Introduction

Non-Centrifugal Cane Sugar (NCS) is a traditional sweetener used in several countries all around the world (Jaffé, 2015). It is mainly produced in "trapiches", artisanal constructions where honey extracted from the cane (*Sacharum Officinarum*) is processed in ovens for evaporating the water and poured into molds, to create the final product (Mujica et al., 2008). Nevertheless, in Colombia, NCS production has been attempted to improve with the installation of factories called "Centrales", where the extracted juice from the cane is processed with industrial equipment (Fedepanela, 2019).

In addition to this, NCS is the "second most important agro-industry with social importance, after coffee, with 220000 hectares" in Colombia (Ministerio de Agricultura y Desarrollo Rural, 2018). In addition, for 2014, Colombia completed a total production of 1.338.554 tons, obtaining around 6.4 ton/ha (Mendieta et al., 2016).

Comfortable environments, with adequate temperature, relative humidity and ventilation

are demonstrated to improve productivity levels, and production capacity (Wolkoff et al., 2021; Teixeira et al., 2017). Additionally, previous studies have been conducted to determine heat efficiency and vapor impact in "trapiches" (Espitia et al., 2020; Velásquez et al., 2019), to identify NCS chemical and sensorial characteristics (Jaffé, 2015; Velásquez et al., 2019; Solís-Fuentes et al., 2019). However, industrial NCS factories have not been studied in any of the areas previously mentioned.

In the same way, studies have shown that high relative humidity allows fungal propagation (Pasanen et al., 1993). Also, unhygienic environments favor the growth of bacteria, generating risks for human consumption, due to their resistance to antibiotics (Verma et al., 2012; Singh et al., 2009). Therefore, it is important to guarantee safe production environments for the final product to be stored.

CFD has proven to be an efficient way to calculate and corroborate strategies for agricultural activities, because in most cases "the long-term field measurement can be very costly and time-consuming" (Tong et al., 2019, p. 2). CFD techniques have been vastly applied to poultry production (Cheng et al., 2021; Tong et al., 2019; Dziubata et al., 2020), swine production (Xie et al., 2019; Kim et al., 2019), cattle (Bustos-Vanegas et al., 2019; Zhou et al., 2019), among others.

In Colombia, normativity has been established to guarantee safe environmental conditions for workers, based on the ASHRAE Handbook Fundamentals, formulated by the American Society of Heating Refrigerating and Air Conditioning Engineers (Ashrae, 2017). In addition, the Ministerio de Trabajo y Seguridad Social (1979) established the standard conditions for work buildings to fulfill.

At the moment, the NCS factory, located in Caparrapí, Colombia, maintain high temperature, resulting in discomfort for the workers, due to the nature of the work. Additionally, relative humidity levels are above 90%, resulting in an unsafe environment for the product and dripping. Consequently, the objectives of this article are to model the real conditions of the place through the use of computational tools and propose an optimal ventilation system to improve the worker comfort.

2.2. Materials and methods

2.2.1. Place description and operation

The production place is in the town of Caparrapí, in Cundinamarca, Colombia. The Caparrapí's Cane Honey Factory is located at coordinates 5°20'39"N, 74°29'30"W, with an altitude of 1271 meters over sea level. The zone presents a mean annual temperature of

23°C (IDEAM, 2015b) and precipitation levels between 1500-2500 mm/year distributed in 100-200 days/year (IDEAM, 2015a). Additionally, average relative humidity varies from 18% to 32% (IDEAM, 2015b), and average wind velocity changes from 0.3km/h to 3.2km/h, with predominance of south winds.

Fedepanela (2019) describes NCS production, in industrial proportions in Colombia, as follows: firstly, the extracted cane juice is gathered in a tank with a 10000 litters capacity. Next, the juice passes through a cleaning process of impurities removal, decantation, and salinity stabilization that last 24 hours. Thereafter, the production begins with the evaporation procedure to lower the juice humidity level and reach the molding point, where the highest temperature processes take place.

Once this point is reached, the juice starts being called honey, and it is poured in the molds, where the drying process takes place through natural convection, presenting high temperatures in the handling of the molds. Thereafter, the workers take the product out of the molds and check the allowed weight on each one. Finally, during the package operation, the product is sealed and stored in boxes (Fedepanela, 2019).

2.2.2. Measurement of environmental conditions

To fully understand the factory operation and the temperature's incidence in workers health, some of the workers were interviewed. Therefore, a registration of the labors was made, to determine the impact of the worker positions inside the factory and its proximity to heat emissions systems. Additionally, a record of the main characteristics of the factory was made, to clarify the function of each part of the factory.

To determine the operating conditions, taken as input for the simulation model, photos were taken with a thermographic camera FLIR Thermacam T640. Temperature photos were taken at 1m of distance from the object, following the manual recommendation. Emissivity from close objects was taken into account to correct the obtained values. Nevertheless, temperature was not taken from objects with radiant surfaces. Through this method, the temperature from evaporators, extractors, walls, ceiling and floor was obtained.

Additionally, the cane honey temperature was measured, while it was being processed, to determine the peak ambient temperatures. Figure **2-1**, shows a range of the measured data from 22°C to surfaces with temperatures above 153°C in the production.

On the other hand, in order to validate the CFD models, data was gathered through manual measures with a heat stress WBGT meter Extech Model HT30. For this purpose, a point

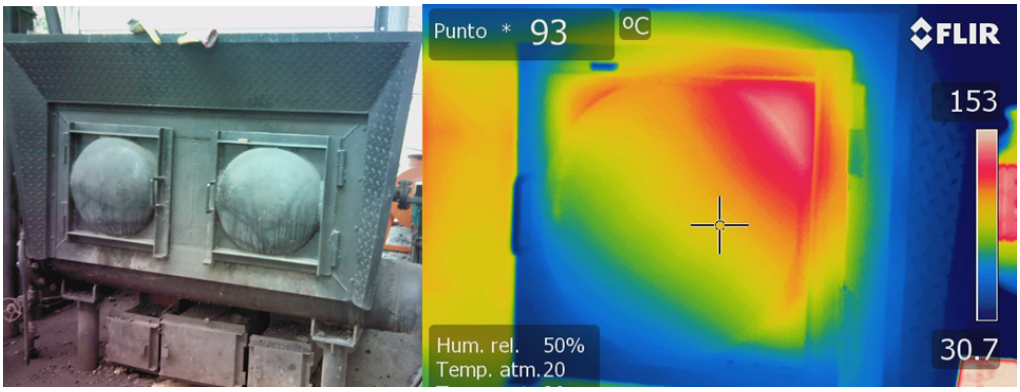

(a) Coal-fired heating system

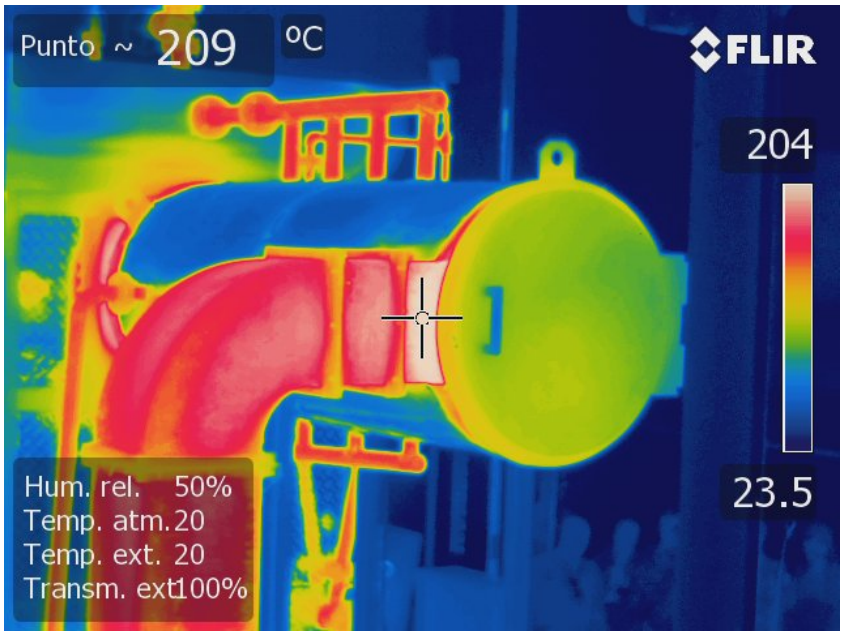

(b) Molding table with cane honey recently poured

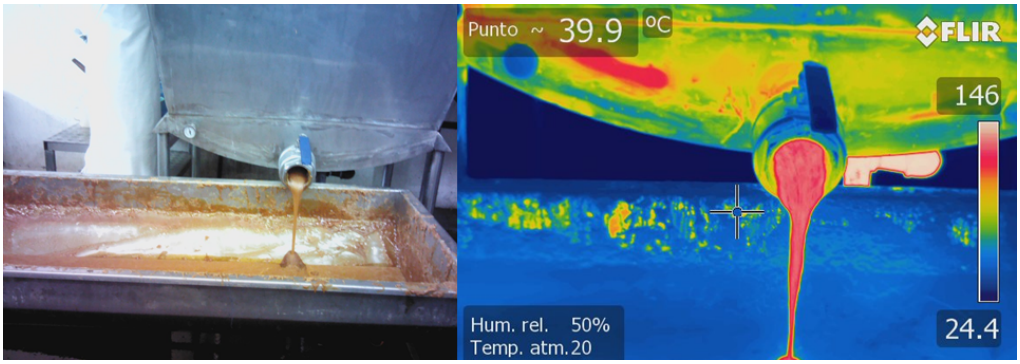

(c) Pouring of the NCS juice in to the honey pans

Figure 2-1.: Measure of working places in Caparrapí's Cane Honey Factory.

cloud was made (Figure **2-2**), where three points were placed in the packaging area (red area), fourteen points were located in the weighing area (green area), twenty-eight points in the molding area (blue area) and eighteen points in the evaporation area (yellow area).

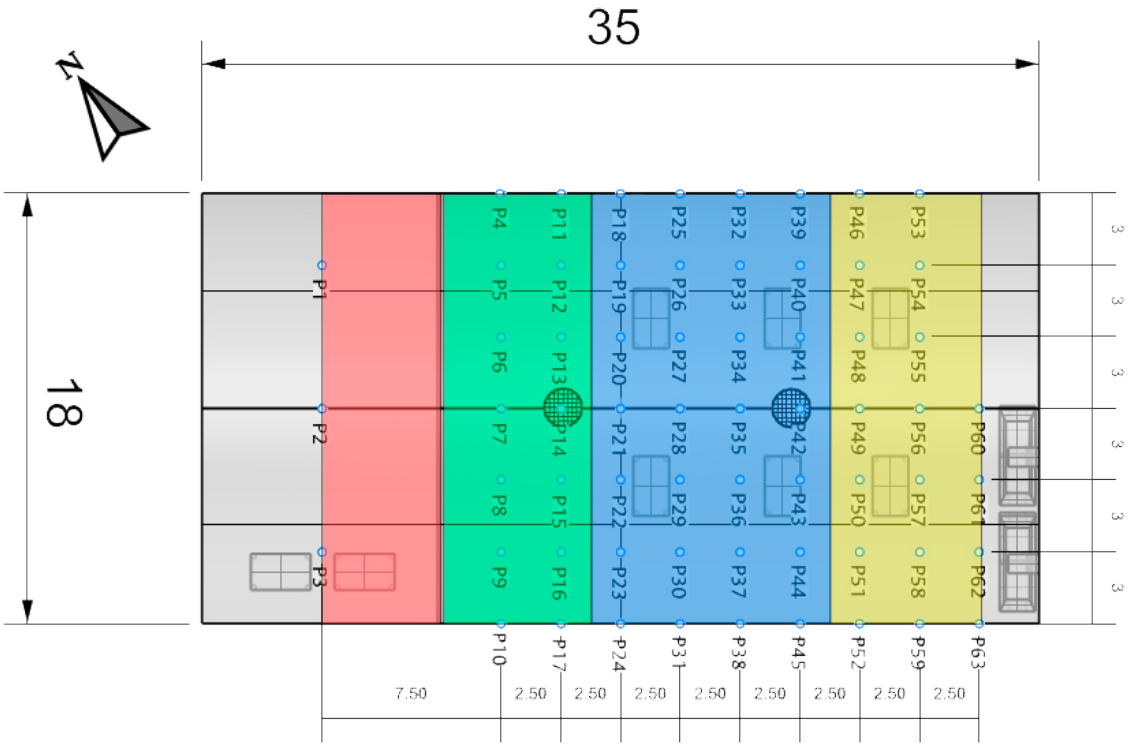

Figure 2-2.: Measure points inside the factory, classified in areas, m.

For each point, variables of temperature, relative humidity, globe temperature, and WBGT index were obtained. These measures were taken at 0.9 m and 1.5 m, due to the height of the work tables and the mean height of the hypothalamus for an average Colombian worker (Swaab et al., 1992; Durán et al., 2016), respectively. Additionally, external conditions for the same variables were measured in three different points, randomly selected, at the beginning and end of each work shift.

Measures were taken before and after the installation of an extractor above the evaporation area. For the first situation, data was gathered in intervals of two hours, from 7 a.m. to 9 a.m., from 9a.m. to 11 a.m and 11 a.m. to 1 p.m. After the installation of the extractors, new data were obtained for comparison in intervals of one hour, from 7 a.m. to 5 p.m., not including lunch break for the workers.

2.2.3. Simulation process

The geometry was designed in the software Rhinoceros 7®, based on the original blueprints (Fedepanela, 2019). Nevertheless, changes were applied after the record of the previously mentioned factory characteristics, to create a model closer to the real conditions of the place. In addition to that, tables were represented fixed to the floor, at their most used position, to avoid errors during the simulation.

Meshes are generated to create the points where equations are evaluated, by "discretizing the space" (Lintermann, 2021). Firstly, the mesh generated for this simulation was designed through a top-down meshing technique, called Octree, where each big area is fragmented into smaller parts. Additionally, a smoothing method was applied, with a bottom-up meshing system, where remaining unnecessary parts are joined together.

The computational model uses the finite volume technique to calculate pressure, temperature, and air velocity variables for each one of the elements, applying the Navier-Stokes equations, due to the complexity of the system (Osorio et al., 2016). Continuity, mass, and energy were calculated by solving the simplified equations (2-1 and 2-2) for steady state calculations for non-isothermal fluids. Additionally, Equation 2-3 is the stress tensor corresponding to Newtonian fluids (Rocha et al., 2013; Osorio-Hernandez et al., 2020).

$$\nabla \cdot (\rho \vec{v}) = 0 \tag{2-1}$$

$$\nabla \cdot (\rho \vec{v} \vec{v}) = \nabla P + \left[\mu_t (\nabla \vec{v} + \nabla \vec{v}^T)\right] \tag{2-2}$$

$$\nabla \cdot (-k \nabla T + \rho \cdot C_p T \vec{v}) = 0 \tag{2-3}$$

Where:

ρ is the fluid density (kg/m^3).

$\vec{v}$ is the velocity vector.

P is the absolute pressure of the location (Pa).

μ_t is the dynamic viscosity of the fluid (kg m^{-1} s^{-1}).

T is temperature (K).

k is thermal conductivity (W m^{-1} K^{-1}).

C_p is specific heat (W kg^{-1} K^{-1}).

On the other hand, to calculate the value of relative humidity, due to vapor interaction inside as a result of the evaporation processes, for each element in the model, Equations 2-4 to 2-7 were used, according to the information reported by Junzeng et al. (2012) and Murray (1967).

$$RH = \frac{e * 100}{e_s} \tag{2-4}$$

$$e = e_{sh} - AP(T - T_{bh}) \tag{2-5}$$

$$e_s = 6.107 \cdot 10^{\left(\frac{7.5 \cdot T_{bh}}{237.3 + T_{bh}}\right)} \tag{2-6}$$

$$e_{sh} = 6.107 \cdot 10^{\left(\frac{7.5 \cdot T}{237.3 + T}\right)} \tag{2-7}$$

Where:

RH is the relative humidity (%).

e is the partial pressure exerted by water vapor (hPa).

e_s is the saturation pressure at dry-bulb temperature (hPa).

A is the psychrometer constant for aired and non-aired psychrometers (constant).

P is the absolute pressure of the location (Pa).

T is dry-bulb temperature (°C).

T_{bh} is wet-bulb temperature (°C).

Turbulence was calculated by the standard k-Epsilon model, due to its utility to "handle various fluid flow conditions", by the comparison between kinetic energy and its dissipation (Mishra & Aharwal, 2018, p. 5). Additionally, the criteria used to determine model convergence was mean square error lower than $1 \cdot 10^{-4}$ for all variables.

Figure **2-3** shows the NCS factory distribution. The building is divided in two parts, to separate the processed NCS from the manufacturing area. The first zone is the packaging area, it contains tables where panela is wrapped through a thermo-sealing process. On the other hand, in the manufacturing area, the evaporation, molding and cooling processes are executed. Also, the first four windows from back to front of the factory, are openings with a filter in them. Contrary to the remaining three windows (back to front), which are made of glass.

The dimensions of the factory are: 18m x 35m x 10.55m, to the top of the ceiling, as shown in Figure **2-2**. The walls are made of plastered brick cladding, windows are singled glazed, the

ceiling is made of fiber cement and the openings have a filter, assumed opened all the time. Table **2-1** shows the heat transfer coefficient of the materials previously listed. Windows dimensions are 2m x 1.1 m.

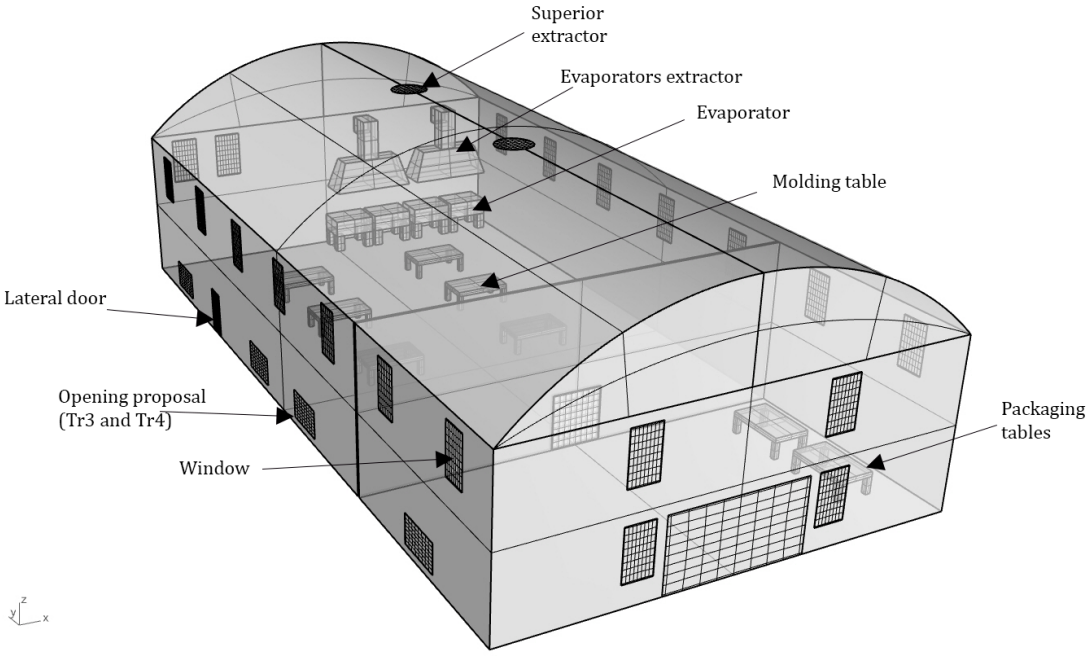

Figure 2-3.: Geometry of the NCS factory located in Caparrapí, Colombia.

Table 2-1.: Properties of the materials of the factory

Material	Heat Transfer Coefficient $W \cdot m^{-2}K^{-1}$
Plastered brick cladding	2.3
Glass (Windows)	6
Fiber Cement	80

Due to the nature of the external conditions present in the factory, 4 treatments were done, to determine the conditions for every change inside the factory. The description for all treatments is described in detail in Table **2-2**.

Table 2-2.: Boundary conditions used for the CFD models.

Source		Description
Treatment 1	CFD Model based on data from February 2022	Initial condition. The created model was based on the data gathered during February 2022. At that moment, no extractors were operating inside the factory. Due to the production dynamics, information was collected only for 7 a.m., 9a.m. and 11a.m. work shifts. Environmental conditions for the production day were measured and assigned as initial values.
Treatment 2	CFD Model based on data from September 2022	Control condition. The created model was based on the data gathered during September 2022. Data were collected during this period, after the installation of an extractor, above the evaporator system, for a critical production day. Environmental conditions for the production day were measured and assigned as initial values.
Treatment 3	CFD Proposed Model	Alternative proposition 1. Lateral openings were proposed, for natural ventilation. All other conditions from Treatment 2 were used.
Treatment 4	CFD Proposed Model	Alternative proposition 2. Mechanical ventilation was added to the openings, with heating and cooling systems. All other conditions from Treatment 3 were used.

Each simulation was run to determine temperature, relative humidity and wet-bulb temperature, for the factory conditions. Furthermore, simulations were made for work hours at 7a.m., 9a.m. and 11a.m. for both scenarios to compare the impact of the extractor installation over the ambient conditions. Also, a simulation was run for the most critical period of time (2p.m. and 3p.m.), after the installation of the extractor (September 2022). Data were not gathered for the evening shifts (2p.m. and 3p.m.) due to labor conditions at the moment of data collection.

The reference values used for the research were obtained from the results obtained from Wolkoff et al. (2021); Varela-Aldás et al. (2020) who show that constant temperature levels above 24∘C, combined with hard labor work can create health problems for workers, when done for extended periods of time, combined with relative humidity superior to 85% lead to "dehydration, dizziness, and even skin troubles (...) caused by physical discomfort, fatigue, loss of psycho-motor performance, concentration and reduced alertness getting dangerous for the health of workers, even putting them at risk of death" (Varela-Aldás et al., 2020, p. 460).

2.2.4. Model validation

Simulations were validated through the determination of the Normalized Mean Square Error (Equation 2-8), by comparing the obtained results with those determined experimentally. Moreover, the comparison of the average conditions was determined by a variance analysis ($P< 0.001$) and a Tukey test with 5% probability, according to the procedure established by the American Society for Testing Materials(ASTM, 2002).

$$NMSE = \frac{1}{n}\sum_{i=1}^{n}\frac{(Y_{pi} - Y_{mi})^2}{Y_{pi}\cdot Y_{mi}} \tag{2-8}$$

Where:

Y_{pi} are predicted values.

Y_{mi} are measured values.

Furthermore, a study was conducted to analyze the propagation of errors resulting from equipment precision. The purpose of this analysis was to investigate whether this factor has an impact on the research findings.

2.3. Results and discussion

Due to the nature and size of the model, an unstructured mesh was designed (Figure **2-4**), following the methodology presented by Alfarawi et al. (2021). The resulting model has 128236 elements, and a total of 34453 nodes. Additionally, the mesh quality was verified through a test, where only 5% of the generated elements had a quality inferior to 0.5.

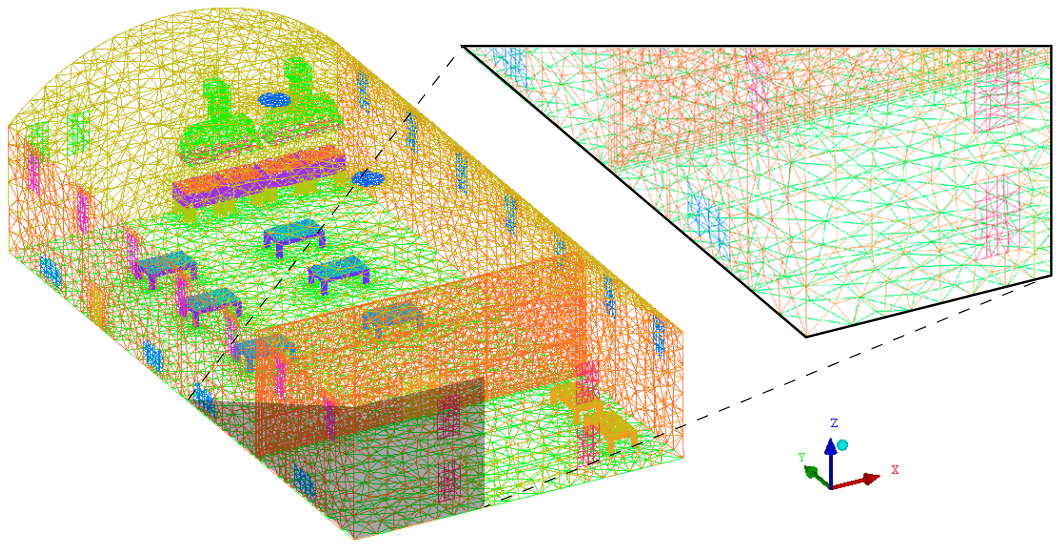

Figure 2-4.: Computed mesh for Caparrapí's Cane Honey Factory model

To determine the concordance of the model, NMSE was established for a maximum value of 0.25. Table **2-3** shows a comparison between the mean of the experimental data and the mean obtained from the simulation data, showing similitude in all values. Additionally, Table **2-4** shows the obtained values for the NMSE test, having a maximum value of 0.0266, demonstrating that the model represents reality accurately.

Table 2-3.: Comparison of simulated and measured data for Temperature (T) and Relative Humidity(T)

February (Tr1)				
	Experimental T [°C]	CFD Model T [°C]	Experimental RH [%]	CFD Model RH [%]
7a.m.	22.82	23.12	81.87	87.65
9a.m.	24.01	24.02	79.94	77.33
11a.m.	23.06	23.85	80.27	81.97
2p.m.	-	-	-	-
3p.m.	-	-	-	-
September (Tr2)				
	Experimental T [°C]	CFD Model T [°C]	Experimental RH [%]	CFD Model RH [%]
7a.m.	20.60	20.79	92.29	92.07
9a.m.	22.81	22.06	81.09	81.53
11a.m.	25.10	24.96	73.59	72.85
2p.m.	26.71	26.73	66.47	68.02
3p.m.	27.18	25.30	63.04	62.98

Table **2-5** shows the statistical analysis done for each one of the treatments. For the 7a.m. work shift, all four treatments behave differently, due to the differences between the obtained mean values, showing a lower temperature in treatment 3, for which the maximum temperature is 23.41°C. Thus, suggesting that natural ventilation can have a positive impact on the conditions present in the morning inside the factory. Nevertheless, treatment 4 presents a higher temperature, because of the proposed alternative for heating the air in morning work shifts (Figure **2-6**f).

Table 2-4.: NMSE values for Temperature (T) and Relative Humidity (RH) variables

	February (Tr1)		September (Tr2)	
	T	HR	T	HR
7a.m.	0.0042	0.0065	0.0032	0.0014
9a.m.	0.0034	0.0110	0.0029	0.0006
11a.m.	0.0080	0.0191	0.0008	0.0148
2p.m.			0.0006	0.0266
3p.m.			0.0079	0.0266

On the other hand, for the 2p.m. work shift, treatment 2 and 3 show a similar behavior, having a difference of less than 1°C. In contrast to this result, treatment 4 presents a mean temperature of 24°C, with a maximum of 26.17°C, near to the evaporator area, as shown in Figure **2-6**. Additionally, as a result of the mean temperature lower than 25°C, the health

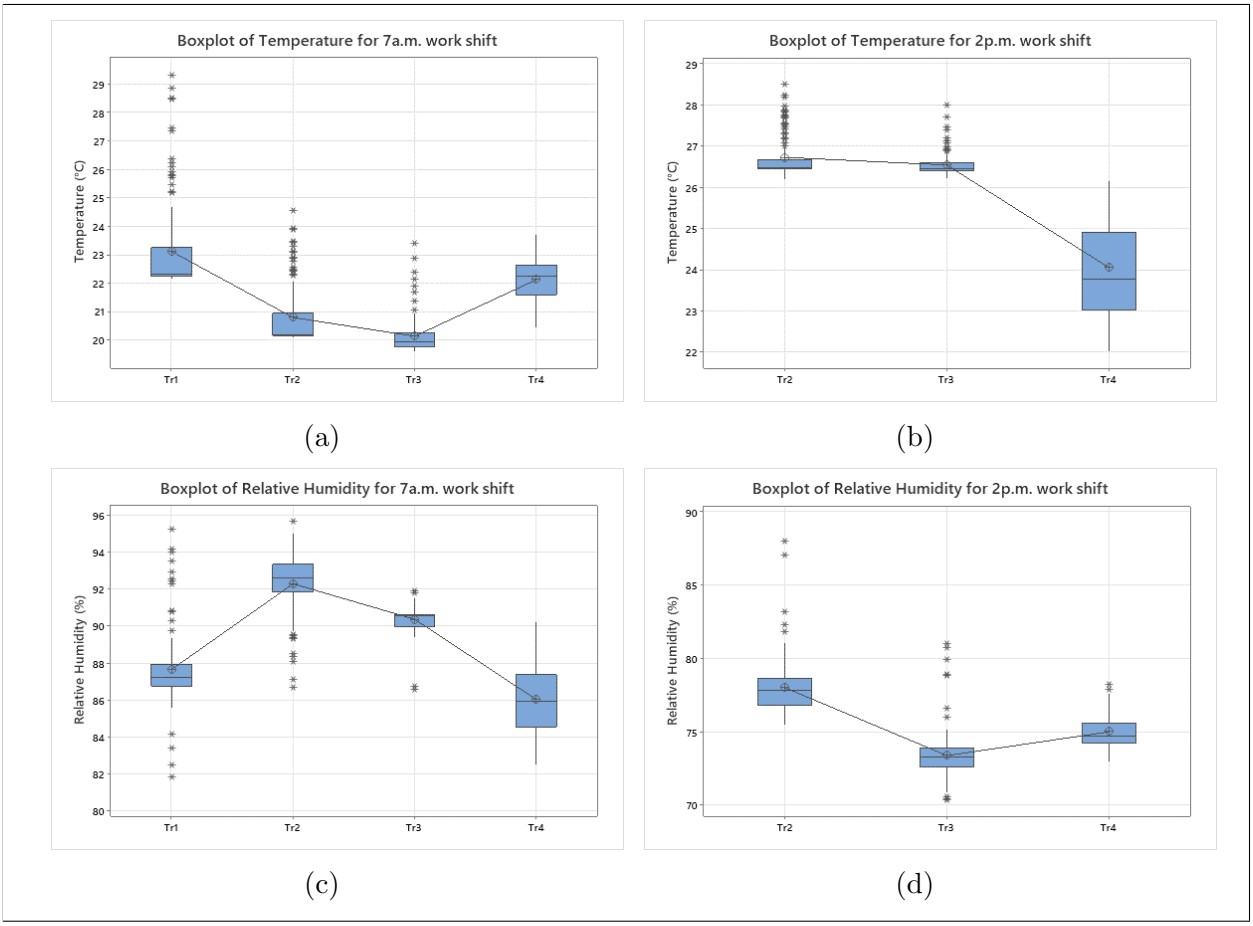

Figure 2-5.: Boxplot graphics of temperature and relative humidity for different work shifts. (a) Temperature for 7a.m. work shift. (b) Temperature for 2p.m. work shift. (c) Relative humidity for 7a.m. work shift. (d) Relative humidity for 2p.m. work shift.

of the workers would not be affected by high temperature exposure (Cai, Lu, & Wang, 2018).

To observe the data distribution, Figure **2-5** shows the boxplot analysis for temperature (Figures **2-5**a and **2-5**b) and relative humidity (Figures **2-5**c and **2-5**d) for treatments 1 to 4. Treatment 1 is not included in the results for 2p.m. work shifts, because the data could not be completely gathered during the first data collection. From the results it can be inferred that treatments 3 and 4 reduce temperature levels inside the factory. Furthermore, it can be seen that data dispersion and extreme values decrease with the implementation of treatment 4. Also, for 7a.m., temperature medians are higher than 22°C for treatment 1 and 4, and closer to 20°C for treatments 2 and 3.

Table 2-5.: Statistical information of temperature for each treatment in 7a.m. and 2p.m. work shifts (°C).

7 a.m.					
Factor	**N**	**Mean**	**Min**	**Max**	**StDev**
$Tr1^A$	126	23.12	22.18	29.35	1.62
$Tr4^B$	126	22.12	20.43	23.72	1.10
$Tr2^C$	126	20.79	20.08	24.58	0.63
$Tr3^D$	126	20.14	19.60	23.41	0.70
2 p.m.					
Factor	**N**	**Mean**	**Min**	**Max**	**StDev**
$Tr2^A$	126	26.73	26.20	28.52	0.52
$Tr3^A$	126	26.55	26.22	28.01	0.28
$Tr4^B$	126	24.05	22.00	26.17	1.22

StDev: Standard Deviation. Treatments followed by the same letters do not differ by the Tukey's test at 0.05. Probability for 7a.m. (P=0.0001, F=192.11). Probability for 2p.m. (P=0.0001, F=460.49)

For relative humidity, data show a smaller variation in its values inside the factory with treatments 3 and 4, as shown in Figures **2-5**c and **2-5**d. Additionally, in the case of relative humidity mean values show a decrease when temperature increases, agreeing with Rocha et al. (2013); Osorio-Hernandez et al. (2020) in cases of coffee installations. Also, median values for treatment 1 and 4 are below 88%, whereas for treatment 2 and 3 the value is closer to 92%, indicating high relative humidity levels for this work shifts, even after the application of the treatments.

Table **2-5** shows the statistical temperature data obtained from the CFD simulations, for the established points (Figure **2-3**). For 7a.m., it is possible to observe that all treatments present statistical difference. For this hour, treatment 1 presents the highest temperature levels, contrasting with treatment 3, where the lowest temperature was obtained, due to the addition of a ventilation system, agreeing with Wolkoff et al. (2021). Additionally, treatment 4 shows a higher temperature level, due to the pre-heating factor described previously.

For 2p.m. work shift, treatments 2 and 3 are part of the same group, indicating similitude between their mean values. This can be caused because the ventilation openings don't guarantee enough air movement and the external air temperature is too high (Wolkoff et al., 2021), showing that the working conditions generate stress for the workers. Additionally, treatment 4 presents a temperature close to 24°C, guaranteeing the limit temperature for a

comfortable environment for workers.

Figure **2-6** shows the environmental temperature inside the NCS factory, for work shifts of 7a.m. and 2p.m. Computational Fluid Dynamic results for 9a.m., 11a.m. and 3p.m. are displayed in Appendix A. Generally speaking, temperature for all work shifts decreased from treatment 1 to treatment 4, showing an improvement in the overall conditions.

Treatment 1 (Figure **2-6**a) shows temperature varying from 22 to 30°C, with a strong increase close to the surroundings of the evaporators. These ambient conditions can cause health problems in workers, when exposed during prolonged periods of time (Taylor, 2006). Additionally, for treatments 2 (Figure **2-6**b), 3 (Figure **2-6**d) and 4 (Figure **2-6**f), at 7a.m., show a constant temperature value, with small increases in the evaporation area.

On the other hand, temperatures from 2p.m. shift (Figure **2-6**) show temperatures over 28°C, with a small decrease for the incorporation of natural ventilation in treatment 3 (Figure **2-6**e), result that agrees with Rocha et al. (2013). Also, treatment 4 (Figure **2-6**g) guarantees a temperature reduction, under 25 °C, providing a more comfortable ambient for the workers, compared to treatment 2 (Figure **2-6**c).

Temperature profiles obtained for 9a.m., 11a.m. and 3 p.m. (Appendix A) show a similar pattern, where treatments 2 and 3 present values of temperature alike, with a bigger temperature decrease for treatment 4. Hence, it is possible to observe that 7a.m. and 2p.m. work shifts present the most critical values.

Relative humidity obtained from the CFD simulations (Table **2-6**) show statistical difference for all treatments, obtaining lower results for treatments 3 and 4. Therefore, along with low air velocities, it can be observed that the conditions for treatment 1 and 2 create the ideal environment for fungus and bacteria to grow (Pasanen et al., 1993; Bakker et al., 2020), causing health problems and deterioration of the product (Jaffé, 2015; Zidan & Azlan, 2022).

7a.m. work shift presents the higher relative humidity values, compared to 2p.m., due to the natural conditions, close to dawn. Furthermore, 7a.m. work shift show mean values higher than 85%, specially in treatment 2, whereas 2p.m. does not reflect values superior to 88.05%, due to the high environmental temperatures during the day, in accordance to the information presented by Osorio-Hernandez et al. (2020); Espitia et al. (2020). Increasing ventilation inside the factory can contribute to further reduce relative humidity (Kolokotroni & Littler, 1995).

With the present temperature and relative humidity conditions, condensation levels can cause dripping (Jeong et al., 2010; Yin et al., 2014), when reaching the dew point temperature of

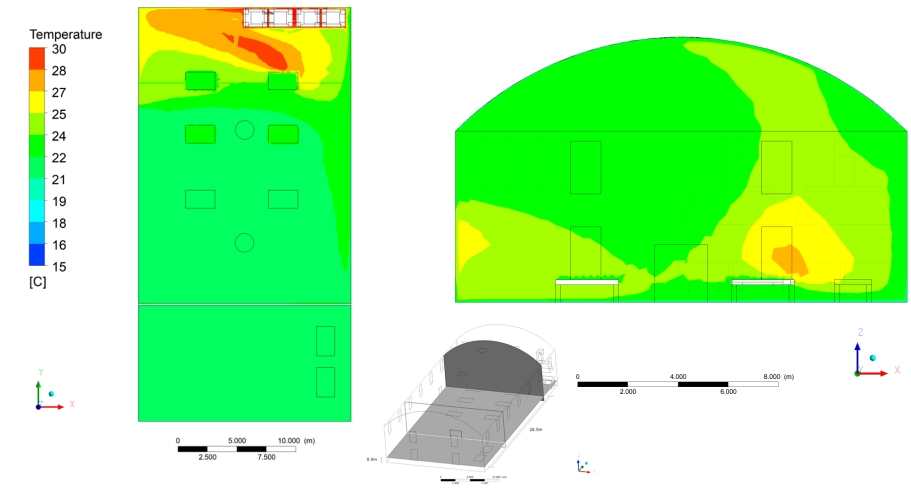

(a) Treatment 1 at 7a.m.

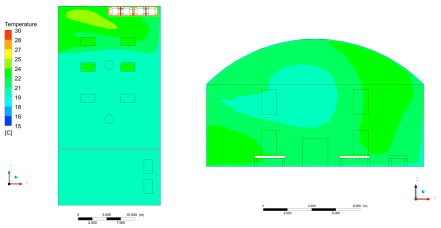

(b) Treatment 2 at 7a.m.

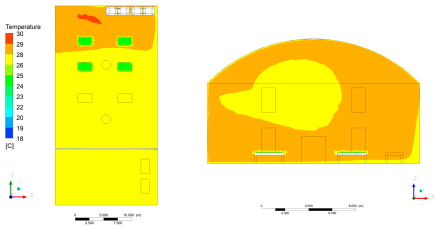

(c) Treatment 2 at 2p.m.

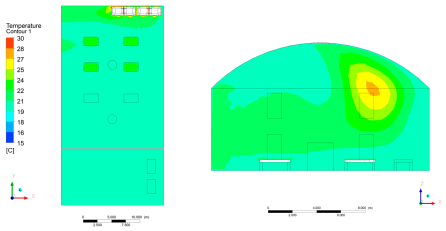

(d) Treatment 3 at 7a.m.

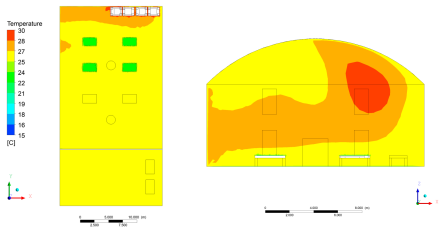

(e) Treatment 3 at 2p.m.

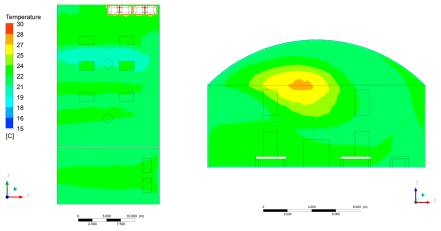

(f) Treatment 4 at 7a.m.

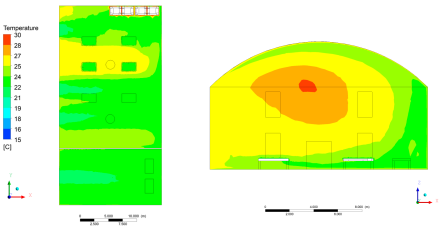

(g) Treatment 4 at 2p.m.

Figure 2-6.: Temperature profiles for treatments 1 to 4

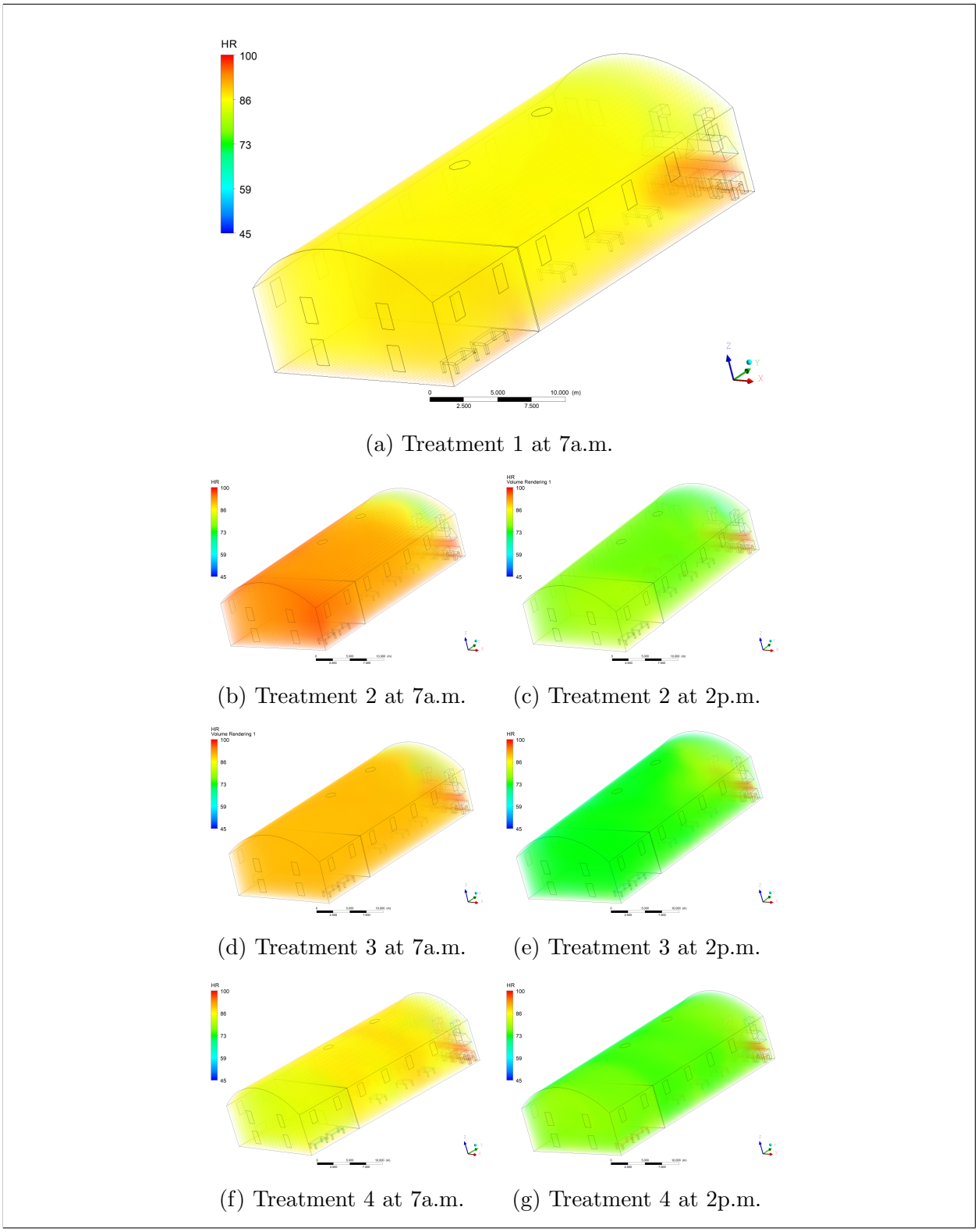

(a) Treatment 1 at 7a.m.

(b) Treatment 2 at 7a.m.

(c) Treatment 2 at 2p.m.

(d) Treatment 3 at 7a.m.

(e) Treatment 3 at 2p.m.

(f) Treatment 4 at 7a.m.

(g) Treatment 4 at 2p.m.

Figure 2-7.: Relative humidity isometric view for treatments 1 to 4

23°C, increasing the risk of damaging the final product by moistening or fungus proliferation (Velásquez et al., 2019; Aguilar-Rivera & Olvera-Vargas, 2021).

Table 2-6.: Statistical information of relative humidity for each treatment in 7a.m. and 2p.m. work shifts (%).

7 a.m.					
Factor	**N**	**Mean**	**Min**	**Max**	**StDev**
$Tr2^{A}$	126	92.29	86.66	95.27	1.95
$Tr3^{B}$	126	90.37	86.58	91.94	1.75
$Tr1^{C}$	126	87.65	81.82	95.27	0.70
$Tr4^{D}$	126	86.03	82.52	90.20	1.73
2 p.m.					
Factor	**N**	**Mean**	**Min**	**Max**	**StDev**
$Tr2^{A}$	126	78.02	75.46	88.05	1.88
$Tr4^{B}$	126	75.00	72.92	78.24	1.74
$Tr3^{C}$	126	73.38	70.31	81.03	1.13

StDev: Standard Deviation. Treatments followed by the same letters do not differ by the Tukey's test at 0.05. Probability for 7a.m. (P=0.0001, F=378.16). Probability for 2p.m. (P=0.0001, F=267.80)

Figure **2-7** shows relative humidity profiles from an isometric view, for treatments 1 to 4. Treatment 1 (Figure **2-7**a) shows a high vapor area, in the proximity of the evaporator, as consequence of the process and lack of extractors in the area. Moreover, treatment 2 at 7a.m. (Figure **2-7**b) displays an increase for the humidity level caused by the evaporators, after the installation of extractors in the area. Nevertheless, it is possible to observe that values above 95% are distributed along the factory, specially in the ceiling. This causes dripping because of condensation, due to the temperature levels, present in the factory, as described before in Table **2-5**.

In addition, it is possible to observe that treatment 3 (Figure **2-7**d) reduces the overall relative humidity approximately 4%, due to the created air flow (Kolokotroni & Littler, 1995), yet not creating favorable conditions to avoid dripping (Jeong et al., 2010). In contrast, treatment 4 (Figure **2-7**f), guarantees a decrease in relative humidity, obtaining a more constant distribution inside the factory, with a maximum value of 90.2%.

On the other hand, for 2p.m. work shift, relative humidity levels show small change for all treatments. Initially, treatment 2 at 2p.m. (Figure **2-7**c) shows relative humidity levels

around 78%, that can cause dripping, due to the high temperatures inside the factory at that hour (Yin et al., 2014). However, treatments 3 and 4 (Figures **2-7**e and **2-7**g, respectively) present relative humidity levels below 75%, having less possibility of dripping.

Relative humidity profiles obtained for 9a.m., 11a.m. and 3 p.m. (Appendix B) show a similar pattern, where treatments 2 and 3 present similar values of relative humidity, with a bigger decrease for treatment 4. Hence, it is possible to observe that 7a.m. and 2p.m. work shifts present the most critical values.

Heat transfer from the environment outside the building influences the inner temperature directly, as shown in the obtained results in Figure **2-6**. In this way, from treatments 1 and 2, it is possible to observe that, due to the solar radiation, heat transfer goes from the exterior to the interior. Additionally, treatment 4 guarantees a change in this condition, because it ensures that air has enough velocity to create convective heat transfer.

2.4. Conclusions

The present study utilizes a Computational Fluids Dynamics technique to create a model that represents reality accurately. In this way, results show a good model approximation of the NCS factory. For instance, the adopted ventilation strategies show a positive impact over the bioclimatic indoor conditions for the NCS product and workers inside the factory.

Additionally, it is possible to observe that heat transfer directly affects the environmental conditions inside the factory, specially through the ceiling. In this way, treatment 4 shows the best alternative to maintain temperature around the limit set.

Treatment 4 showed the best environmental conditions, guaranteeing an increase in temperature during cold work shifts and lowering temperature during hot periods of time. Furthermore, relative humidity levels decreased with this treatment, resulting in less dripping processes and reduce risk of damage in the product, due to the increase in temperature levels, for critical cold hours.

The study showed the importance of air flow inside this type of constructions. In this way, it is advisable to make the proposed changes with the model, to change the inner conditions of the factory. Furthermore, future studies can study ways to improve the heat exchange and air movement for different parts of the factory.

References

Aguilar-Rivera, N., & Olvera-Vargas, L. A. (2021). Innovations for Sustainable Production of Traditional and Artisan Unrefined Non-centrifugal Cane Sugar in Mexico. In *World sustainability series* (pp. 313–330). doi: 10.1007/978-3-030-78825-4_19

Alfarawi, S. S., El-sawi, A., & Omar, H. (2021). Exploring discontinuous meshing for cfd modelling of counter flow heat exchanger. *Journal of Advanced Research in Numerical Heat Transfer*, *5*(1), 26–34.

Ashrae. (2017). *Ashrae handbook fundamentals 2017: Inch-pound edition.* American Society of Heating, Refrigerating and Air-Conditioning Engineers. Retrieved from https://books.google.com.co/books?id=6VhRswEACAAJ

ASTM. (2002). *Guide for statistical evaluation of indoor air quality models (d5157-97).* American Society for Testing Materials. Retrieved from https://www.astm.org/d5157-19.html doi: https://doi.org/10.1520/D5157-19

Bakker, A., Siegel, J. A., Mendell, M. J., Prussin, A. J., Marr, L. C., & Peccia, J. (2020). Bacterial and fungal ecology on air conditioning cooling coils is influenced by climate and building factors. *Indoor air*, *30*(2), 326–334. doi: https://doi.org/10.1111/ina.12632

Bustos-Vanegas, J. D., Hempel, S., Janke, D., Doumbia, M., Streng, J., & Amon, T. (2019). Numerical simulation of airflow in animal occupied zones in a dairy cattle building. *Biosystems Engineering*, *186*, 100–105. doi: https://doi.org/10.1016/j.biosystemseng.2019.07.002

Cai, X., Lu, Y., & Wang, J. (2018). The impact of temperature on manufacturing worker productivity: Evidence from personnel data. *Journal of Comparative Economics*, *46*(4), 889–905. doi: 10.1016/j.jce.2018.06.003

Cheng, Q., Feng, H., Meng, H., & Zhou, H. (2021). Cfd study of the effect of inlet position and flap on the airflow and temperature in a laying hen house in summer. *Biosystems Engineering*, *203*, 109–123. doi: https://doi.org/10.1016/j.biosystemseng.2021.01.009

Durán, P., Merker, A., Briceño, G., Colón, E., Line, D., Abad, V., ... Hagenäs, L. (2016). Colombian reference growth curves for height, weight, body mass index and head circumference. *Acta Paediatrica*, *105*(3), e116-e125. Retrieved from https://onlinelibrary.wiley.com/doi/abs/10.1111/apa.13269 doi: https://doi.org/10.1111/apa.13269

Dziubata, Z., Trokhaniak, V., Rogovskii, I., Titova, L., Luzan, P., & Popyk, P. (2020). Using cfd simulation to investigate the impact of fresh air valves on poultry house aerodynamics in case of a side ventilation system.
doi: https://doi.org/10.35633/inmateh-62-16

Espitia, J., Velásquez, F., López, R., Escobar, S., & Rodríguez, J. (2020). An engineering ap-

proach to design a non-centrifugal cane sugar production module: A heat transfer study to improve the energy use. *Journal of Food Engineering*, *274*, 109843. Retrieved from https://www.sciencedirect.com/science/article/pii/S0260877419304868 doi: https://doi.org/10.1016/j.jfoodeng.2019.109843

Fedepanela. (2019). *PROTOCOLO DE TRAZABILIDAD PARA OBTENCIÓN DE PANELA*. BOGOTÁ, D.C.. Unpublished writing.

IDEAM. (2015a). *Mapa de precipitación total anual (mm)*. Cundinamarca, Colombia.

IDEAM. (2015b). *Mapa de temperatura media anual (°c)*. Cundinamarca, Colombia.

Jaffé, W. R. (2015). Nutritional and functional components of non centrifugal cane sugar: A compilation of the data from the analytical literature. *Journal of Food Composition and Analysis*, *43*, 194–202. doi: 10.1016/j.jfca.2015.06.007

Jeong, K., Kessen, M. J., Bilirgen, H., & Levy, E. K. (2010). Analytical modeling of water condensation in condensing heat exchanger. *International Journal of Heat and Mass Transfer*, *53*(11-12), 2361–2368. doi: https://doi.org/10.1016/j.ijheatmasstransfer.2010.02.004

Junzeng, X., Qi, W., Shizhang, P., & Yanmei, Y. (2012). Error of saturation vapor pressure calculated by different formulas and its effect on calculation of reference evapotranspiration in high latitude cold region. *Procedia Engineering*, *28*, 43-48. Retrieved from https://www.sciencedirect.com/science/article/pii/S187770581200690X (2012 International Conference on Modern Hydraulic Engineering) doi: https://doi.org/10.1016/j.proeng.2012.01.680

Kim, R.-w., Kim, J.-g., Lee, I.-b., Yeo, U.-h., & Lee, S.-y. (2019). Development of a vr simulator for educating cfd-computed internal environment of piglet house. *biosystems engineering*, *188*, 243–264. doi: https://doi.org/10.1016/j.biosystemseng.2019.10.024

Kolokotroni, M., & Littler, J. (1995). Effectiveness of extractor fans in reducing airborne moisture in homes. *Indoor Air*, *5*(1), 69-75. Retrieved from https://onlinelibrary.wiley.com/doi/abs/10.1111/j.1600-0668.1995.00011.x doi: https://doi.org/10.1111/j.1600-0668.1995.00011.x

Lintermann, A. (2021). Computational meshing for cfd simulations. In K. Inthavong, N. Singh, E. Wong, & J. Tu (Eds.), *Clinical and biomedical engineering in the human nose: A computational fluid dynamics approach* (pp. 85–115). Singapore: Springer Singapore. Retrieved from https://doi.org/10.1007/978-981-15-6716-2_6 doi: 10.1007/978-981-15-6716-2_6

Mendieta, O., García, M., Peña, A., & Rodríguez, J. (2016). *Las buenas prácticas de manufactura en la producción de panela* (1st ed.; Corpoica, Ed.). Mosquera (Colombia).

Ministerio de Agricultura y Desarrollo Rural. (2018). Cadena Agroindustrial De La Panela. *El Renacer del Campo*, 2018.

Ministerio de Trabajo y Seguridad Social. (1979). *RESOLUCIÓN 2400 DE 1979.* BOGOTÁ, D.C.. Retrieved from

https://minvivienda.gov.co/sites/default/files/normativa/2400 - 1979.pdf

Mishra, P., & Aharwal, K. R. (2018, aug). A review on selection of turbulence model for cfd analysis of air flow within a cold storage. *IOP Conference Series: Materials Science and Engineering*, *402*(1), 012145. doi: https://dx.doi.org/10.1088/1757-899X/402/1/012145

Mujica, M., Guerra, M., & Soto, N. (2008). Efecto de la variedad, lavado de la caña y temperatura de punteo sobre la calidad de la panela granulada. *Interciencia*, *33*, 598–603.

Murray, F. W. (1967). On the computation of saturation vapor pressure. *Journal of Applied Meteorology and Climatology*, *6*(1), 203 - 204. doi: https://10.1175/1520-0450(1967)006<0203:OTCOSV>2.0.CO;2

Osorio, J. A., Ferreira, I. d. F., Olivera, K. S., Barreto, L., & Norton, T. (2016, 01). A CFD based approach for determination of ammonia concentration profile and flux from poultry houses with natural ventilation. *Revista Facultad Nacional de Agronomía Medellín*, *69*, 7825 - 7834. doi: http://dx.doi.org/10.15446/rfna.v69n1.54750

Osorio-Hernandez, R., Osorio-Saraz, J., Sullivan-Oliveira, K., Aristizaba, I., & Arango, J. (2020). Computational fluid dynamics assessment of effect of different openings configurations on the thermal environment of a facility for coffee wet processing. *Journal of Agricultural Engineering*, *51*(1), 21–26. doi: 10.4081/jae.2020.892

Pasanen, P., Pasanen, A.-L., & Jantunen, M. (1993). Water condensation promotes fungal growth in ventilation ducts. *Indoor Air*, *3*(2), 106–112. doi: https://doi.org/10.1111/j.1600-0668.1993.t01-2-00005.x

Rocha, D. K. S. O., Martins, J. H., Martins, M. A., Saraz, J. A. O., & Filho, A. F. L. (2013). Three-dimensional modeling and simulation of heat and mass transfer processes in porous media: An application for maize stored in a flat bin. *Drying Technology*, *31*(10), 1099-1106. doi: https://doi.org/10.1080/07373937.2013.775145

Singh, S., Dubey, A., Tiwari, L., & Verma, A. (2009). Microbial profile of stored jaggery: a traditional indian sweetener. *Sugar Tech*, *11*(2), 213–216. doi: https://doi.org/10.1007/s12355-009-0034-4

Solís-Fuentes, J. A., Hernández-Ceja, Y., del Rosario Hernández-Medel, M., García-Gómez, R. S., Bernal-González, M., Mendoza-Pérez, S., & del Carmen Durán-Domínguez-de Bazúa, M. (2019). Quality improvement of jaggery, a traditional sweetener, using bagasse activated carbon. *Food Bioscience*, *32*, 100444. Retrieved from https://www.sciencedirect.com/science/article/pii/S2212429218308071 doi: https://doi.org/10.1016/j.fbio.2019.100444

Swaab, D., Hofman, M., Mirmiran, M., Ravid, R., & van Leeuwen, F. (1992). Anatomy of the human hypothalamus (chiasmatic and tuberal region). *The Human Hypothalamus in Health and Disease*, 3.

Taylor, N. A. (2006). Challenges to temperature regulation when work-

ing in hot environments. *Industrial health*, *44*(3), 331–344. doi: https://doi.org/10.2486/indhealth.44.331

Teixeira, L., Talaia, M., & Meles, B. (2017). Assessment of thermal comfort in a portuguese metalworking industry. *Occupational Ergonomics*, *13*(S1), 59–70. doi: https://doi.org/10.3233/OER-170254

Tong, X., Hong, S.-W., & Zhao, L. (2019). Cfd modelling of airflow pattern and thermal environment in a commercial manure-belt layer house with tunnel ventilation. *Biosystems engineering*, *178*, 275–293. doi: https://doi.org/10.1016/j.biosystemseng.2018.08.008

Varela-Aldás, J., Fuentes, E. M., Ruales, B., & Ichina, C. (2020). Construction of a wbgt index meter using low cost devices. In *International conference on information technology & systems* (pp. 459–468). doi: https://doi.org/10.1007/978-3-030-40690-5_45

Velásquez, F., Espitia, J., Mendieta, O., Escobar, S., & Rodríguez, J. (2019). Non-centrifugal cane sugar processing: A review on recent advances and the influence of process variables on qualities attributes of final products. *Journal of Food Engineering*, *255*(November 2018), 32–40. doi: 10.1016/j.jfoodeng.2019.03.009

Verma, A., Singh, S., Singh, S., & Dubey, A. (2012). 16s rdna sequence based characterization of bacteria in stored jaggery in indian jaggery manufacturing units. *Sugar Tech*, *14*(4), 422–427. doi: https://doi.org/10.1007/s12355-012-0162-0

Wolkoff, P., Azuma, K., & Carrer, P. (2021). Health, work performance, and risk of infection in office-like environments: The role of indoor temperature, air humidity, and ventilation. *International Journal of Hygiene and Environmental Health*, *233*, 113709. doi: https://doi.org/10.1016/j.ijheh.2021.113709

Xie, Q., Ni, J.-Q., Bao, J., & Su, Z. (2019). A thermal environmental model for indoor air temperature prediction and energy consumption in pig building. *Building and Environment*, *161*, 106238. doi: https://doi.org/10.1016/j.buildenv.2019.106238

Yin, Y., Wang, R., Zhai, X., & Ishugah, T. (2014). Experimental investigation on the heat transfer performance and water condensation phenomenon of radiant cooling panels. *Building and environment*, *71*, 15–23. doi: https://doi.org/10.1016/j.buildenv.2013.09.016

Zhou, B., Wang, X., Mondaca, M. R., Rong, L., & Choi, C. Y. (2019). Assessment of optimal airflow baffle locations and angles in mechanically-ventilated dairy houses using computational fluid dynamics. *Computers and Electronics in Agriculture*, *165*, 104930. doi: https://doi.org/10.1016/j.compag.2019.104930

Zidan, D., & Azlan, A. (2022). Non-centrifugal sugar (ncs) and health: a review on functional components and health benefits. *Applied Sciences*, *12*(1), 460. doi: https://doi.org/10.3390/app12010460

3. Comfort indexes of work conditions in a Non-Centrifugal Cane Sugar Factory in Colombia

Abstract

Non-Centrifugal Cane Sugar (NCS) production is characterized by its social and economical impact on rural communities, in Colombia. In this way, the incorporation of industrial factories for NCS production has been proposed to improve the rural economy and reduce risk for workers. Nevertheless, this type of factories present high temperature levels, by radiation, endangering the workers' health and performance. On account of this problems, the objectives of this study were to predict the current WBGT Index levels and propose alternatives to the situation present at the work place. Results show that the factory presents heat stress for work shifts from 10a.m. to 4p.m., and further actions should be taken to reduce heat impact on workers, such as reducing times for work shifts, every hour.

3.1. Introduction

Non-Centrifugal Cane Sugar (NCS), also known as panela, jaggery or kokuto, is a traditional sweetener made based on the extracted juice from sugar cane (Jaffé, 2015). NCS is commonly produced in "trapiches", which are artisanal buildings to process the juice (Mendieta et al., 2016). For instance, in Colombia, new centers have been installed for NCS production in industrial quantities, called "Centrales" (Fedepanela, 2019).

Furthermore, NCS has an important social and economic impact in Colombia, being the "second most important agro-industry (...) after coffee, with 220000 hectares", being the only labor of 350000 families (Ministerio de Agricultura y Desarrollo Rural, 2019). Also, until 2014, Colombia was the second largest NCS producer in the world, with a total of 1.338.554 tons of NCS, with a yield of 6.4 ton/ha (Mendieta et al., 2016).

NCS production is characterized by high superficial temperatures (above 105°C), and high vapor emission (Jaffé, 2015). Nevertheless, Wolkoff et al. (2021) showed that a comfortable

environment in the work site, guarantees higher production and improves productivity levels. Additionally, several studies have demonstrated that heat stress can cause illnesses (Budd, 2008; Ahmed et al., 2020) and, in extreme cases, death (Schickele, 1947).

Moreover, NCS production has been studied to determine its chemical characteristics (Jaffé, 2015; Velásquez et al., 2019), the heat transfer efficiency of the production process (Espitia et al., 2020). Nevertheless, industrial factories for NCS productions haven't been studied previously.

For determining heat comfort, CFD tools present a great alternative, because they reduce costs of in-field measurements and avoid time-consuming processes, specially in rural areas (Tong et al., 2019). WBGT Index calculation through CFD models has been studied previous, showing results that fit properly to reality (Xue & TY, 2002; Yuan, Farnham, & Emura, 2021; Ghani, Mahgoub, Bakochristou, & ElBialy, 2021).

In Colombia, dispositions for measuring and work place adaptation are ruled by the Ministerio de Trabajo y Seguridad Social (1979), with the "Resolución 2400 DE 1979". Nevertheless, standard limit values and calculations are taken from Ministério do Trabalho e Previdência (2021), from Brazil, due to the lack of normativity on this topic, in Colombia.

Currently, Caparrapí's NCS Factory present a production with elevated temperature and relative humidity levels, resulting in affections for the work environment for workers. Therefore, the objectives of this article are to predict the current WBGT Index levels and propose alternatives to the situation present at the work place, to guarantee avoiding thermal stress, through the application of Computational Fluid Dynamics (CFD) tools.

3.2. Materials and methods

3.2.1. Place description

The production place is in Caparrapí, in Cundinamarca, Colombia. The Caparrapí's Cane Honey Factory is located at coordinates 5°20'39"N, 74°29'30"W, at 1271 meters above sea level. The zone presents a mean annual temperature of 23°C (IDEAM, 2015b) and precipitation levels between 1500-2500 mm/year distributed in 100-200 days/year (IDEAM, 2015a).

The process for manufacturing NCS, as described byFedepanela (2019) is as follows: firstly, the extracted cane juice is gathered in a tank with a 10000 litters capacity. Later, the juice passes through a cleaning process of impurities removal, decantation, and salinity stabilization that lasts 24 hours. Thereafter, the juice passes through the evaporator, to extract water from the cane juice and reach the molding point, where the highest temperature processes

take place.

Base conditions were determined to be input values in the simulation model. For this, photos were taken with a thermographic camera FLIR Thermacam T640. With the help of this camera, temperature from evaporators, walls, ceiling, extractors and floor was obtained.

Furthermore, cane honey temperature was determined during its processing, to determine the peak ambient temperatures. Figure **2-1**, shows a range of the measured data from 20°C to surfaces with temperatures above 209°C in the work place.

At the moment the juice reaches this point, the juice starts being called honey, and it is poured in the molds. Once there, the deposited honey dries, by heat exchange with the environment.Thereafter, workers remove the molds and weight the product, to determine the group it is going to be packed in. Finally, during the package operation, the product is sealed and stored in boxes (Fedepanela, 2019).

3.2.2. Simulation procedure

Operating conditions for the Computational Fluid Dynamics Model were extracted from photographs taken with a thermographic camera, as shown in Figure **3-1**. With the help of this method, temperature levels from all operation points were extracted. Moreover, the processing temperature was taken during the realization of the tasks, to calculate surface temperatures.

Geometry was designed in the software Rhinoceros 7®, based on the original blueprints, provided by Fedepanela (2019). However, the resulting model presents changes, compared to the original blueprint, due to the current factory characteristics, to create a model closer to the real conditions of the place. In addition to that, tables were represented fixed to the floor, at their most used position, to avoid errors during the simulation.

Meshes are generated to establish points where equations are evaluated, by "discretizing the space" (Lintermann, 2021). In the first place, a top-down meshing technique was applied to generate the initial mesh, called Octree, where each big area is fragmented into smaller parts. Thereafter, a smoothing method was applied, with a bottom-up meshing system, where remaining smaller parts are joined together.

The computational model uses the finite volume technique to calculate pressure, temperature, and air velocity variables for each one of the elements, applying the Navier-Stokes equations, due to the complexity of the system (Osorio et al., 2016). Continuity, mass, and

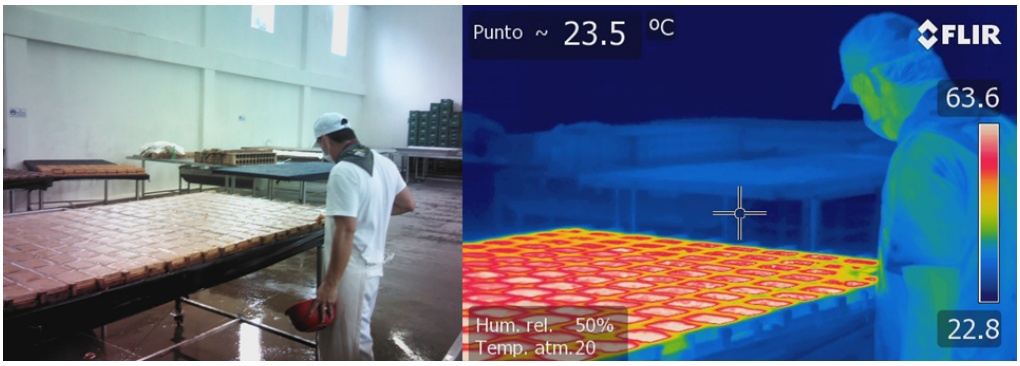

(a) Molding procedure

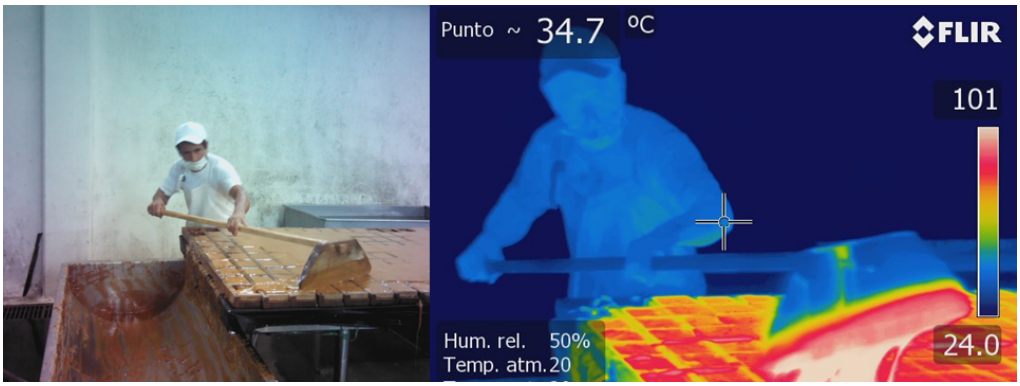

(b) Molding procedure with measured temperature

(c) Beating process with worker temperatures

Figure 3-1.: Temperature measure through thermographic images

energy were calculated by solving the simplified equations (3-1 and 3-2) for steady state calculations for non-isothermal fluids. Additionally, Equation 3-3 is the stress tensor corresponding to Newtonian fluids (Rocha et al., 2013; Osorio-Hernandez et al., 2020).

$$\nabla \cdot (\rho \vec{v}) = 0 \tag{3-1}$$

$$\nabla \cdot (\rho \vec{v}\vec{v}) = \nabla P + \left[\mu_t (\nabla \vec{v} + \nabla \vec{v}^T)\right] \tag{3-2}$$

$$\nabla \cdot (-k \nabla T + \rho \cdot C_p T \vec{v}) = 0 \tag{3-3}$$

Where:

ρ is the fluid density (kg/m^3).

$\vec{v}$ is the velocity vector.

P is the absolute pressure of the location (Pa).

μ_t is the dynamic viscosity of the fluid (kg m^{-1} s^{-1}).

T is temperature (K).

k is thermal conductivity (W m^{-1} K^{-1}).

C_p is specific heat (W kg^{-1} K^{-1}).

On the other hand, to calculate the value of relative humidity, due to vapor interaction inside as a result of the evaporation processes, for each element in the model, Equations 3-4 to 3-7 were used, according to the information reported by Junzeng et al. (2012) and Murray (1967).

$$RH = \frac{e * 100}{e_s} \tag{3-4}$$

$$e = e_{sh} - AP(T - T_{bh}) \tag{3-5}$$

$$e_s = 6.107 \cdot 10^{\left(\frac{7.5 \cdot T_{bh}}{237.3 + T_{bh}}\right)} \tag{3-6}$$

$$e_{sh} = 6.107 \cdot 10^{\left(\frac{7.5 \cdot T}{237.3 + T}\right)} \tag{3-7}$$

Where:

RH is the relative humidity (%).

e is the partial pressure exerted by water vapor (hPa).

e_s is the saturation pressure at dry-bulb temperature (hPa).

A is the psychrometer constant for aired and non-aired psychrometers (constant).

P is the absolute pressure of the location (Pa).

T is dry-bulb temperature (°C).

T_{bh} is wet-bulb temperature (°C).

Turbulence was calculated by the standard k-Epsilon model, due to its utility to "handle various fluid flow conditions", by the comparison between kinetic energy and its dissipation (Mishra & Aharwal, 2018, p. 5). Additionally, the criteria used to determine model convergence was mean square error lower than $1 \cdot 10^{-4}$ for all variables.

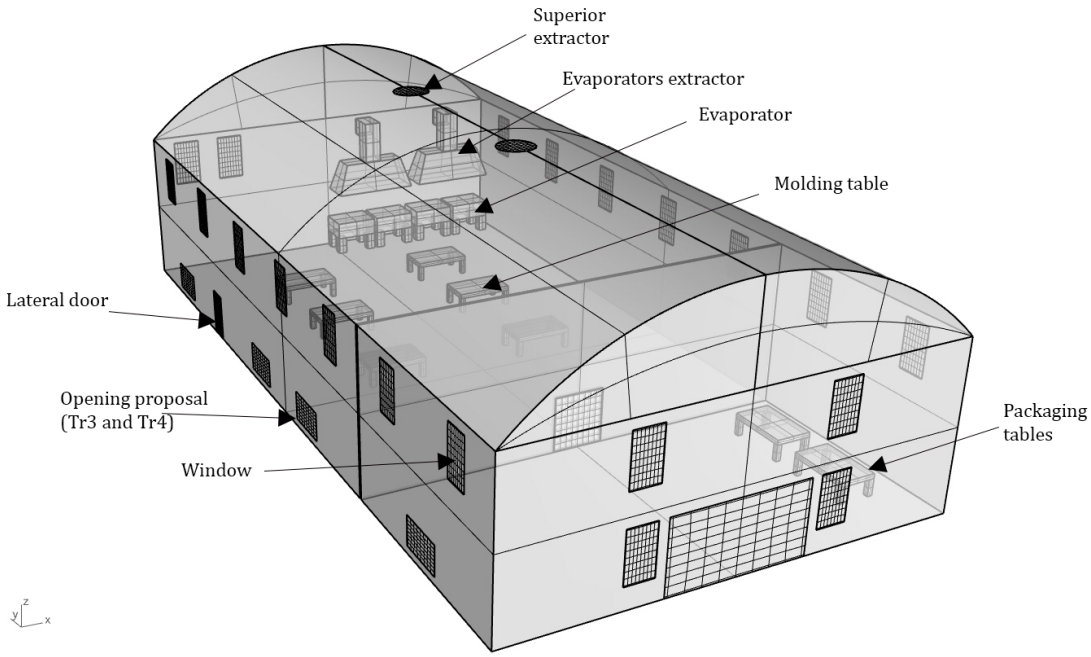

Figure 3-2.: Geometry of the NCS factory located in Caparrapí, Colombia.

Figure **3-2** show the NCS factory distribution. The dimensions of the factory are: 18m x 35m x 10.55m, to the top of the ceiling. In the frontal section of the building, packaging tasks are performed, as shown in Figure **3-2**. Additionally, inside the factory exists a division in areas according to the task: evaporation area, where the evaporation of water from the cane juice is conducted; molding area, where the NCS juice is deposited into molds and cools; weighing area, where the workers guarantee the expected weight of the product is achieved.

The walls are made of plastered brick cladding, windows are singled glazed, the ceiling is made of fiber cement and the openings have a filter, assumed opened all the time. For treatments 3 and 4, openings were proposed in the lower section of the building, with dimensions of 2m x 1.1m. Table **3-1** shows the heat transfer coefficient of the materials previously listed.

Table 3-1.: Properties of the materials of the factory

Material	Heat Transfer Coefficient $W \cdot m^{-2}K^{-1}$
Plastered brick cladding	2.3
Glass (Windows)	6
Fiber Cement	80

Due to the nature of the external conditions present in the factory, 4 treatments were done, to determine the conditions for every change inside the factory. The description for all treatments is described in detail, in Table **3-2**.

Table 3-2.: Boundary conditions used for the CFD models

Source		Description
Treatment 1	CFD Model based on data from February 2022	Initial condition. The created model was based on the data gathered during February 2022. At that moment, no extractors were operating inside the factory. Due to the production dynamics, information was collected only for 7 a.m., 9a.m. and 11a.m. work shifts. Environmental conditions for the production day were measured and assigned as initial values.
Treatment 2	CFD Model based on data from September 2022	Control condition. The created model was based on the data gathered during September 2022. Data were collected during this period, after the installation of an extractor, above the evaporator system, for a critical production day. Environmental conditions for the production day were measured and assigned as initial values.
Treatment 3	CFD Proposed Model	Alternative proposition 1. Lateral openings were proposed, for natural ventilation. All other conditions from Treatment 2 were used.
Treatment 4	CFD Proposed Model	Alternative proposition 2. Mechanical ventilation was added to the openings, with heating and cooling systems. All other conditions from Treatment 3 were used.

Each simulation was run to determine temperature, relative humidity, globe temperature and wet-bulb temperature, for the specific conditions. Furthermore, simulations were made for work hours at 7a.m., 9a.m. and 11a.m. for both scenarios to compare the impact of the extractor installation over the ambient conditions. Also, a simulation was run for the most critical period of time (2p.m. and 3p.m.), after the installation of the extractor (September 2022).

3.2.3. Model validation

Simulations were validated through the determination of the normalized mean square error (Equation 3-8), by comparing the obtained results with those determined experimentally.

Furthermore, the comparison of the established conditions was determined by a variance analysis (P< 0.001) and a Tukey test with 5% probability, according to the procedure established by the American Society for Testing Materials (ASTM, 2002).

$$NMSE = \frac{1}{n}\sum_{i=1}^{n}\frac{(Y_{pi} - Y_{mi})^2}{Y_{pi} \cdot Y_{mi}} \tag{3-8}$$

Where:

Y_{pi} are predicted values.

Y_{mi} are measured values.

Additionally, an error propagation study was performed based on the equipment precision, to determine whether this characteristic affects the obtained results of the research.

3.2.4. WBGT Index determination and interpretation

Thermal comfort was evaluated through the calculation and measurement of the Wet Bulb Globe Temperature (WBGT) index is a measure of heat stress in outdoor environments that takes into account temperature, humidity, wind speed, and solar radiation (Yaglou, Minaed, et al., 1957). The WBGT index is calculated using a formula that combines the three temperature readings: the wet bulb temperature, which reflects the cooling effect of sweat evaporation; the dry bulb temperature, which measures the ambient air temperature; and the globe temperature, which accounts for radiant heat from the sun and other radiation sources (Kakaei et al., 2019).

In Colombia, the Ministerio de Trabajo y Seguridad Social (1979) approved the WBGT index as the default comfort index to determine thermal stress and its sources, due to the influence of radiation, measured with the help of the globe thermometer. WBGT Index for indoor conditions is determined by equation (3-9), as reported by Yoshida et al. (2020).

$$\text{WBGT} = 0.7 \cdot T_{wb} + 0.3 \cdot T_g \tag{3-9}$$

Where:

T_{wb} is wet-bulb temperature.

T_g is globe temperature.

Wet-bulb temperature was determined with Equation 3-10, as reported by Stull (2011). Additionally, the globe temperature (Equation 3-11) was determined according to the research presented by Abreu et al. (2011) and Dimiceli et al. (2013), for indoor environments.

$$T_{wb} = T \cdot \arctan[0.151977(RH + 8.313659)^{1/2}] + \arctan(T + RH) - \arctan(RH - 1.676331) + 0.00391838(RH)^{3/2} \cdot \arctan(0.023101 \cdot RH) - 4.686035 \quad (3\text{-}10)$$

$$T_g = 0.456 + 1.0335 * T \quad (3\text{-}11)$$

Where:

RH is relative humidity (%).

T is dry-bulb temperature (°C)

In order to analyze the results, the standard values presented by the Ministério do Trabalho e Previdência (2021) from Brazil were taken, due to the similarity with the tasks operated by the workers. In this way, the selected activity from the document was "weight-bearing work or vigorous arm movements movements with the arms" (Ministério do Trabalho e Previdência, 2021, p. 13), with a metabolic rate of 495 W.

Furthermore, data was gathered from each point previously described, in order to compare with the results obtained from the simulations. For this purpose, a WBGT meter Extech Model HT30 was used, to calculate the index at a height of 1.6 m above floor level.

Additionally, Table **3-3** presents the maximum values allowed for workers, depending on the activity, measured by the metabolic rate in Watts (W). For this study, the reference maximum was set to 21.9°C.

Table 3-3.: WBGT Index maximum permitted values. Adapted from Ministério do Trabalho e Previdência (2021).

Metabolic rate [W]	WBGT Index Max
100	31.7
101	31.6
103	31.5
...	...
487	22
495	21.9
503	21.8
...	...
593	20.8
602	20.7

3.3. Results and discussion

An unstructured mesh was designed (Figure **3-3**), following the methodology presented by Alfarawi et al. (2021). The resulting mesh has 128236 elements, and a total of 34453 nodes. Moreover, the mesh quality was established with a maximum quality value of 0.5, for a 10% of the model. For this purpose, a test was run, where only 5% of the generated elements had a quality inferior to 0.5.

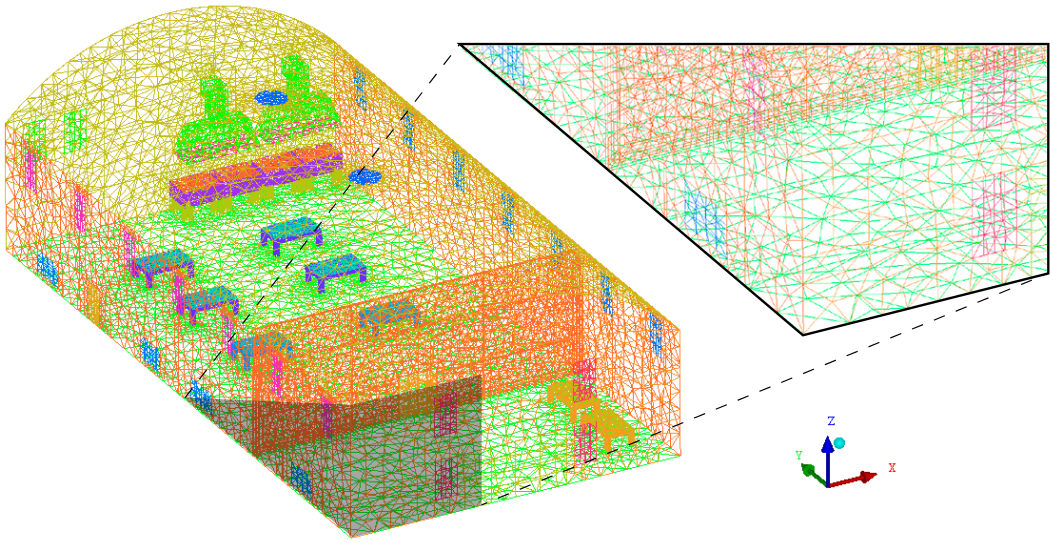

Figure 3-3.: Computed mesh for Caparrapí's Cane Honey Factory model

Table **3-4** shows a comparison of means for the experimental data and the obtained data from the CFD model. It is possible to observe that Treatment 1 present similar values, with differences below 1°C. Also, Treatment 2 shows similarity between values.

Table 3-4.: Comparison of simulated and measured means for WBGT Index, °C

	February (Tr1)		September (Tr2)	
	Experimental WBGT	CFD Model WBGT	Experimental WBGT	CFD Model WBGT
7a.m.	21.84	21.64	19.99	19.85
9a.m.	22.81	21.98	20.50	21.24
11a.m.	22.07	21.16	23.57	23.75
2p.m.	-	-	24.90	24.50
3p.m.	-	-	23.02	23.56

On the other hand, Table **3-5** shows the Normalized Mean Square Error for the WBGT Index, comparing the experimental data, with the results obtained from the simulation.

With this, it can be noted that all error values are lower than the established limit of 0.25. Therefore, the obtained model represents reality precisely (ASTM, 2002).

Table 3-5.: NMSE for WBGT Index values

	WBGT February	WBGT September
7a.m.	0.0198	0.0004
9a.m.	0.0021	0.0014
11a.m.	0.0035	0.0016
2p.m.	-	0.0037
3p.m.	-	0.0016

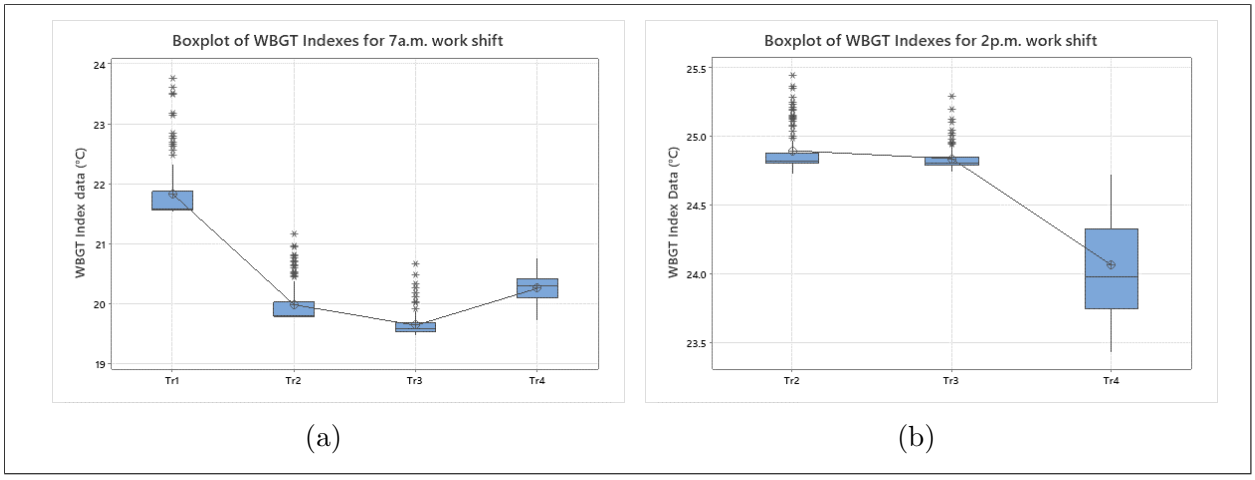

(a) (b)

Figure 3-4.: Boxplot graphics of WBGT index for different work shifts

Figure **3-4** shows the data distribution for the calculated WBGT Indexes, for each treatment. WBGT Indexes for 7a.m. work shifts (Figure **3-4**a) present a media of 21.64°C. Firstly, Treatment 1 presents points above 23°C, exceeding the allowed maximum for the tasks. Also, for Treatments 2 and 3, WBGT index show a decrease in their value. Finally, Treatment 4 shows a increase in the mean WBGT Index, without surpassing the established limit.

On the other hand, for 2p.m. work shift (Figure **3-4**b), conditions show a higher WBGT Index level. For treatments 2 and 3, WBGT conditions show a mean value above 24.5°C, whereas Treatment 4 mean is around 24°C. This demonstrates that work activities generate high thermal stress for workers, presenting similar results to Budd (2008).

Table **3-6** shows the statistical data obtained by the analysis done for Treatments 1 to 4. In the case of 7a.m. work shift, Treatment 1 present the higher mean value, followed by Treatment 4. Maximum values show that Treatment 1 , consequently showing that ventilation can help reduce heat stress levels, as reported by (Osorio-Hernandez et al., 2020; Budd, 2008; Yoshida et al., 2020).

Table 3-6.: Statistical information of WBGT Index for each treatment in 7a.m. and 2p.m. work shifts (°C)

7a.m.					
Factor	**N**	**Mean**	**Min**	**Max**	**StDev**
$Tr1^{A}$	126	21.84	21.54	23.77	0.50
$Tr4^{B}$	126	20.26	19.73	20.75	0.34
$Tr2^{C}$	126	19.99	19.77	21.16	0.19
$Tr3^{D}$	126	19.64	19.48	20.66	0.22
2p.m.					
Factor	**N**	**Mean**	**Min**	**Max**	**StDev**
$Tr2^{A}$	126	24.90	24.73	25.45	0.16
$Tr3^{A}$	126	24.84	24.74	25.29	0.09
$Tr4^{B}$	126	24.07	23.43	24.72	0.38

StDev: Standard Deviation. Treatments followed by the same letters do not differ by the Tukey's test at 0.05. Probability for 7a.m. (P=0.0000, F=1050.52). Probability for 2p.m. (P=0.0000, F=460.49)

On the contrary, 2p.m. work shift shows statistical similarity between Treatment 2 and 3, with a minimum value around 24.7°C. Additionally, Treatment 4 shows the lowest values, with a mean of 24.07°C, demonstrating the reduction of heat stress inside the factory. However, data show that heat stress level isn't reduced enough with the proposed ventilation system.

Figure **3-5** presents a graphical representation of the obtained WBGT Index for 7a.m. and 2p.m. work shifts. 9a.m., 11a.m. and 3p.m. are displayed on Appendix C. On the one hand, 7a.m. work shift show a similar distribution for Treatments 1 and 2 (Figures **3-5**a, and **3-5**b, respectively), with an increase in the WBGT level in the proximity of the evaporation area. In contrast, Treatments 3 and 4 (Figures **3-5**d, and **3-5**f, respectively) show a more steady distribution along the factory, with lower WBGT level close to the ventilation areas.

On the other hand, for 2p.m. work shift, Treatment 2 and 3 (Figures **3-5**c and **3-5**e) show a similar behavior, with a small reduction in the WBGT index results in some points close to

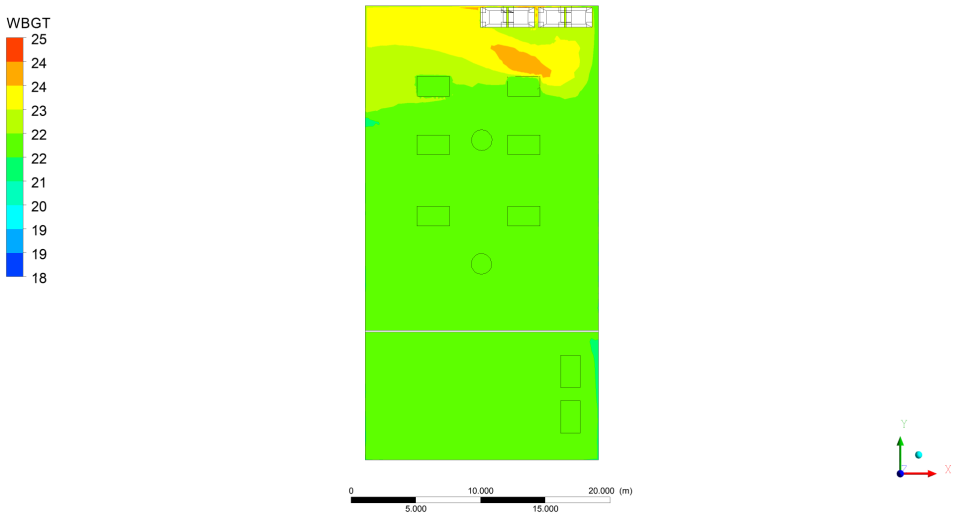

(a) Treatment 1 at 7a.m.

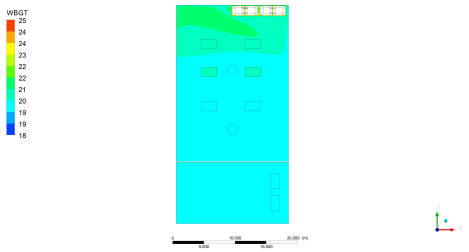

(b) Treatment 2 at 7a.m.

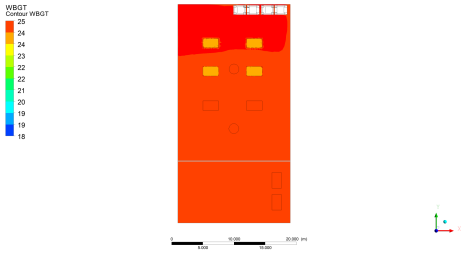

(c) Treatment 2 at 2p.m.

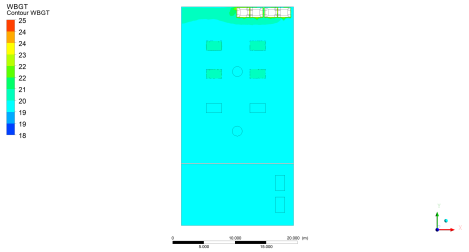

(d) Treatment 3 at 7a.m.

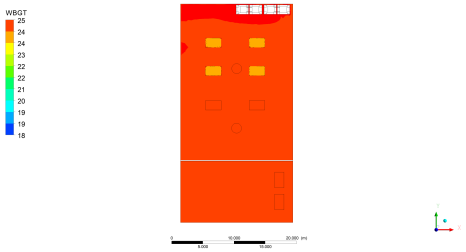

(e) Treatment 3 at 2p.m.

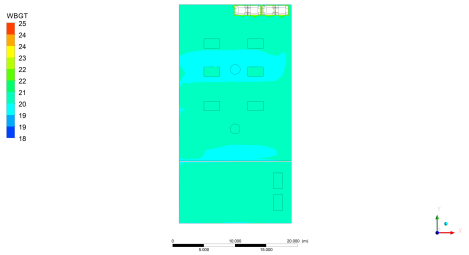

(f) Treatment 4 at 7a.m.

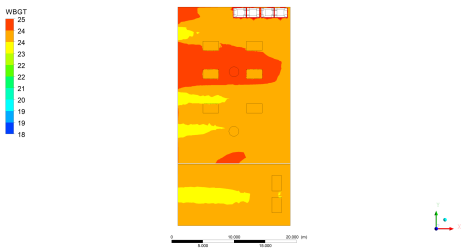

(g) Treatment 4 at 2p.m.

Figure 3-5.: WBGT Index profiles for treatments 1 to 4, °C

the evaporation area. Additionally, Treatment 4 **3-5**g shows a decrease in the WBGT levels caused by the ventilation systems and the air movement inside the factory. Nevertheless, high WBGT levels are present in general, specially in the molding area.

With the results shown, it is possible to observe that workers are not comfortable and present high thermal stress, because of WBGT Index results above 25°C. It is advisable to reduce work shifts, between hours could help lower the heat stress (Budd, 2008), as well as implementing specialized clothing for high temperature processes (Yoshida et al., 2020), to reduce the risk of illnesses by heat stress and improve the production performance.

Heat transfer, specially through solar radiation, shows a direct impact in the obtained results of the temperature of the WBGT Index (Figure **3-5**). Firstly, it is possible to observe that at 2 p.m., the highest values are presented. Additionally, treatment 4 shows that 25°C is reached, to guarantee the maximum limit allowed.

3.4. Conclusions

A Computational Fluid Dynamics model was created to predict the WBGT Index values for all points inside the Non-Centrifugal Cane Sugar Factory, located in Caparrapí, Colombia. It was possible to observe that the model presents a fit approximation to reality, corroborated with Treatments 1 and 2.

In the same way, Treatment 3 and 4 present a reduction in the overall thermal comfort inside the factory. For instance, Treatment 4 showed a higher reduction of the WBGT Index, yet maintaining a higher level than the recommended limit. For this, alternatives were proposed to decrease the heat stress in workers, by changing their activity shifts.

This study proved that studying human comfort can help reduce heat stress problems, associated to the WBGT Index. Therefore, it is advisable to conduct the proposed changes, to create better conditions for the factory. Additionally, future studies can investigate the impact of other strategies in the WBGT Index and create new alternatives.

References

Abreu, P. G. d., Abreu, V. M. N., Franciscon, L., Coldebella, A., & Amaral, A. G. d. (2011, dez.). Estimativa da temperatura de globo negro a partir da temperatura de bulbo seco. *Revista Engenharia na Agricultura - REVENG*, *19*(6), 557–563. doi: https://10.13083/reveng.v19i6.273

Ahmed, H. O., Bindekhain, J. A., Alshuweihi, M. I., Yunis, M. A., & Matar, N. R. (2020). Assessment of thermal exposure level among construction workers in uae using wbgt, hsi and twl indices. *Industrial health*, *58*(2), 170–181.

Alfarawi, S. S., El-sawi, A., & Omar, H. (2021). Exploring discontinuous meshing for cfd modelling of counter flow heat exchanger. *Journal of Advanced Research in Numerical Heat Transfer*, *5*(1), 26–34.

ASTM. (2002). *Guide for statistical evaluation of indoor air quality models (d5157-97).* American Society for Testing Materials. Retrieved from https://www.astm.org/d5157-19.html doi: https://doi.org/10.1520/D5157-19

Budd, G. M. (2008). Wet-bulb globe temperature (wbgt)—its history and its limitations. *Journal of Science and Medicine in Sport*, *11*(1), 20-32. Retrieved from https://www.sciencedirect.com/science/article/pii/S1440244007001478 (Heat Stress in Sport) doi: https://doi.org/10.1016/j.jsams.2007.07.003

Dimiceli, V. E., Piltz, S. F., & Amburn, S. A. (2013). Black globe temperature estimate for the wbgt index. In H. K. Kim, S.-I. Ao, & B. B. Rieger (Eds.), *Iaeng transactions on engineering technologies: Special edition of the world congress on engineering and computer science 2011* (pp. 323–334). Dordrecht: Springer Netherlands. Retrieved from https://doi.org/10.1007/978-94-007-4786-9_26 doi: 10.1007/978-94-007-4786-9_26

Espitia, J., Velásquez, F., López, R., Escobar, S., & Rodríguez, J. (2020). An engineering approach to design a non-centrifugal cane sugar production module: A heat transfer study to improve the energy use. *Journal of Food Engineering*, *274*, 109843. Retrieved from https://www.sciencedirect.com/science/article/pii/S0260877419304868 doi: https://doi.org/10.1016/j.jfoodeng.2019.109843

Fedepanela. (2019). *PROTOCOLO DE TRAZABILIDAD PARA OBTENCIÓN DE PANELA.* BOGOTÁ, D.C.. Unpublished writing.

Ghani, S., Mahgoub, A. O., Bakochristou, F., & ElBialy, E. A. (2021). Assessment of thermal comfort indices in an open air-conditioned stadium in hot and arid environment. *Journal of Building Engineering*, *40*, 102378. Retrieved from https://www.sciencedirect.com/science/article/pii/S2352710221002345 doi: https://doi.org/10.1016/j.jobe.2021.102378

IDEAM. (2015a). *Mapa de precipitación total anual (mm).* Cundinamarca, Colombia.

IDEAM. (2015b). *Mapa de temperatura media anual (°c).* Cundinamarca, Colombia.

Jaffé, W. R. (2015). Nutritional and functional components of non centrifugal cane sugar: A compilation of the data from the analytical literature. *Journal of Food Composition and Analysis*, *43*, 194–202. doi: 10.1016/j.jfca.2015.06.007

Junzeng, X., Qi, W., Shizhang, P., & Yanmei, Y. (2012). Error of saturation vapor pressure calculated by different formulas and its effect on calculation of reference evapotranspiration in high latitude cold region. *Procedia Engineering*, *28*, 43-48. Retrieved from

https://www.sciencedirect.com/science/article/pii/S187770581200690X (2012 International Conference on Modern Hydraulic Engineering) doi: https://doi.org/10.1016/j.proeng.2012.01.680

Kakaei, H., Omidi, F., Ghasemi, R., Sabet, M. R., & Golbabaei, F. (2019). Changes of wbgt as a heat stress index over the time: A systematic review and meta-analysis. *Urban Climate*, *27*, 284–292.

Lintermann, A. (2021). Computational meshing for cfd simulations. In K. Inthavong, N. Singh, E. Wong, & J. Tu (Eds.), *Clinical and biomedical engineering in the human nose: A computational fluid dynamics approach* (pp. 85–115). Singapore: Springer Singapore. Retrieved from https://doi.org/10.1007/978-981-15-6716-2_6 doi: 10.1007/978-981-15-6716-2_6

Mendieta, O., García, M., Peña, A., & Rodríguez, J. (2016). *Las buenas prácticas de manufactura en la producción de panela* (1st ed.; Corpoica, Ed.). Mosquera (Colombia).

Ministerio de Agricultura y Desarrollo Rural. (2019). *Cadena agroindustrial de la panela.*

Ministerio de Trabajo y Seguridad Social. (1979). *RESOLUCIÓN 2400 DE 1979.* BOGOTÁ, D.C.. Retrieved from https://minvivienda.gov.co/sites/default/files/normativa/2400 - 1979.pdf

Ministério do Trabalho e Previdência. (2021). *Portaria n.º 426 de 07 de outubro de 2021.* Retrieved from https://www.gov.br/trabalho-e-previdencia/pt-br/composicao/orgaos-especificos/secretaria-de-trabalho/inspecao/seguranca-e-saude-no-trabalho/sst-portarias/2021/portaria-mtp-no-426-anexos-i-vibracao-e-iii-calor-da-nr-09.pdf (Anexo 3)

Mishra, P., & Aharwal, K. R. (2018, aug). A review on selection of turbulence model for cfd analysis of air flow within a cold storage. *IOP Conference Series: Materials Science and Engineering*, *402*(1), 012145. doi: https://dx.doi.org/10.1088/1757-899X/402/1/012145

Murray, F. W. (1967). On the computation of saturation vapor pressure. *Journal of Applied Meteorology and Climatology*, *6*(1), 203 - 204. doi: https://10.1175/1520-0450(1967)006<0203:OTCOSV>2.0.CO;2

Osorio, J. A., Ferreira, I. d. F., Olivera, K. S., Barreto, L., & Norton, T. (2016, 01). A CFD based approach for determination of ammonia concentration profile and flux from poultry houses with natural ventilation. *Revista Facultad Nacional de Agronomía Medellín*, *69*, 7825 - 7834. doi: http://dx.doi.org/10.15446/rfna.v69n1.54750

Osorio-Hernandez, R., Osorio-Saraz, J., Sullivan-Oliveira, K., Aristizaba, I., & Arango, J. (2020). Computational fluid dynamics assessment of effect of different openings configurations on the thermal environment of a facility for coffee wet processing. *Journal of Agricultural Engineering*, *51*(1), 21–26. doi: 10.4081/jae.2020.892

Rocha, D. K. S. O., Martins, J. H., Martins, M. A., Saraz, J. A. O., & Filho, A. F. L.

(2013). Three-dimensional modeling and simulation of heat and mass transfer processes in porous media: An application for maize stored in a flat bin. *Drying Technology*, *31*(10), 1099-1106. doi: https://doi.org/10.1080/07373937.2013.775145

Schickele, E. (1947). Environment and fatal heat stroke: an analysis of 157 cases occurring in the army in the us during world war ii. *The Military Surgeon (United States)*, *100*(3), 235–256.

Stull, R. (2011). Wet-bulb temperature from relative humidity and air temperature. *Journal of Applied Meteorology and Climatology*, *50*(11), 2267–2269. doi: 10.1175/JAMC-D-11-0143.1

Tong, X., Hong, S.-W., & Zhao, L. (2019). Cfd modelling of airflow pattern and thermal environment in a commercial manure-belt layer house with tunnel ventilation. *Biosystems engineering*, *178*, 275–293. doi: https://doi.org/10.1016/j.biosystemseng.2018.08.008

Velásquez, F., Espitia, J., Mendieta, O., Escobar, S., & Rodríguez, J. (2019). Non-centrifugal cane sugar processing: A review on recent advances and the influence of process variables on qualities attributes of final products. *Journal of Food Engineering*, *255*(November 2018), 32–40. doi: 10.1016/j.jfoodeng.2019.03.009

Wolkoff, P., Azuma, K., & Carrer, P. (2021). Health, work performance, and risk of infection in office-like environments: The role of indoor temperature, air humidity, and ventilation. *International Journal of Hygiene and Environmental Health*, *233*, 113709. doi: https://doi.org/10.1016/j.ijheh.2021.113709

Xue, H., & TY, B. (2002). An occupant-coupled cfd model for local wbgt analysis in a ventilated enclosure. *Journal of the Human-Environment System*, *5*(2), 79–86. doi: https://doi.org/10.1618/jhes.5.79

Yaglou, C., Minaed, D., et al. (1957). Control of heat casualties at military training centers. *Arch. Indust. Health*, *16*(4), 302–16.

Yoshida, S., Yoshida, A., & Kinoshita, S. (2020). Chapter 5 - evaluation methods of adaptation cities. In H. Takebayashi & M. Moriyama (Eds.), *Adaptation measures for urban heat islands* (p. 115-159). Academic Press. doi: https://doi.org/10.1016/B978-0-12-817624-5.00005-1

Yuan, J., Farnham, C., & Emura, K. (2021). Effect of different reflection directional characteristics of building facades on outdoor thermal environment and indoor heat loads by cfd analysis. *Urban Climate*, *38*, 100875. doi: https://doi.org/10.1016/j.uclim.2021.100875

4. Noise mapping technique for an unrefined sugar cane processing factory in Colombia

Abstract

Noise monitoring in production factories is a tool used to visualize and address sound level problems. The objective of this study was to characterize the current noise situation inside the unrefined sugar cane factory, located in Caparrapí, Colombia, through mapping techniques and determine alternatives, if necessary. For this purpose, the allowed duration for current sound levels was calculated for 69 points inside the factory along with the daily noise dose experimented by the workers. Results show that there are some points with high sound levels, mainly occasioned by the reflection in walls. Nevertheless, it can be observed that the factory presents noise levels under the allowed maximum, with certain areas that could present higher levels, with changes in the activities done in it.

Keywords: mapping, sound level, time-weighted average, unrefined sugar cane, acoustic environment.

4.1. Introduction

Panela, also known as non-centrifugal cane sugar (NCS), is "a natural sweetener obtained by concentration of the sugar cane juice in installations named 'trapiches' and presented in different forms" (Mujica et al., 2008). Panela is also a product extracted and transformed from sugar cane (*Saccharum officinarum*). In Colombia, panela production is "the second most important agro-industry with social importance, after coffee, with 220000 hectares" (Ministerio de Agricultura y Desarrollo Rural, 2019). Moreover, in 2014, Colombia produced 1.388.554 tons, with a yield of 6.4 ton/ha (Mendieta et al., 2016).

On the other hand, production in Colombia is characterized for lacking technification systems for cane production and posterior processing, presenting high vapor production and high temperature levels (Rodriguez et al., 2004; Velásquez et al., 2019). For instance, studies have been conducted to characterize the final product, where its nutritional content

was determined and its quality improved (Jaffé, 2015; Velásquez et al., 2019; Solís-Fuentes et al., 2019). Additionally, García et al. (2017) studied the smell characteristics, its influence.

In addition, the production process has been studied in terms of the efficiency starting from the crop and the incidence of light, climate, temperature over its yield. Moreover, the inner environmental conditions during the non-centrifugal sugar manufacture have been studied, based on worker welfare analyzing specially temperature, heat transfer and relative humidity (Espitia et al., 2020; Velásquez et al., 2019).

To counter production problems and raise panela production levels in Colombia, there were installed production factories denominated "centrals" with productions up to 250 kg/h (Fedepanela, 2019). The principal difference between traditional and industrial production is on the sugar cane juice concentration process, where the industrial process gathers the juice produced by farmers to transform it, while the traditional process skips this step (Fedepanela, 2019). For this type of production, studies have been conducted in Colombia, to determine the environmental conditions for the operators inside the factory (Alvarez-Carpintero & Osorio-Hernandez, 2021). Nevertheless, environmental conditions associated with noise have never been studied in this production area.

Previously, several studies have been done to determine and map sound levels in cities (Luzzi & Vassiliev, 2005; King et al., 2010; Conde-Santos et al., 2008) and inside production factories, such as concrete production (Ahmed & Gadelmoula, 2022), rubber production (Lim et al., 2018), Fatty Acid Plant Area (Hasibuan et al., 2020), among others. Additionally, National Institute for Occupational Safety and Health (NIOSH) (1998), establishes the standard recommendations for exposure limits and calculation procedures.

Additionally, in Colombia, normativity establishes recommended noise limits, along with standard procedures and calculations. For this type of constructions, the recommended limit is 75 dBA (Ministerio de Ambiente, vivienda y Desarrollo Territorial, 2006). In the same way, determination and monitoring of noise levels is necessary to prevent diseases, such as temporal or permanent audition loss, raising of arterial pressure, which can cause cardiac and nervous disorders, and lower productivity levels in production sites (Organización Internacional del Trabajo, 2010).

To generate a complete study on the non-centrifugal sugar cane factory located in Caparrapí, Colombia, this article has the objective to describe the current noise situation of the production factory through mapping tools.

4.2. Materials and methods

4.2.1. Site description

The production facility is located in the municipality of Caparrapí, in Cundinamarca, Colombia, at geographic coordinates 5◦20'39"N, 74◦29'30"W, and an altitude of 1271 meters above sea level. This area is characterized by a mean annual temperature of 23◦C (IDEAM, 2015b) and annual precipitation levels ranging from 1500-2500 mm/year, which are distributed across 100-200 days/year (IDEAM, 2015a).

In Colombia, the industrial production of non-centrifugal sugar cane follows a standardized process that involves several steps. First, the extracted cane juice is collected in a tank with a capacity of 10000 liters. The juice is then subjected to a cleaning process to remove impurities, followed by a 24-hour period of decantation and salinity stabilization. Afterward, the juice undergoes an evaporation process to reduce its moisture content and reach the molding point.

At this stage, the juice is referred to as honey and is poured into molds where the drying process occurs through natural convection. Workers remove the product from the molds and verify the allowed weight for each one, a process characterized by high levels of noise. Finally, the product is sealed and stored in boxes during the packaging process.

4.2.2. Sound level measure

To conduct the mapping process, data was collected at 63 points within the working area, as illustrated in Figure **4-1**. The selection of these points took into account the distribution of labor within the factory and their spatial proximity to critical work areas, including mold tables, evaporators, and packaging sites. The points were categorized based on the respective area in which they were located, which included the packaging area (red area), weighing area (blue area), molding area (green area), and evaporation area (yellow area).

In addition, the boxes depicted in the diagram within the red, blue, and yellow areas correspond to the tables utilized in each production process.

At each of the 63 designated points, sound levels were measured in dBA using a sound level meter. Measurements were taken by moving from one point to another at two-hour intervals within a three-hour time frame: 7 to 9 a.m., 9 to 11 a.m., and 11 a.m. to 1 p.m.

The production process is characterized by a cyclical pattern in which the sound level oscillates between a low level for 120 seconds and a loud 2-second noise, which repeats every two hours while workers remove non-centrifugal sugar cane from the molds. Once the sugar

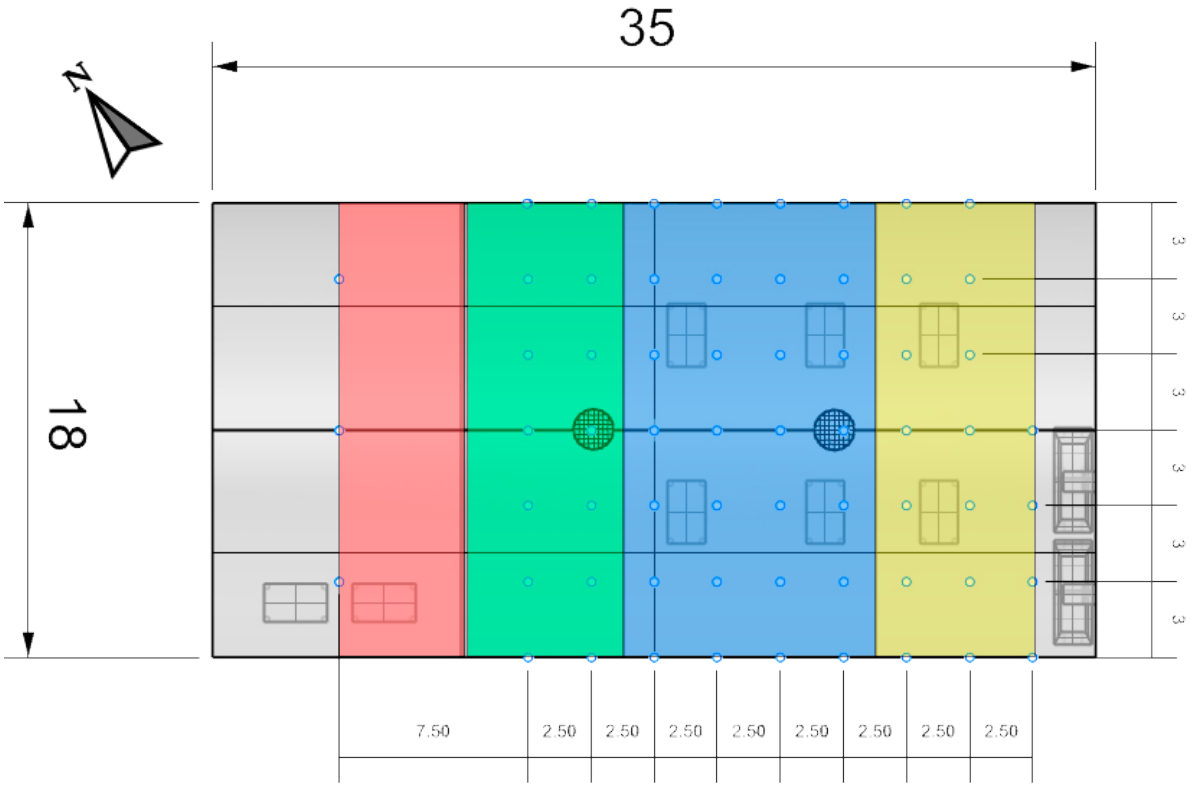

Figure 4-1.: Measure points inside the factory, m.

cane is weighed and ready for packing, the process restarts from the molding stage. The work shifts are 10 hours long each day.

Sound levels were measured in dBA using a PCE-322A sonometer with a range of 30 to 130 dB and a precision of ±1.4dB, corresponding to a net with A-weighting (Ahmed & Gadelmoula, 2022). The device was programmed to calculate the average level for each point. Finally, data was measured at 1.6 m above floor level.

4.2.3. Noise data analysis

First, during the data analysis process, the normality distribution was checked to verify the validity of the information in each point.

Daily noise dose is the permitted sound level during a day of work with an 8-h shift, reaching its limit at 85dBA (NIOSH, 1998). After the data validation, the daily noise dose was calculated with the equation:

$$D = \left[\frac{C_1}{D_1} + \frac{C_2}{D_2} + \ldots + \frac{C_n}{D_n}\right] * 100 \quad (4\text{-}1)$$

Where C_n is the total time of exposure at a specified noise level and Tn is the exposure duration for which noise at this level becomes hazardous (NIOSH, 1998).
Also, NIOSH (1998), reports the following equation for calculating the allowed exposure levels:

$$T(min) = \frac{480}{2^{(L-85)/3}} \quad (4\text{-}2)$$

Where 480 are shifts with 8 hours and L is the exposure level, measured in dB. 3 is the exchange rate (NIOSH, 1998).

Finally, the time-weighted average is the exposure level translated to an 8-hours shift, in case the working system is stablished differently (NIOSH, 1998), calculated as:

$$TWA = 10 * \log(\frac{D}{100}) + 85 \quad (4\text{-}3)$$

Subsequently, a regression technique was employed to determine the most suitable fit for graphing the distribution of sound levels inside the factory using level curves. Using Surfer 21 software (Gold Surfer Inc., USA), maps were generated to depict the average levels and TWA levels. The root-mean-square error was analyzed to select the model that most closely reflected reality.

Furthermore, the study included an analysis of the propagation of errors associated with equipment precision to ascertain whether such precision had any influence on the research outcomes.

4.3. Results and discussion

Table **4-1** shows a sample of the measured sound levels and the calculated reference duration, based on each one of the shifts (7 to 9 a.m., 9 to 11 a.m. and 11 a.m. to 1 p.m.). Additionally, the daily noise dose was obtained, based on the exposure time and the allowed duration calculated previously. Finally, the time-weighted average was calculated using equation 4-3, showing low noise levels for the duration of the daily shifts, in accordance with previous reports with higher noise levels (Ahmed & Gadelmoula, 2022).
As stated before, the current analysis evaluates the standard conditions for each time gap of two hours. Generally speaking, the three-time gaps maintain the same sound levels throughout the shifts, presenting variations no higher to 4dB. The noise levels for the space between points was determined by a minimum curvature regression.

Table 4-1.: Sound level and reference duration sample

X	Y	Sound level - 7-9 a.m.	Sound level - 9-11 a.m.	Sound level - 11-1 p.m.	Allowed duration, T 7-9(h)	Allowed duration, T 9-11(h)	Allowed duration, T 11-1(h)	%D	TWA
3	0	64.3	68.2	62.0	955.4	388.0	1625.5	0.066	53.2
9	0	58.9	63.5	62.7	3327.0	1149.4	1382.8	0.040	51.0
15	0	67.0	69.4	65.1	512.0	294.1	794.2	0.110	55.4
0	5	63.3	60.8	69.9	1203.8	2144.9	262.0	0.153	56.8
3	5	62.8	62.4	61.6	1351.2	1482.0	1782.9	0.037	50.7
6	5	64.8	62.0	62.1	851.2	1625.5	1588.4	0.044	51.4
9	5	64.8	63.4	63.8	851.2	1176.3	1072.4	0.058	52.6
(...)	(...)	(...)	(...)	(...)	(...)	(...)	(...)	(...)	(...)

Figure 2 shows the generated maps with the average levels for each one of the time gaps. Firstly, it is possible to observe a raise in the sound levels near the walls during the three-time lapses. This could be explained by the usage of certain tools during the panela manufacturing process, also attributing the reflected sound from the walls (Ahmed & Gadelmoula, 2022).

Furthermore, the packaging area (red) has a prominent noise level, explained by the sound of the engines used by packaging machines. Additionally, the place in which the task is performed is in the proximity of a wall, causing the effect mentioned previously.

The weighing area shows an overall similitude between the three-time lapses. Nevertheless, from 7 to 11 a.m., the registered sound levels were higher in comparison to the registered data from 11 to 1 p.m. This represents the sound levels when the weighing task is being done, which was performed by the workers at the time of the data gathering, who usually have loud conversations while they complete the task. These traditional customs produce levels over 70 dB and makes the area a warning zone where the levels can potentially pass the permitted levels.

On the other hand, the molding area presents sound levels that vary from one another. Each time gap shows a different peak zone that can be attributed to the table change after completion of the tasks. Also, it is important to note that in the proximities of the tables where the workers receive the sound, the levels stay constant, with an average of 65 dB.

Finally, the evaporation area presents average levels of 67dB in the tables, with an increase in the proximities of the evaporators up to around 76 dB. This phenomenon occurs due to the high-pressure vapor ejection through the pipes destined to evaporate the water of the sugar cane juice. Additionally, during the 11 to 1 p.m. time-lapse, there is an increase in the sound level in a small area in the upper part of the map. This can be explained by the habit of opening the lateral door to let the air move inside the factory, due to the high temperatures, causing higher reflection of the sound behind the door (Ahmed & Gadelmoula, 2022). The high sound levels over 75 dB in this area make it another warning zone, due to the possibility to surpass the allowed sound limit.

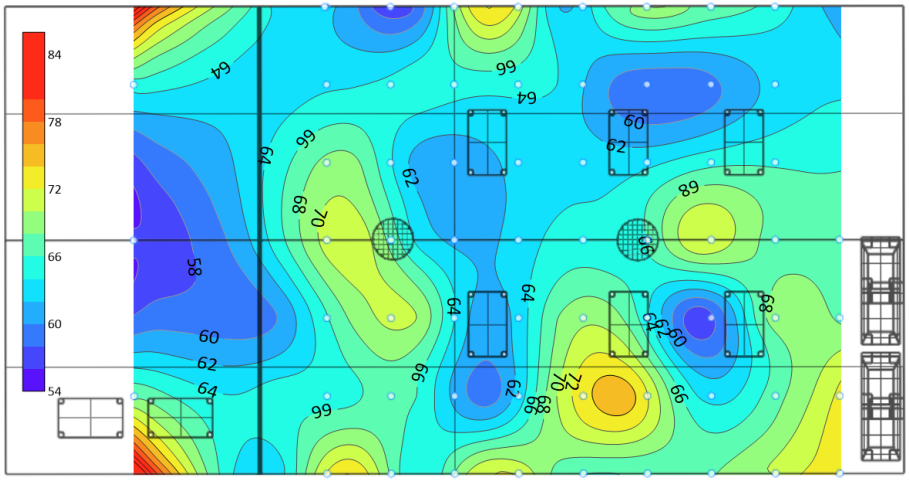

(a) 7 a.m. - 9 a.m.

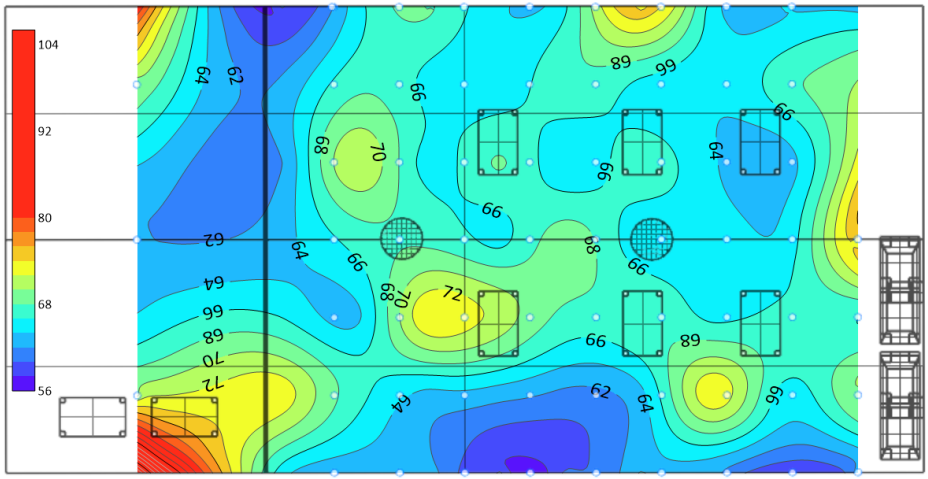

(b) 9 a.m. - 11 a.m.

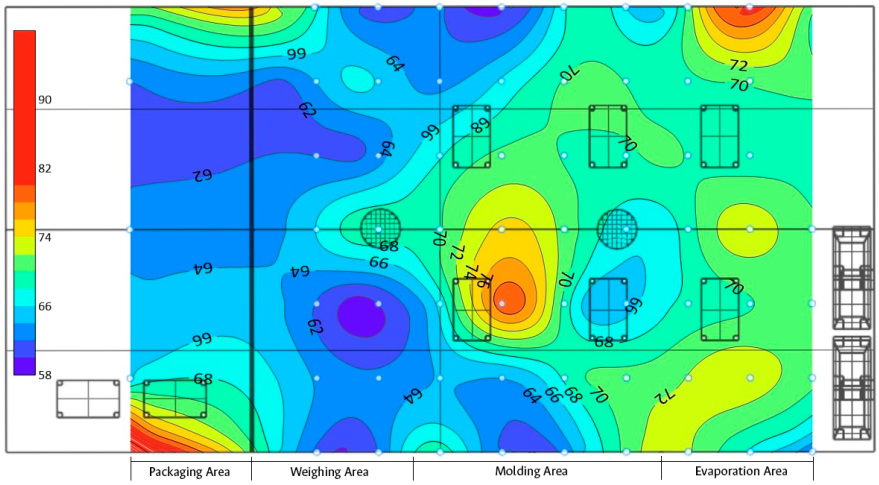

(c) 11 a.m. - 1 p.m.

Figure 4-2.: Contour maps for noise in working measures, dBA: (a) 7-9 a.m. (b) 9–11 a.m. (c) 11–1 p.m.

Figure **4-3** shows the time-weighted average distribution around the factory. These results go in consonance with previous studies, where sound levels increase in the proximity to walls and surfaces (Ahmed & Gadelmoula, 2022; Lim et al., 2018). Additionally, the map reaffirms the previously mentioned warning areas, with the presence of peaks in the molding and evaporation areas.

Furthermore, noise levels inside the factory are below the recommended levels, as presented in Figure **4-2** and Figure **4-3**. This shows that workers present no stress due to noise levels, therefore not having major affectations to their health (Organización Internacional del Trabajo, 2010). Additionally, the obtained results show the importance of sound mapping in agro-industrial productions, an area that has not been studied before.

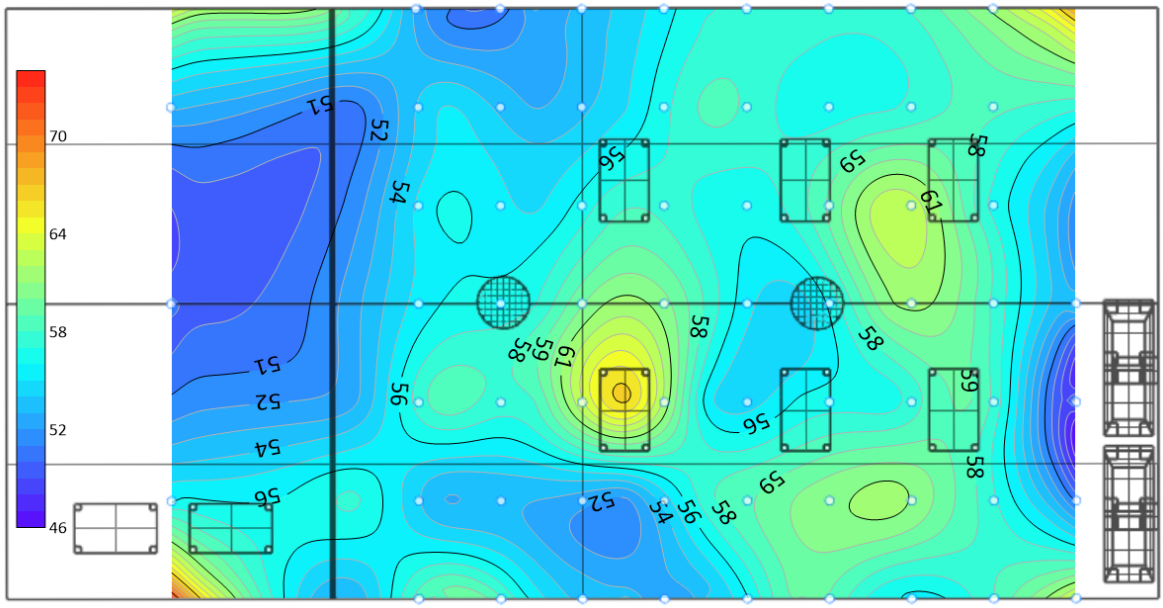

Figure 4-3.: TWA noise levels, dBA

Spaces with high noise levels, specially in the packaging area, can be decreased with the incorporation of noise reducing strategies. For instance, to avoid noise coming from the exterior area, it is possible to incorporate natural cover, to reduce heat exchange and guarantee a reduction in noise levels. Additionally, inside the factory, it is possible to change the times at which the tasks are performed, in order to reduce the noise accumulation, specially in the weighing and molding area.

4.4. Conclusions

This study uses a regression technique to map the sound levels registered through data gathering in the unrefined sugar cane factory, located in Caparrapí, Colombia. The results showed a general noise activity inside the allowed limits, with some exceptions in the proximity of the high noise activities.

The implementation of noise-reducing strategies, such as natural cover and modification of task schedules, can be effective in diminishing elevated noise levels, particularly in critical areas such as the packaging, weighing, and molding areas. These measures can significantly improve the overall work environment and reduce the risk of noise-induced health issues among workers.

High noise zones can be analyzed carefully, with the help of the maps, for the workers to avoid practices with high incidence in the sound levels. Finally, the addition of any device to change the environmental conditions inside the factory, such as fans, extractors or refrigerants could raise the studied levels. Additionally, this study shows the potentiality of applying sound mapping to agricultural production, due to the nature of the activities developed in that kind of task.

References

Ahmed, S. S., & Gadelmoula, A. M. (2022). Industrial noise monitoring using noise mapping technique: a case study on a concrete block-making factory. *International Journal of Environmental Science and Technology*, *19*(2), 851–862. Retrieved from https://doi.org/10.1007/s13762-020-02982-9 doi: 10.1007/s13762-020-02982-9

Alvarez-Carpintero, J., & Osorio-Hernandez, R. (2021, July). Thermal analysis for an unrefined sugar cane processing factory in colombia by using cfd. In *Proceedings of the European Conference on Agricultural Engineering AgEng2021* (pp. 733–739). Universidade de Évora.

Conde-Santos, L., Matias, C., Vieira, F., & Valado, F. (2008, October). Noise mapping of industrial sources. In (p. 1-12). Retrieved from https://dialnet.unirioja.es/servlet/libro?codigo=788358

Espitia, J., Velásquez, F., López, R., Escobar, S., & Rodríguez, J. (2020). An engineering approach to design a non-centrifugal cane sugar production module: A heat transfer study to improve the energy use. *Journal of Food Engineering*, *274*, 109843. Retrieved from https://www.sciencedirect.com/science/article/pii/S0260877419304868 doi: https://doi.org/10.1016/j.jfoodeng.2019.109843

Fedepanela. (2019). *PROTOCOLO DE TRAZABILIDAD PARA OBTENCIÓN DE PANELA*. BOGOTÁ, D.C.. Unpublished writing.

García, J. M., Narváez, P. C., Heredia, F. J., Orjuela, Á., & Osorio, C. (2017). Physicochemical and sensory (aroma and colour) characterisation of a non-centrifugal cane sugar ("panela") beverage. *Food Chemistry*, *228*, 7–13. doi: 10.1016/j.foodchem.2017.01.134

Hasibuan, C., Sutrisno, F., & Pranatal, B. (2020, 02). The instensity measurement and noise mapping in fatty acid plant area at pt. xyz. *Simetrikal: Journal of Engineering and Technology*, *2*, 20-27. doi: 10.32734/jet.v2i1.3556

IDEAM. (2015a). *Mapa de precipitación total anual (mm).* Cundinamarca, Colombia.

IDEAM. (2015b). *Mapa de temperatura media anual (°c).* Cundinamarca, Colombia.

Jaffé, W. R. (2015). Nutritional and functional components of non centrifugal cane sugar: A compilation of the data from the analytical literature. *Journal of Food Composition and Analysis*, *43*, 194–202. doi: 10.1016/j.jfca.2015.06.007

King, E., Murphy, E., & Rice, H. (2010, 11). Implementation of the eu environmental noise directive: Lessons from the first phase of strategic noise mapping and action planning in ireland. *Journal of environmental management*, *92*, 756-64. doi: 10.1016/j.jenvman.2010.10.034

Lim, M., Lee, Y., Lee, F. W., & Heng, G. (2018, 01). Strategic noise mapping prediction for a rubber manufacturing factory in malaysia. *E3S Web of Conferences*, *65*, 05019. doi: 10.1051/e3sconf/20186505019

Luzzi, S., & Vassiliev, A. V. (2005). A comparison of noise mapping methods in italian and russian experiences. In (p. 1051-1056). S. Hirzel Verlag. Retrieved from `https://books.google.com.co/books?id=EJ88HQAACAAJ`

Mendieta, O., García, M., Peña, A., & Rodríguez, J. (2016). *Las buenas prácticas de manufactura en la producción de panela* (1st ed.; Corpoica, Ed.). Mosquera (Colombia).

Ministerio de Agricultura y Desarrollo Rural. (2019). *Cadena agroindustrial de la panela.*

Ministerio de Ambiente, vivienda y Desarrollo Territorial. (2006). *RESOLUCION 0627 DE 2006.* BOGOTÁ, D.C..

Mujica, M., Guerra, M., & Soto, N. (2008). Efecto de la variedad, lavado de la caña y temperatura de punteo sobre la calidad de la panela granulada. *Interciencia*, *33*, 598–603.

NIOSH. (1998). *Occupational Noise Exposure* (No. 98-126). Cincinnati: National Institute for Occupational Safety and Health. doi: 10.1121/1.4778162

Organización Internacional del Trabajo. (2010). *La salud y la seguridad en el trabajo: El ruido en el lugar de trabajo.* Organización Internacional del Trabajo.

Rodriguez, G., Garcia, H., Roa, Z., & Santacoloma, P. (2004). Producción de panela como estrategia de diversificación en la generación de ingresos en áreas rurales de América Latina Producción de panela como estrategia de diversificación en áreas rurales de America Latina. *FAO*, 98.

Solís-Fuentes, J. A., Hernández-Ceja, Y., del Rosario Hernández-Medel, M., García-Gómez, R. S., Bernal-González, M., Mendoza-Pérez, S., & del Carmen Durán-Domínguez-de Bazúa, M. (2019). Quality improvement of jaggery, a traditional sweetener, using bagasse activated carbon. *Food Bioscience*, *32*, 100444. Retrieved from `https://www.sciencedirect.com/science/article/pii/S2212429218308071` doi: https://doi.org/10.1016/j.fbio.2019.100444

Velásquez, F., Espitia, J., Mendieta, O., Escobar, S., & Rodríguez, J. (2019). Non-centrifugal cane sugar processing: A review on recent advances and the influence of process variables on qualities attributes of final products. *Journal of Food Engineering*, *255*(November 2018), 32–40. doi: 10.1016/j.jfoodeng.2019.03.009

5. Conclusions and recommendations

5.1. Conclusions

With the use of Computational Fluid Dynamics tools it was possible to obtain the principal bioclimatic characteristics, with a close approximation to reality. Therefore, the results showed that temperature and relative humidity levels create an uncomfortable environment for workers, specially in hours with high solar incidence.

With the application of the CFD tools it was possible to determine that temperature and relative humidity levels are elevated, causing damage in the products and affecting the workers health. Additionally, the proposed treatments show that these problems can be corrected with the addition of natural or forced convection, guaranteeing a suitable environment.

Similarly, WBGT Index show that in early work shifts the workers do not present thermal stress. Nevertheless, during the hours with the highest temperatures, employees present difficulties to maintain the work rhythm and can exceed their capacity. In this way, possible solutions were presented, to help correct these problems.

Additionally, the study analyzed the current noise situation inside the factory. Results show that noise levels are proper for workers, for continuous shifts of 8 hours. Nevertheless, there are certain areas with high noise risks, where actions might be required to correct, in case other processes are added.

Finally, the proposed model shows an improvement in the environmental temperature and relative humidity levels, along with the WBGT Index for comfort. Nevertheless, in hours with high solar radiation it is necessary to implement additional strategies, to reduce heat stress.

A. Appendix: Temperature profiles for treatments 1 to 4 at 9a.m., 11 a.m. and 3p.m. work shifts

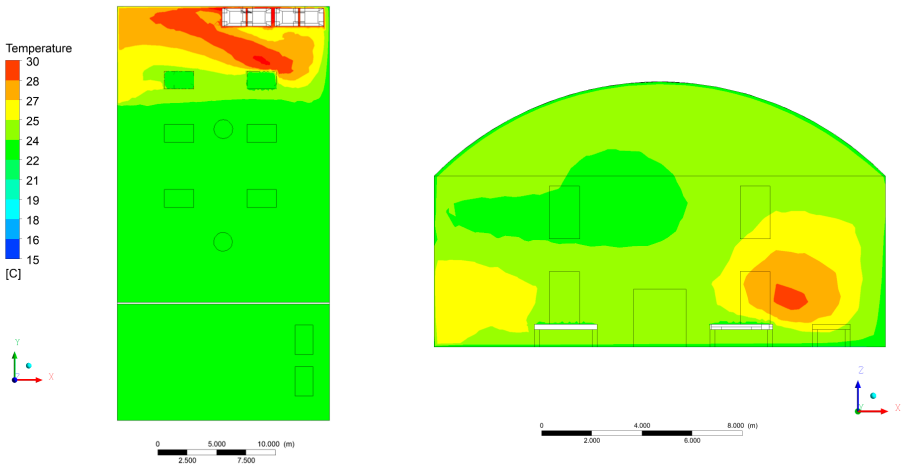

(a) Treatment 1 at 9a.m.

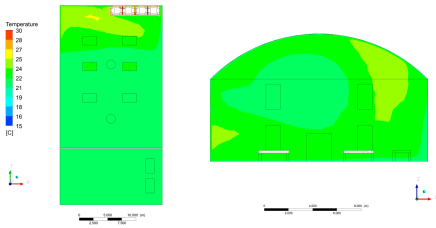

(b) Treatment 2 at 9a.m.

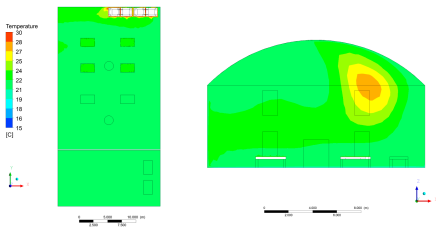

(c) Treatment 3 at 9a.m.

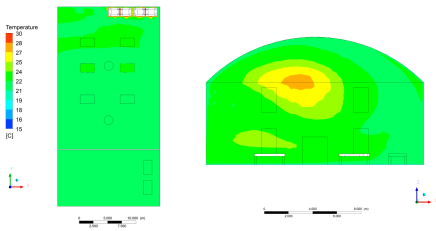

(d) Treatment 4 at 9a.m.

Figure A-1.: Temperature profiles for treatments 1 to 4 for 9a.m. work shift

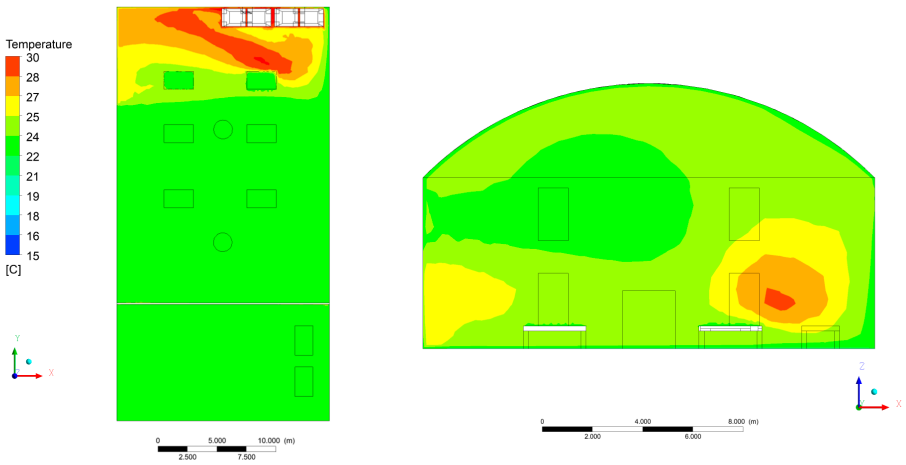

(a) Treatment 1 at 9a.m.

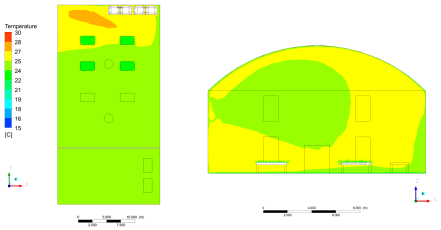

(b) Treatment 2 at 9a.m.

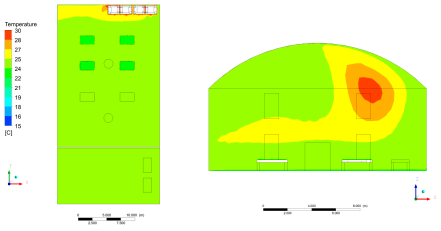

(c) Treatment 3 at 9a.m.

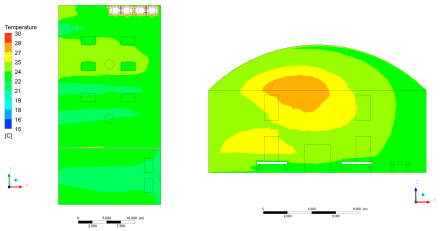

(d) Treatment 4 at 9a.m.

Figure A-2.: Temperature profiles for treatments 1 to 4 for 11a.m. work shift

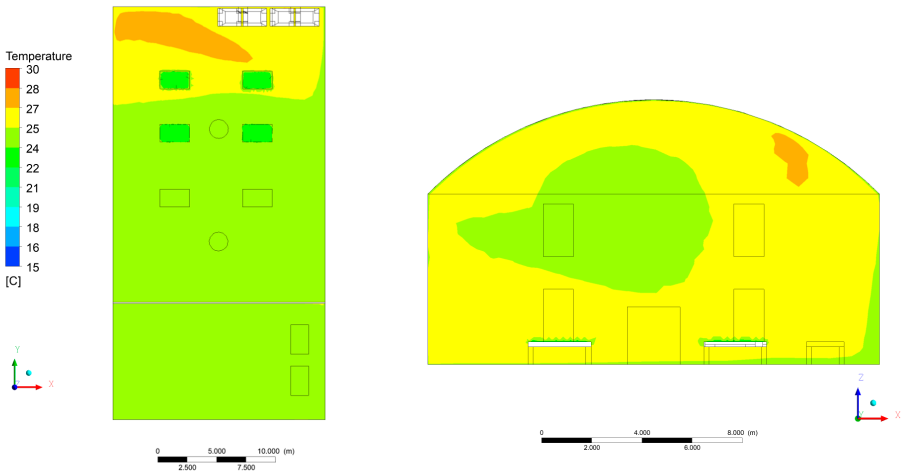

(a) Treatment 1 at 3p.m.

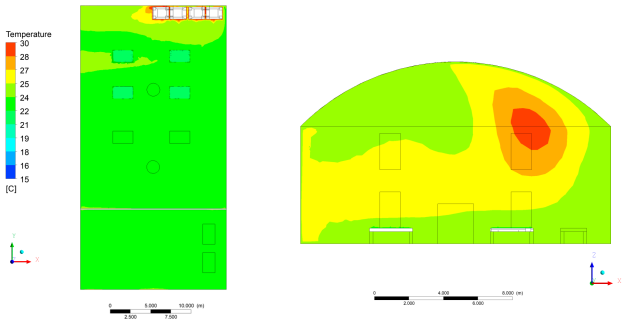

(b) Treatment 2 at 3p.m.

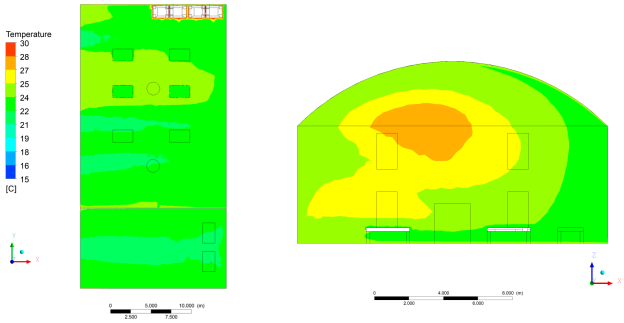

(c) Treatment 3 at 3p.m.

Figure A-3.: Temperature profiles for treatments 1 to 4 for 3p.m. work shift

B. Appendix: Relative humidity profiles for treatments 1 to 4 at 9a.m., 11 a.m. and 3p.m. work shifts

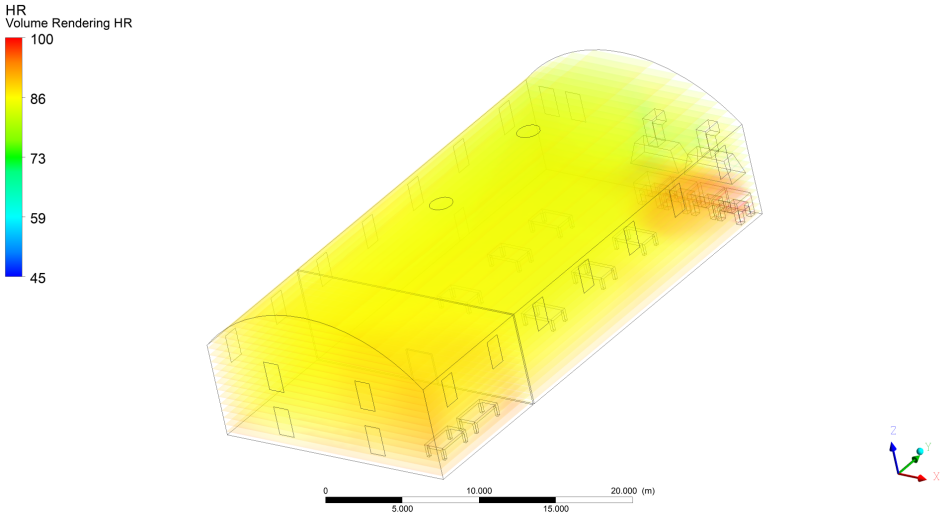

(a) Treatment 1 at 9a.m.

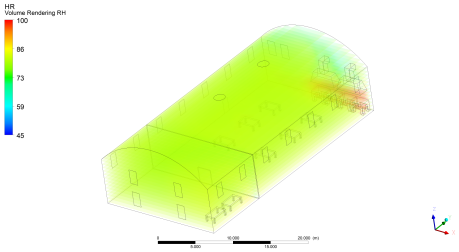

(b) Treatment 2 at 9a.m.

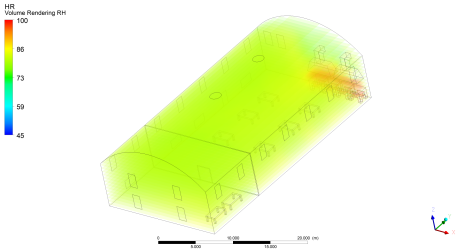

(c) Treatment 3 at 9a.m.

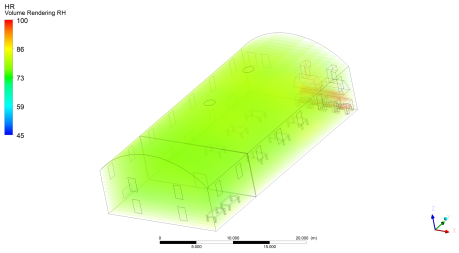

(d) Treatment 4 at 9a.m.

Figure B-1.: Relative humidity profiles for treatments 1 to 4 for 9a.m. work shift

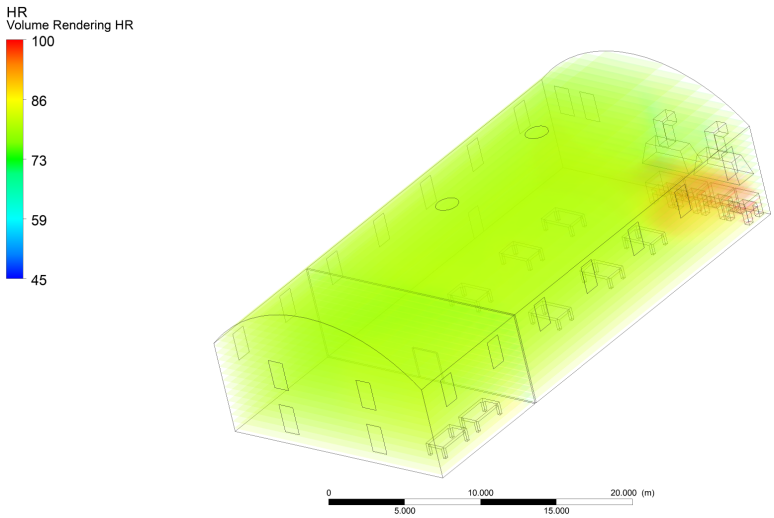

(a) Treatment 1 at 9a.m.

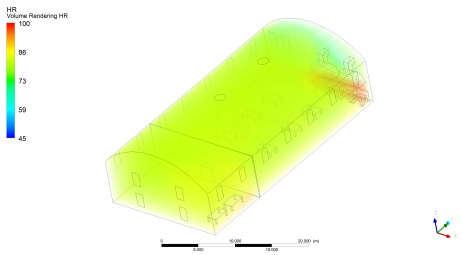

(b) Treatment 2 at 9a.m.

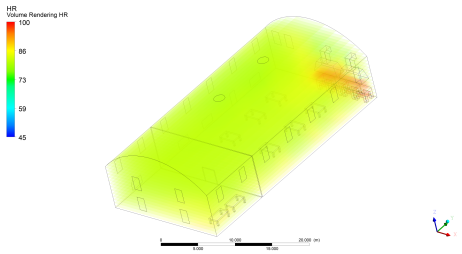

(c) Treatment 3 at 9a.m.

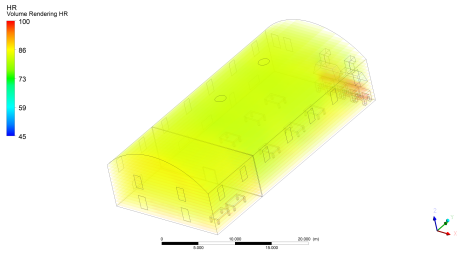

(d) Treatment 4 at 9a.m.

Figure B-2.: Relative humidity profiles for treatments 1 to 4 for 11a.m. work shift

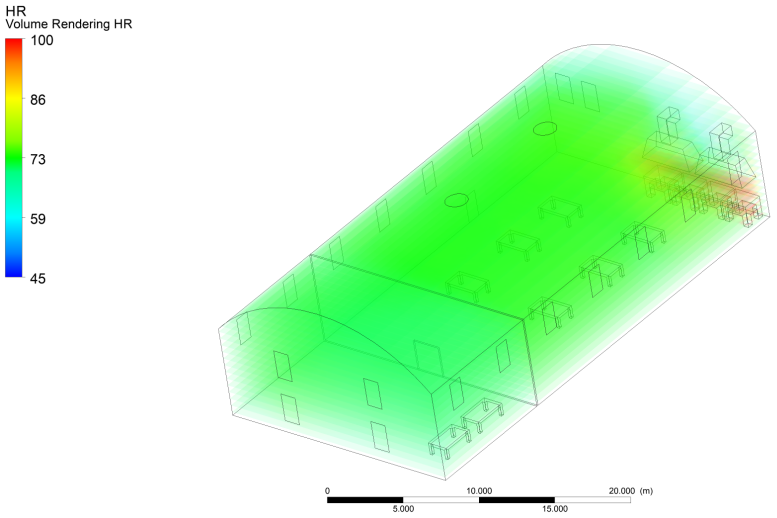

(a) Treatment 1 at 3p.m.

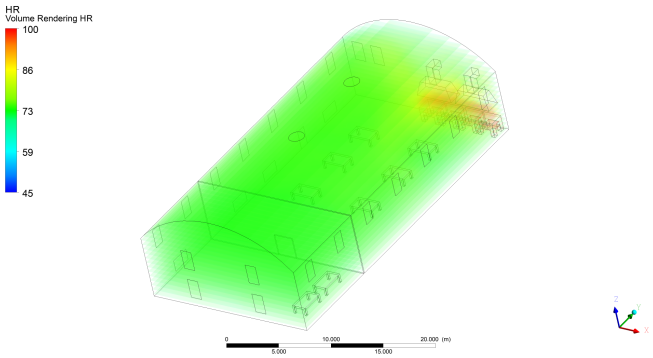

(b) Treatment 2 at 3p.m.

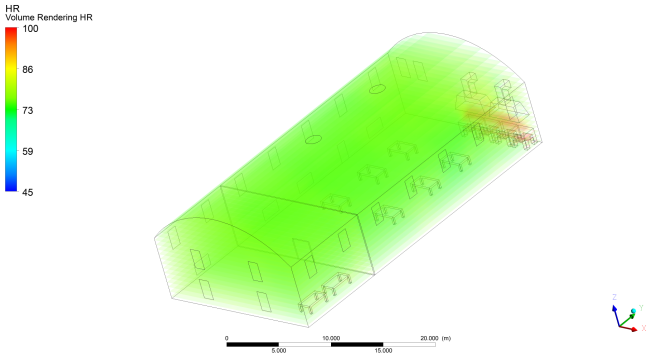

(c) Treatment 3 at 3p.m.

Figure B-3.: Relative humidity profiles for treatments 1 to 4 for 3p.m. work shift

C. Appendix: WBGT Index maps for treatments 1 to 4 at 9a.m., 11a.m. and 3p.m.

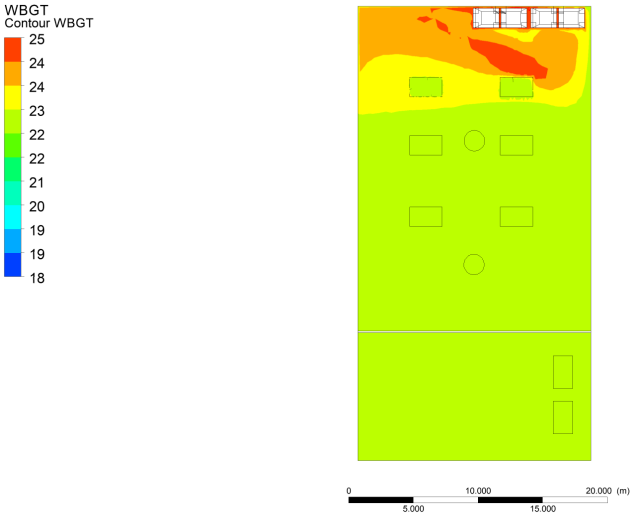

(a) Treatment 1 at 9a.m.

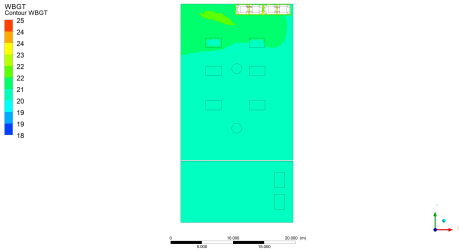

(b) Treatment 2 at 9a.m.

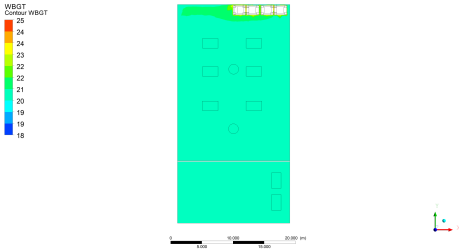

(c) Treatment 3 at 9a.m.

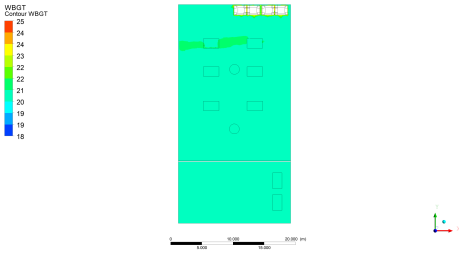

(d) Treatment 4 at 9a.m.

Figure C-1.: WBGT profiles for treatments 1 to 4 for 9a.m. work shift

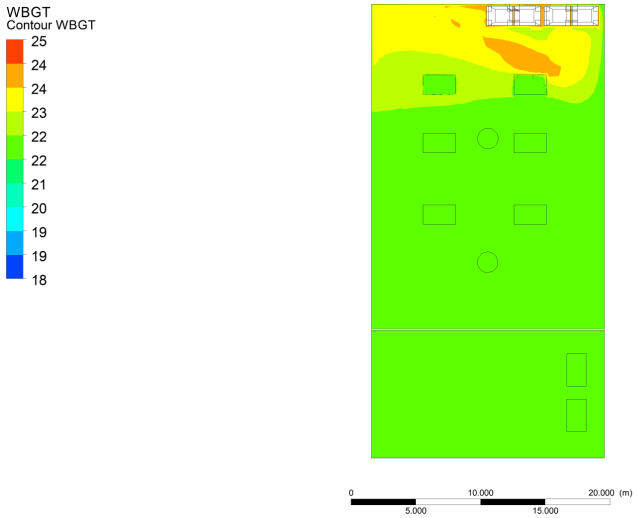

(a) Treatment 1 at 11a.m.

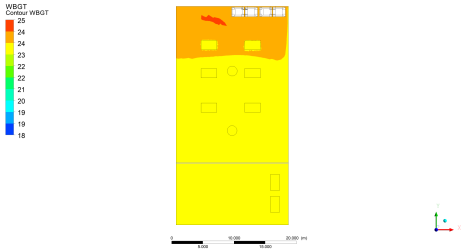

(b) Treatment 2 at 11a.m.

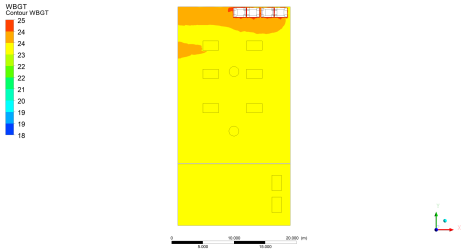

(c) Treatment 3 at 11a.m.

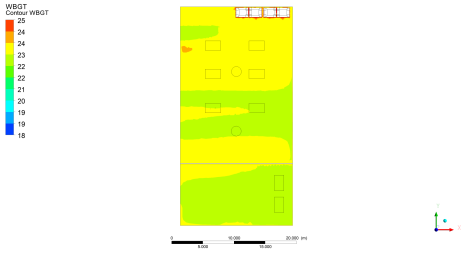

(d) Treatment 4 at 11a.m.

Figure C-2.: WBGT profiles for treatments 1 to 4 for 11a.m. work shift

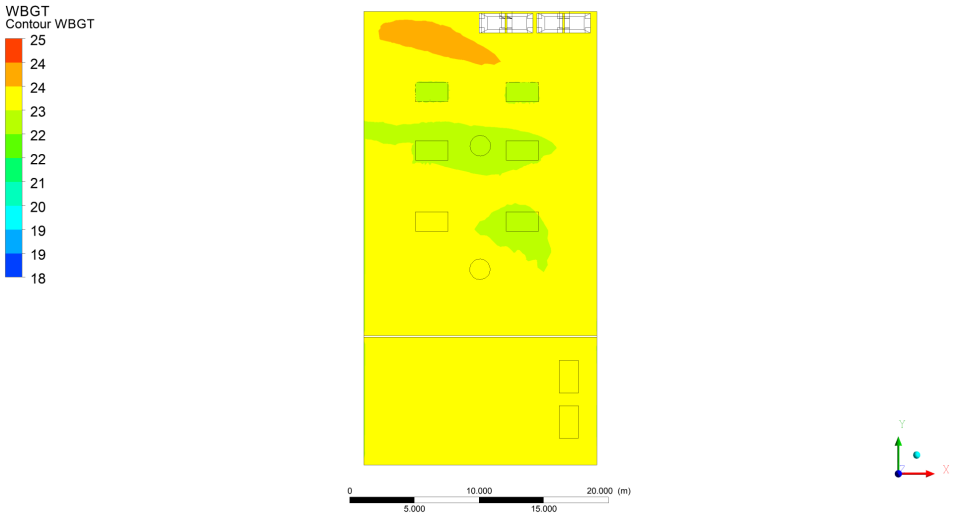

(a) Treatment 1 at 3p.m.

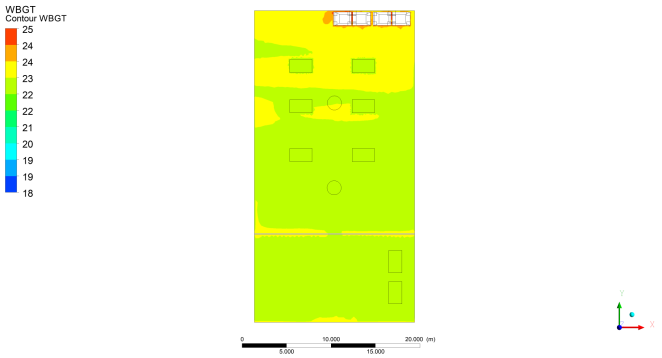

(b) Treatment 2 at 3p.m.

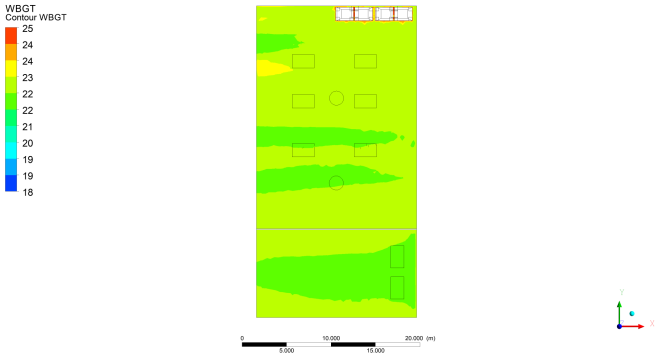

(c) Treatment 3 at 3p.m.

Figure C-3.: WBGT profiles for treatments 1 to 4 for 3p.m. work shift